Journal of Archaeological Science: Reports 27 (2019) 101957

Contents lists available at ScienceDirect

Journal of Archaeological Science: Reports

journal homepage: www.elsevier.com/locate/jasrep

Introducing the Peabody-Yale Reference Obsidians (PYRO) sets: Open-source calibration and evaluation standards for quantitative X-ray fluorescence analysis

Ellery Frahm

Yale Archaeological XRF ExoLab (YAXX), Council on Archaeological Studies, Department of Anthropology, Yale University, New Haven, CT, USA
Anthropology Division, Peabody Museum of Natural History, Yale University, New Haven, CT, USA

ARTICLE INFO

Keywords:
Obsidian sourcing
EDXRF
Portable XRF
Accuracy
Reproducibility
Transparency
Collaboration

ABSTRACT

A series of well-characterized specimens, known as the Peabody-Yale Reference Obsidians (PYRO) sets, has been designed to aid with calibrating and assessing X-ray fluorescence analysis (XRF) data, including portable XRF (pXRF) measurements, for obsidian sourcing. Each of these ten matched sets consists of 35 specimens: 20 specimens for calibration and 15 specimens for evaluation. These sets include not only obsidians with common geochemical compositions (i.e., alkaline rhyolites) but also rarer ones (i.e., peralkaline rhyolitic, trachytic, and andesitic specimens, including East African Rift obsidians). When used as described, the PYRO sets are suitable to calibrate and evaluate XRF data for obsidians worldwide. A set can be borrowed following loan policies of the Peabody Museum of Natural History, which will also accession a set. Publishing all source information – from their names and GPS coordinates to the datasets used for the recommended values – not only allows the sets to be replicated by others but also fulfills the demands of scientific transparency. Their main purpose is facilitating collaborations and "big data" projects, and the PYRO sets were designed to complement existing protocols for calibration and evaluation. In short, the sets are intended as a tool for almost anyone (e.g., a student who borrows an instrument to source artifacts) to meet – and even exceed – experts' practices involving transparency, accuracy, and reproducibility.

1. Introduction

This paper introduces a collection of well-characterized obsidian specimens designed to aid archaeologists with calibrating and assessing quantitative X-ray fluorescence analysis (XRF) data for sourcing research. Known as the Peabody-Yale Reference Obsidians (PYRO) sets, each of these ten matched sets consists of 35 specimens mounted within 25-mm epoxy discs (Fig. 1): 20 specimens for calibration and 15 independent specimens for evaluation. These sets include not only obsidians with common alkaline rhyolitic compositions but also peralkaline rhyolitic, trachytic, and andesitic specimens, including five obsidians that occur within the East African Rift region and sanukite from Japan. Consequently, when utilized as described here, the PYRO sets are suitable for calibrating and evaluating XRF data for obsidian sources and artifacts throughout the world. A set can be borrowed freely by researchers, following loan policies of the Peabody Museum of Natural History, which will also accession a set. Publishing all of the obsidian source information – from the source names and GPS coordinates to the datasets used for the recommended values – not only permits the sets to be replicated by others but also fulfills the demands of scientific transparency.

Soon after the pioneering work of Renfrew and his colleagues to attribute Mediterranean and Mesopotamian obsidian artifacts to their volcanic sources with optical emission spectroscopy (Cann and Renfrew, 1964; Renfrew et al., 1965, Renfrew et al., 1966, Renfrew et al., 1968), University of California-Berkeley researchers and Shell Development scientists successfully used XRF to source American obsidians (Heizer et al., 1965; Weaver and Stross, 1965; Jack and Carmichael, 1968). This, however, was not "XRF" as most readers would recognize it now. The instrument was a General Electric wavelength-dispersive "XRF" (WDXRF) that needed two different hardware configurations (i.e., different dispersing crystals and X-ray counters) and two hours per artifact to measure a spectrum and produce its tracing on paper (Weaver and Stross, 1965). The intensity of each X-ray peak was approximated from such tracings in units of photon counts per second, a procedure that, with practice, took another 15 min per specimen. These data, without conversion to elemental concentrations, were used to make source identifications, which, according to Weaver

E-mail address: ellery.frahm@yale.edu.

https://doi.org/10.1016/j.jasrep.2019.101957
Received 23 May 2019; Received in revised form 16 July 2019; Accepted 30 July 2019
Available online 28 August 2019
2352-409X/

and Stross (1965:91), were "suggestive but by no means conclusive." Today, the spectral computations are largely automated and almost instantaneous. This should not come as a surprise given the processing power available at our fingertips. NASA's Apollo Guidance Computer during the late 1960s was capable of 40 operations per second, while an iPhone is capable of over 600 billion operations per second. Nevertheless, five decades later, XRF remains a comparative method of elemental analysis that is predicated on calibration.

The proliferation of portable XRF (pXRF) instruments in obsidian artifact sourcing has been met with both caution and enthusiasm. Regarding the former, as I have observed elsewhere (Frahm, 2014:115), many criticisms of pXRF-based studies focus more on the users' methods and knowledge than (perceived) technological limitations of the instruments. Regarding the latter, as I mentioned at a recent conference (Frahm, 2019), pXRF is (literally) changing the faces of elemental analysis in archaeological science. Measuring obsidian specimens and artifacts no longer occurs only in expert analysts' labs. This, in turn, creates opportunities for coordinated, international collaborations that were not previously possible. In 2013, a colleague and I (Frahm and Doonan, 2013:1427) suggested that pXRF had the potential to change experts' roles within such projects:

> This, however, is not to undermine the role of the expert analyst, and we strongly contend that experts should not show distain for these instruments because they appear to undermine their own accrued expertise. On the contrary, the proliferation of [pXRF] instruments should, and most likely will, raise the demand for expert knowledge to ensure their effective deployment in archaeology. It might not be the expert who actually pulls the trigger, but it will almost certainly be the expert who decides when the trigger is pulled and, more importantly, at what the instrument is aimed.

We also proposed that archaeological science should expect to see a phase of initial experimentation before methods eventually become more firmly developed. Shackley (1998:4) warned, years before the first pXRF analyzers, that the field of obsidian sourcing should avoid settling into an established and unchallenged framework – what Kuhn (1962) termed "normal science" in his *The Structure of Scientific Revolutions* (1962) – and falling "into an abyss of tautological analyses" (4). The pXRF "revolution" is not only technological but also methodological and epistemological.

To realize the potential for "big data" in obsidian sourcing, as recently discussed by Golitko (2019), there are lessons to be learned from the past – specifically, the past of compositional analysis in archaeological science. During the 1980s and 1990s, elemental data from ceramic analyses were compiled in the Smithsonian Archaeometric Research Collections and Records (SARCAR) database, which was meant to integrate and curate such datasets (Bishop et al., 1983). Debates began, though, when SARCAR advocates excluded data from certain studies and techniques that they considered to lack sufficient rigor (e.g., Bishop, 1992; Harbottle and Bishop, 1992). In a review paper on the state of ceramic chemical analyses, including "growth in laboratories providing compositional analytical services for archaeological" materials, Prudence Rice (1996:173) argued:

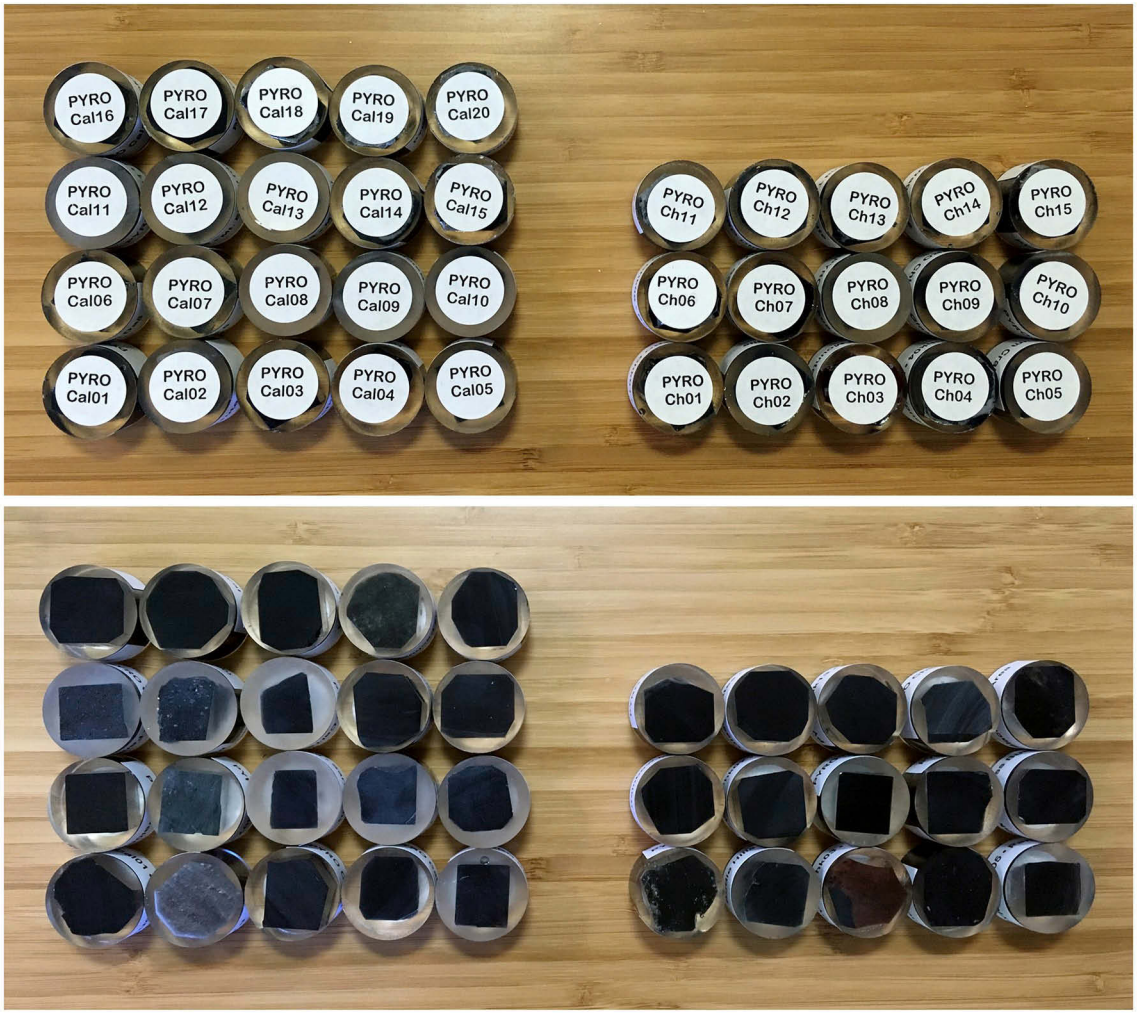

Fig. 1. One of the ten PYRO sets: 35 well-characterized specimens 20 for calibration and 15 for evaluation mounted in 25-mm epoxy discs.

> Apart from questions of accuracy and interpretation, it is worth noting that other recent critiques have targeted the suitability of specific methods of compositional analysis… These authors… dismiss… these methods on the grounds that they represent ad hoc, often cursory, single-purpose endeavors or pilot studies, and are rarely adequate for database comparisons. It might be claimed that at least some of these authors are arguing from a rather elitist position of enlightened self-interest, as they are ultimately advocating that their own worldwide ceramic database (e.g., the existing SARCAR database) be enshrined. However, the greater comparability in ceramic data is of concern to all researchers, incorporating basic, pragmatic questions… as well as loftier issues of scientific legitimacy… The issue in the future will revolve around how to achieve the desired comparable standards while, at the same time, avoiding the appearance of arbitrarily dictating "good" versus "bad" scientific paradigms and curbing the rights of researchers to select their methods and carry out their investigations freely.

Her observations remain equally relevant now given that, as reported by Grave et al. (2012:1674), the "archaeological applications of pXRF continue to be cautiously treated, principally because of a perceived lack of analytic rigor or understanding." For example, Speakman – then at the Smithsonian – and colleagues argued that "it is not the analytical technique that is flawed, but rather the general lack of experience and knowledge of the users" (Speakman et al., 2011:3484). These obstacles must be addressed before "big data" obsidian projects can become a reality, otherwise such efforts could face the unceremonious fate of SARCAR (Blackman and Bishop, 2007:333).

Key points of contention regarding pXRF of obsidian artifacts surround quantification of the elemental data – namely, the use (or not) of standards not only to calibrate measurements but also to evaluate their accuracy, which Shackley (2012b) has labeled "the ugly side of pXRF applications in archaeology" (see also Shackley, 2010; Speakman and Shackley, 2013). Experts' critiques have been, in general, more programmatic than pragmatic and were even, in at least one instance, published in all capitalized letters ("WE CANNOT ESTABLISH VALIDITY IF WE DON'T PROVIDE… THE ANALYSIS OF STANDARDS," Shackley, 2010:19). Nevertheless, as discussed in Section 2.2, the recent literature indicates that pXRF users are, indeed, listening and endeavoring to address these concerns, albeit to varying degrees of success. Furthermore, the options that experts have advocated are not without their own issues, as elucidated in Section 2.1, implying that there is a lack of critical self-reflection in our field. In short, potential collaborators have been presented with two basic options. The first is to purchase what are known as certified or standard reference materials (CRMs or SRMs), which (1) are sometimes prohibitively expensive (e.g., NIST SRM #278 [powdered obsidian] costs $442, while NIST SRMs #610 and #612 [trace elements within glass] cost $539 each) and (2) frequently are not particularly well-suited to obsidians. The second option is to rely on an "obsidian" calibration that was developed at the University of Missouri Research Reactor (MURR) in 2012 and is implemented, installed, and sold by only one manufacturer of pXRF instruments. Its constituent obsidian sources have not been published, so its use does not alleviate objections to taking a "black box" (Speakman et al., 2011:3484) or "trust me" (Shackley, 2010:19) approach. Furthermore, neither of these two calibration options are especially strong with regard to data evaluation.

A cognate issue was recognized by scientists and conservators working on XRF analyses of bronzes, brasses, and other copper alloys (Heginbotham et al., 2011), and a working group led to the creation of the Copper CHARM (Cultural Heritage Alloy Reference Material) Set (Heginbotham et al., 2015), a collection of 17 SRMs that served as one inspiration for the PYRO sets. The working group commissioned MBH Analytical Ltd. to produce and distribute this set of SRMs. As of this writing, the SRMs cost between $394 and $567 each (the mean is ~$500), so the total cost is ~$8500. This poses a barrier for most smaller projects. For example, one researcher, seeking advice, commented online that "the cost of purchasing [a set] is expensive and outside the budget of my project" (ResearchGate, 2019). In contrast, the PYRO sets are not for sale. Nor does this project use a "cost recovery" model, whereby direct and indirect production costs are recuperated via fees. Instead, the PYRO sets were always intended to be freely available for others to borrow or replicate.

The purpose of the PYRO sets is to facilitate a transition to more settled protocols for pXRF-based sourcing and, in turn, more collaborations. It was designed to complement existing methods of calibration and evaluation, as discussed in the following sections. To give an example here, various researchers report, as routine practice, measurements of SRM RGM-1 (or its replacement, RGM-2) in order to demonstrate accuracy, and consequently, the PYRO check set includes a specimen of Glass Mountain obsidian, the source material for RGM-1/2. In 2012, a question occurred to me: "How do I, as a postdoc moving from post to post, maintain the consistency of my data as I use different pXRF instruments?" I discuss my earlier endeavors toward this end in Section 2.3, but our students and I are increasingly faced with variations on this issue as we work and form collaborations around the world. The PYRO sets reflect the newest development in my answer to this question. In short, these sets are intended as a tool for almost anyone (e.g., a Master's student who borrows an instrument to analyze the obsidian artifacts in a museum collection) to meet – and even exceed – experts' practices and their assertions regarding transparency, accuracy, and reproducibility.

2. Past and current practices

Before discussing the intended protocols for PYRO use and the choices made in developing the sets, it is necessary to consider (1) calibration and data evaluation procedures used by XRF labs that specialize in sourcing obsidian artifacts, (2) methods used in pXRF-based studies to address the same issues, and (3) my prior approaches to pXRF calibration and assessment.

2.1. Protocols of EDXRF laboratories

How are recent benchtop energy-dispersive XRF (EDXRF) instruments calibrated – and their calibrations evaluated – in laboratories that specialize in analyses of obsidian artifacts? It is typical for these instruments to be calibrated using powdered SRMs from agencies such as the United States Geological Survey (USGS) and United States National Institute of Standards and Technology (NIST). For example, Shackley et al. (2016:63) list a set of 20 SRMs for calibration at the Geoarchaeological XRF Lab (formerly at the University of California-Berkeley, now in New Mexico):

> A suite of 16 specific [USGS] standards are used for the best fit regression calibration… G-2 (basalt), AGV-2 (andesite), GSP-2 (granodiorite), SY-2 (syenite), BHVO-2 (hawaiite), STM-1 (syenite), QLO-1 (quartz latite), RGM-1 (obsidian), W-2 (diabase), BIR-1 (basalt), SDC-1 (mica schist), BCR-2 (basalt), TLM-1 (tonalite), SCO-1 (shale), NOD-A-1 (manganese), NOD-P-1 (manganese). Four other standards include: [NIST SRM] 278 (obsidian), BR-E (basalt) from the Centre de Recherches Pétrographiques et Géochimiques in France, and JR-1 and JR-2 (obsidian) from the Geological Survey of Japan.

This list includes four obsidian SRMs, and while many of these other rocks are volcanic (e.g., diabase, basalts), there are metamorphic (mica schist) and sedimentary (shale) rocks as well. For example, the two manganese nodules (NOD-A-1 and NOD-P-1) are rock concretions, formed on an ocean bed, that consist of concentric layers of manganese and iron hydroxide minerals – such nodules are very different from obsidians, both in elemental composition and geological origin.

The McMaster Archaeological XRF Lab (MAX Lab) uses thirteen of the same SRMs – or their direct substitutions (e.g., RGM-2 in place of

RGM-1) – for instrument calibration:

> These comprise AGV-2 (andesite), BCR-2 (basalt), BHVO-2 (hawaiite), BIR-1a (basalt), GSP-2 (granodiorite), QLO-1 (quartz latite), RGM-2 (rhyolite), SDC-1 (mica schist), STM-2 (syenite), TLM-1 (tonalite), and W-2a (diabase) from the US Geological Service [USGS], plus JR-1 and JR-2 (both obsidian) from the Geological Survey of Japan (Carter et al., 2018:178).

The SRMs used at Geochemical Research Laboratory (GRL), located in California, include "up to 30 international rock standards" from the USGS, NIST, Geological Survey of Japan, Centre de Recherches Pétrographiques et Géochimiques, and elsewhere (Hughes, 2015:295). This is also the protocol for the Northwest Research Obsidian Studies Laboratory (NWROSL) in Oregon. One reason that these labs use the same or similar SRMs is that they are "related" in a sense. Shackley (2011a) points out that "these laboratories are, in part, daughter labs of the 1970s… instrument at Berkeley" (11). That is, the founders of these laboratories either worked at (i.e., Hughes), studied at (i.e., Carter), or worked near (i.e., Skinner at Biosystems Analysis) the University of California-Berkeley. Therefore, it makes sense that these four facilities constitute a distinct community of practice.

It should be no surprise, therefore, that calibration checks are identical at these labs. All of them report their values with a measurement of USGS RMG-1 or 2 ("RGM-1 is analyzed during each sample run… to check machine calibration," Shackley et al., 2016:64; see also Skinner and Thatcher, 2003; Carter et al., 2013; Hughes, 2015). There are two problems to this approach to evaluate data accuracy. First, as illustrated in Figs. 2a-d, accurate elemental concentration data for one standard do not mean that measurements are accurate for other concentrations. This is the reason that Hall (2016) recommends using more than one known standard to monitor calibration. It takes analyses of multiple standards to differentiate among those scenarios shown in Fig. 2a versus 2b-d. Even two standards (Figs. 3a-d) might not reveal accuracy problems in certain ranges.

This is a valid concern due to the second problem. Note that RMG-1/2 is used not only as an accuracy check but also as one of the calibration standards. It is typically recommended that check standards not be included among the calibration standards in order to act as an independent means of accuracy verification (e.g., Beckhoff et al., 2006:393; Hibbert, 2007:133; Barrett et al., 2012:206). Checking accuracy using a standard included within the calibration set can yield false confidence in the measurements. Accuracy is expected to be greatest when measuring a calibration standard and might not reflect data quality across wider compositions. The solution is straightforward: analyzing multiple known standards, not included in the calibration, as unknowns.

2.2. Protocols of recent pXRF studies

A review of peer-reviewed articles published in the last few years suggests that researchers are endeavoring, in a variety of ways, to evaluate and/or improve the quality of their pXRF data for obsidian sourcing. Some researchers rely entirely on a factory-installed MURR/Bruker calibration but report no means to assess its accuracy or reproducibility (e.g., Pintar et al., 2016; Reepmeyer et al., 2016; Fernández et al., 2017; Grebennikov et al., 2018; Matsumoto et al., 2018). Others who rely on this calibration, though, also measured either a SRM (e.g., USGS Glass Mountain rhyolitic obsidian RGM-2 in Panich, 2016; USGS Hawaiian basalt BHVO-2 in Gaffney and Summerhayes, 2018) or well-characterized specimen (e.g., Sierra de Pachuca obsidian from Mexico in Neri et al., 2015; Shirataki-Akaishiyama obsidian from Japan in Lynch et al., 2018). Similarly, Mendelsohn (2018) utilized the MURR/Bruker calibration, but she notes that "control samples were run at the beginning and end of each day, so that any changes in the readout of the machine could be observed" (640). Others chose to compare their measurements to those from an obsidian-focused lab (e.g., NWROSL in Ebert et al., 2015; Geoarchaeological XRF Lab in Liebmann, 2017). There is, on occasion, a more sophisticated approach. For example, McCoy et al. (2014) first used the factory-set MURR/Bruker calibration and then applied their own regression analysis based on a set of nine SRMs, followed by measurements of USGS SRM BHVO-2 alongside their artifacts "as a quality check" (471).

Without the MURR/Bruker obsidian calibration, those researchers using pXRF instruments from other manufacturers have devised their own procedures. At the Elemental Analysis Facility of Chicago's Field

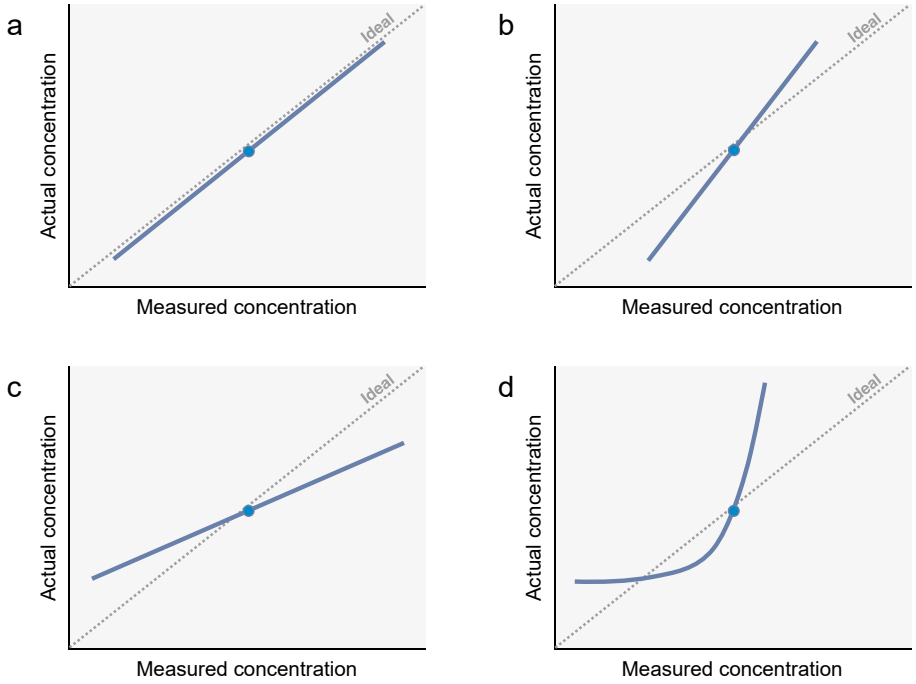

Fig. 2. Four fictional trends illustrate that reporting accuracy for a single standard (circular dot) could reflect not only (a) excellent accuracy across a range of values but also (b and c) an undetected systematic error or even (d) nonlinear behavior.

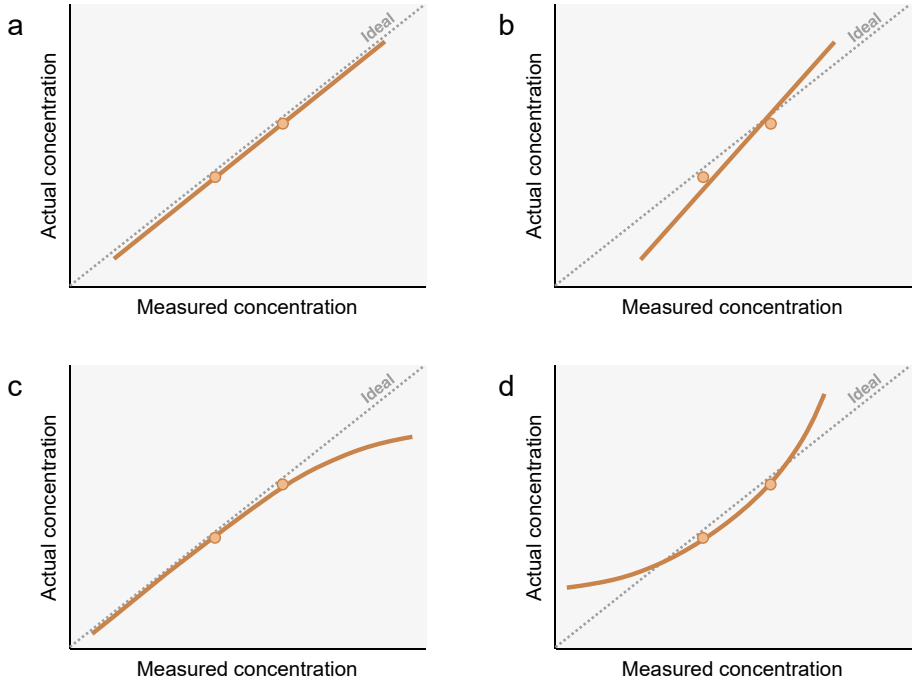

Fig. 3. Like Fig. 2, these four fictional trends illustrate that reporting accuracy for two standards (circular dots) could reflect not only (a) excellent accuracy across a wide range of values but also (b) an undetected systematic error or even (c and d) nonlinear behavior.

Museum of Natural History, Millhauser et al. (2015) utilized two well-characterized obsidians – Sierra de Pachuca, Mexico and Little Glass Buttes, Oregon, USA – as a means to "provide a basis, albeit minimal, for reporting the precision and accuracy" of their Innov-X instrument (138). Riebe et al. (2018:27) explain that researchers at this museum later developed a more sophisticated approach in order to correct and calibrate their Thermo Niton instrument:

> Building off of the ["Mining" mode that uses] fundamental parameters provided by the instrument manufacturer, Mark Golitko… created a calibration correction to increase instrumental precision. Golitko analyzed 21 in-house obsidian standards using both pXRF and LA-ICP-MS (calibrated with NIST 610, NIST 612, and Glasses Buttes and Sierra Pachuca obsidian; Glascock, 1999) and generated linear regression lines to correct fundamental parameters output [with "user factors"].

Abedi et al. (2018) and other GéObs Project researchers similarly adjust the FP-based "Mining" data from their Thermo Niton instrument. Specimens from five obsidian sources in Turkey (i.e., Bingöl A and B, Nemrut Dağ, Meydan Dağ, Pasinler) were measured with both pXRF and ICP-MS, providing a means to derive custom "user factors" to bring the former into line with the latter. At the University of Manchester, Campbell and Healey (2016) likewise "fine-tuned" their Thermo Niton calibration for obsidian sourcing in Southwest Asia. Specifically, they explain (380):

> The raw results from the instrument are already subject to built-in internal calibration. However, to provide data comparable to that obtained from other techniques as well as control for potential instrumental variation through time, a further calibration is required. For this, we used a composite reference set of international standards and obsidian artifact samples to provide an obsidian-specific calibration. The former were analyzed as compressed powder pellets and included NIST 278 (obsidian), BIR-1 (basalt), BCR-2 (basalt), and W-2a (diabase), among others. The obsidian artifact samples were thick with flat faces and had been previously analyzed… by laser-ablation ICP-MS by Poidevin… and using EPMA by Frahm (for technique see Frahm, 2010)… This comparative data was used to create a custom calibration using a simple linear regression.

Thus, these three sets of archaeologists (Campbell and Healey, 2016; Abedi et al., 2018; Riebe et al., 2018) all use FP-based correction together with a custom calibration based on regression analysis of obsidian specimens and/or geological standards. In each instance, however, these researchers had to assemble their own calibration materials due to the lack of an available set.

2.3. My calibration protocol development

In a review paper (Frahm and Doonan, 2013), a colleague and I predicted that pXRF methods were entering a time of experimentation and evaluation. Killick's (2015) "awkward adolescence" is also an apt description for this period of methodological development. My own calibration methods are no exception. When I first analyzed obsidian specimens and artifacts with pXRF (Frahm, 2007), I relied entirely upon the factory calibration and, as a result, found that the reported concentrations exhibited systematic errors, sometimes off by a factor of two or three. In 2012, I tried two different calibration approaches. In one study, I calibrated the data relative to the means of published values for Aegean obsidians analyzed with other techniques, including NAA, ICP-OES/MS, and XRF (Frahm et al., 2014a). In the other study, the initial factory-calibrated values were "fine-tuned" using linear regression analysis and 18 matched obsidian specimens also analyzed by NAA and EDXRF at MURR (Frahm, 2013). I further developed this latter approach in time to bring a pXRF instrument (a Niton XL2) to Armenia for the 2012 field season to conduct obsidian sourcing.

Specifically, in 2012, I selected 24 obsidian specimens from Turkey (Sarıkamış, Meydan Dağ, Erzurum, and Kars-Digor 1), Georgia (Chikiani), and Armenia (Aghvorik, Geghasar 1 and 2, Gutansar, Hatis, Kamakar, Pokr Arteni, Satanakar, and Sevkar, among others) to use as calibration standards (Frahm, 2014). Matched subsamples from all of them were previously analyzed by NAA and EDXRF at MURR and by electron microprobe analysis (EMPA) at the University of Minnesota (Frahm, 2012). These obsidian specimens were mounted in epoxy discs and, as a result, have survived numerous trans-Atlantic flights. In 2017,

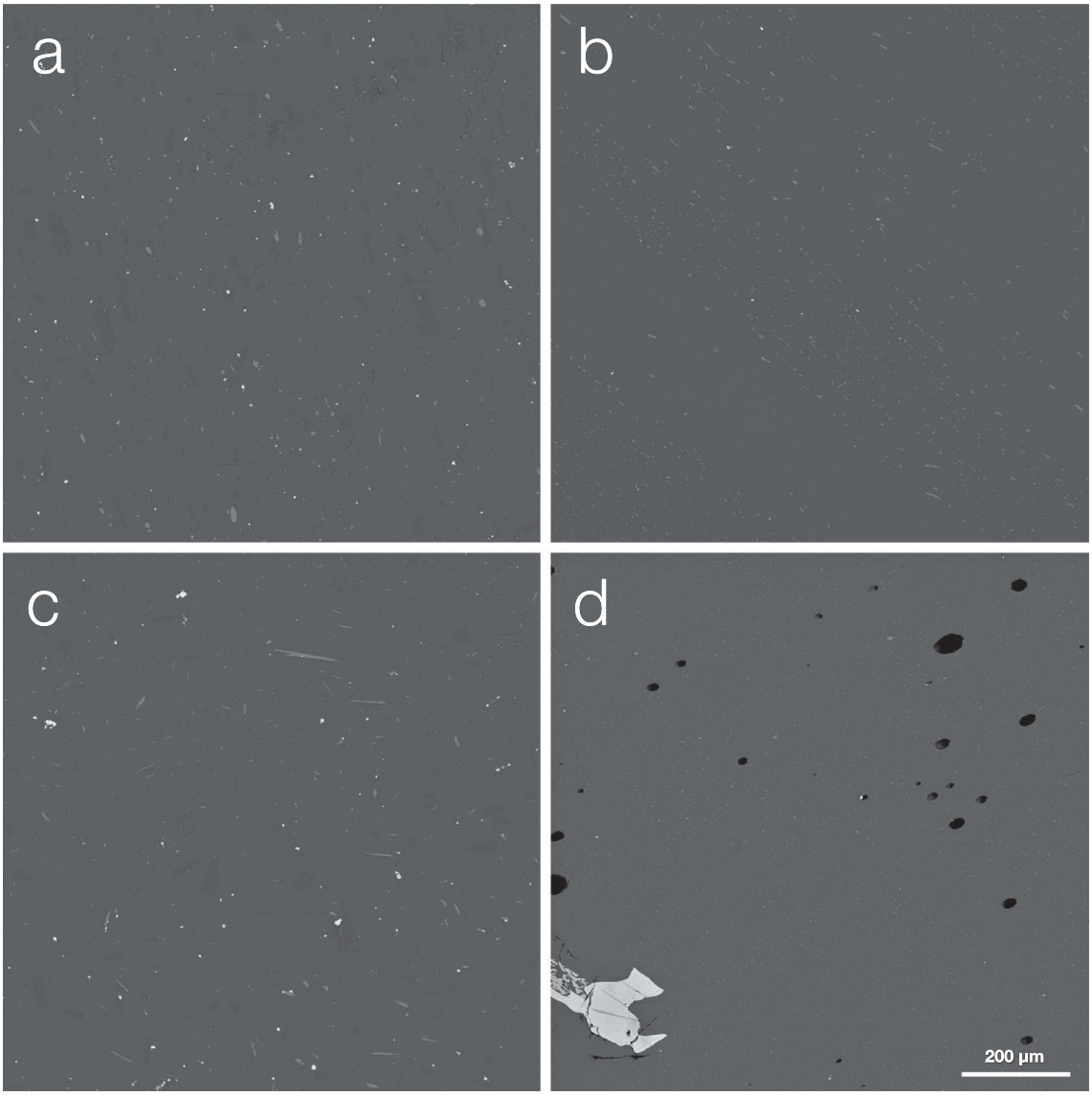

Fig. 4. Backscattered electron (BSE) microscopy of Glass Mountain obsidian reveals the presence of microscopic mineral inclusions that vary in grain size, amount, orientation, and composition. The brighter minerals have a higher mean atomic number (e.g., magnetite, Fe_3O_4) than the darker ones (e.g., feldspar, $KAlSi_3O_8$ – $NaAlSi_3O_8$ – $CaAl_2Si_2O_8$). The large inclusion in the lower left corner of (d) exhibits intergrowths of titanomagnetite ($Fe_{3-x}Ti_xO_4$) and ilmenite ($FeTiO_3$), indicative of a process known as oxy-exsolution, meaning that the obsidian was exposed to oxygen at a high temperature (i.e., to the atmosphere when it erupted). The black ovals in the same image are bubbles in the glass. The field of view for all four BSE images is 1 × 1 mm. Images collected by the author at the Electron Microprobe Laboratory, Department of Earth Sciences, University of Minnesota.

I streamlined this calibration set down to 20 specimens, occasionally supplemented by powdered USGS SRMs (e.g., AGV-1 andesite, BHVO-1 basalt, G-2 granite; Frahm et al., 2017b; Frahm and Tryon, 2018a). This calibration set allowed me to integrate the datasets from a series of pXRF instruments (including five Niton models) over a six-year span.

There were two main shortcomings of this original calibration set. First, there was only one set, which yielded logistical challenges for collaborations. Second, it did not include obsidians with atypical geochemical compositions, such as those created along the East African Rift system (Brown et al., 2013). Consequently, to source obsidian artifacts from Kenyan archaeological sites (Frahm et al., 2017a; Frahm and Tryon, 2018b), a new calibration set was necessary. This took the form of 27 matched specimens, generously contributed by Frank Brown and Harry Merrick, from the obsidian source database in Brown et al. (2013), which includes EMPA, NAA, and XRF measurements. These specimens were divided between two groups: primary calibration standards (n = 12) and secondary check standards (15). This two-fold approach – calibration with one collection of well-characterized obsidians and evaluation with another – became a model for the PYRO sets.

3. FAQs about the PYRO sets and their development

The following sections consider four frequently asked questions (FAQs) about the PYRO sets and choices made during their development: (1) What are (and aren't) the PYRO sets?; (2) Why not use SRMs?; (3) Is there an effect from microscopic minerals?; and (4) Are these sets useful for other micro- and non-destructive analytical techniques? Other topics, such as specimen preparation and data reduction in order to derive recommended values, are addressed later.

3.1. What are (and aren't) the PYRO sets?

X-rays measured by XRF instruments must be corrected for a series

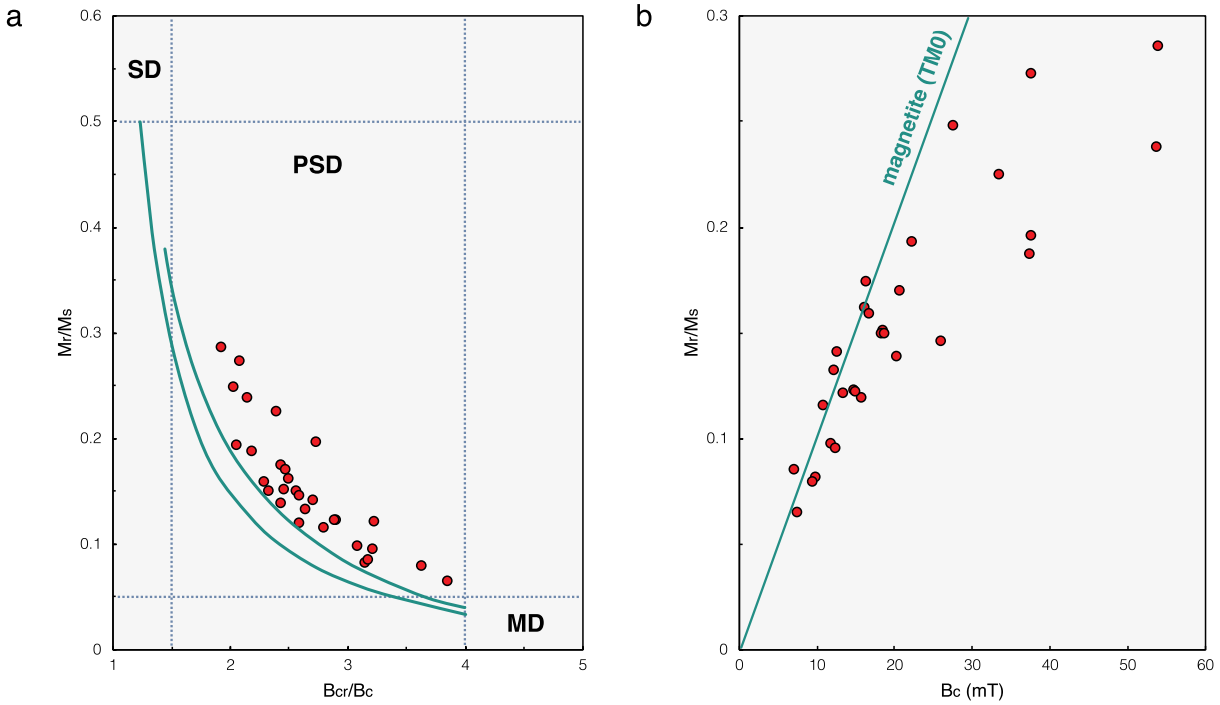

Fig. 5. (a) Day plot (B_{cr}/B_c vs. M_r/M_s) of Glass Mountain obsidian specimens with magnetic domain boundaries (dotted blue lines) and magnetite mixing curves (solid green lines) from Dunlop (2002). All specimens fall in the pseudo-single domain (PSD) region of the Day plot, not in the single domain (SD) or multi-domain (MD) regions. Magnetite grains exhibit PSD behavior in the 0.1–20 μm size range. (b) Glass Mountain obsidian data (B_c vs. M_r/M_s) with the compositional line for magnetite with zero Ti content (Fe_3O_4; TM0) is based on theoretical calculations by Wang and Van der Voo (2004). Measurements taken at the Institute for Rock Magnetism, University of Minnesota.

of phenomena that occur within a specimen (e.g., absorption, attenuation, secondary fluorescence) to convert the raw signals into quantitative elemental concentrations. There are different approaches to correction, including empirical methods in which the relationships between (1) measured intensities of X-ray peaks and (2) their corresponding concentrations are established via direct comparison to well-characterized standards, often dozens of them, that are similar in composition. This is the basis of the "obsidian" calibration that was devised by MURR in 2012 (Glascock and Ferguson, 2012) – based on an earlier set of obsidian specimens (Glascock, 2011:175) – and has been implemented, installed, and sold by Bruker Corporation with their Tracer instruments (Speakman, 2012). This MURR/Bruker obsidian calibration and its constituent obsidians have been described, even within the recent literature, in a range of ways: from "machine-specific quantification protocols" (Gaffney and Summerhayes, 2018) derived from "40 obsidian sources analyzed by multiple methods at MURR" (Fernández et al., 2017) to a "factory-installed calibration" (Liebmann, 2017) based on "40 international standards provided by MURR" (Reepmeyer et al., 2016). The obsidian compositions, as determined by NAA and ICP-MS, are reported in an unpublished "white paper" commissioned by Bruker AXS (Glascock and Ferguson, 2012), as are the analyses by pXRF (Speakman, 2012). Their sources are not specified in the white papers hosted on Bruker's website, nor are they published in a peer-reviewed journal or elsewhere. The obsidian sources are specified in an Excel file included among the documentation with a Bruker instrument, but will this information be widely available in a decade or two? Thus, there is a dearth of transparency and reproducibility, and this calibration is unique to one manufacturer, which is not healthy for our discipline. Furthermore, as noted in Section 2.2, researchers can become dependent on this calibration and overlook evaluating data accuracy or reproducibility.

Another approach to correction is fundamental parameters (FP), which uses a physics-based model to mathematically describe relationships between measured X-ray intensities and elemental concentrations, accounting for various parameters (e.g., attenuation coefficients for scattering and photoelectric absorption, X-ray fluorescent and absorption edge energies, Coster-Kronig transition probabilities, Rayleigh and Compton scattering cross sections). Based on inter-laboratory tests that led to commissioning the Copper CHARM Set, Heginbotham et al. (2011) found that the best-ranked XRF instruments used FP correction calibrated with standards, whereas instruments with empirical correction consistently ranked lower. Specifically, they point out:

> Through this study, one common characteristic of higher-performing laboratories has become clear: the use of fundamental parameters software calibrated with standards… For both major and minor elements, it is very clear that laboratories using fundamental parameters software calibrated with standards… performed consistently more accurately than laboratories using other methods… In comparison, all other factors examined in this study appear to be relatively poorly correlated with laboratory accuracy. The consensus of the group is that options should be explored for ways in which existing instruments that currently use empirical or standardless FP methods could be upgraded to use FP with standards… It seems apparent that, as a first step, movement toward the wider adoption of quantification methods utilizing FP with standards offers the possibility of significant improvements in inter-laboratory reproducibility. (185, 187)

Consequently, the PYRO sets are designed to be used as standards for FP-corrected data. Specifically, for pXRF instruments such as the Olympus Vanta or Thermo Niton, the instrument software allows the factory calibration to be adjusted using linear regression (i.e., values for the slope and intercept of the linear regression equation are input as "cal factors" or "user factors"). No claim is made here regarding the suitability (or lack thereof) of the PYRO sets for empirical approaches. This has simply not been systematically investigated at this point, nor has it been a priority given the demonstrated superiority of FP with

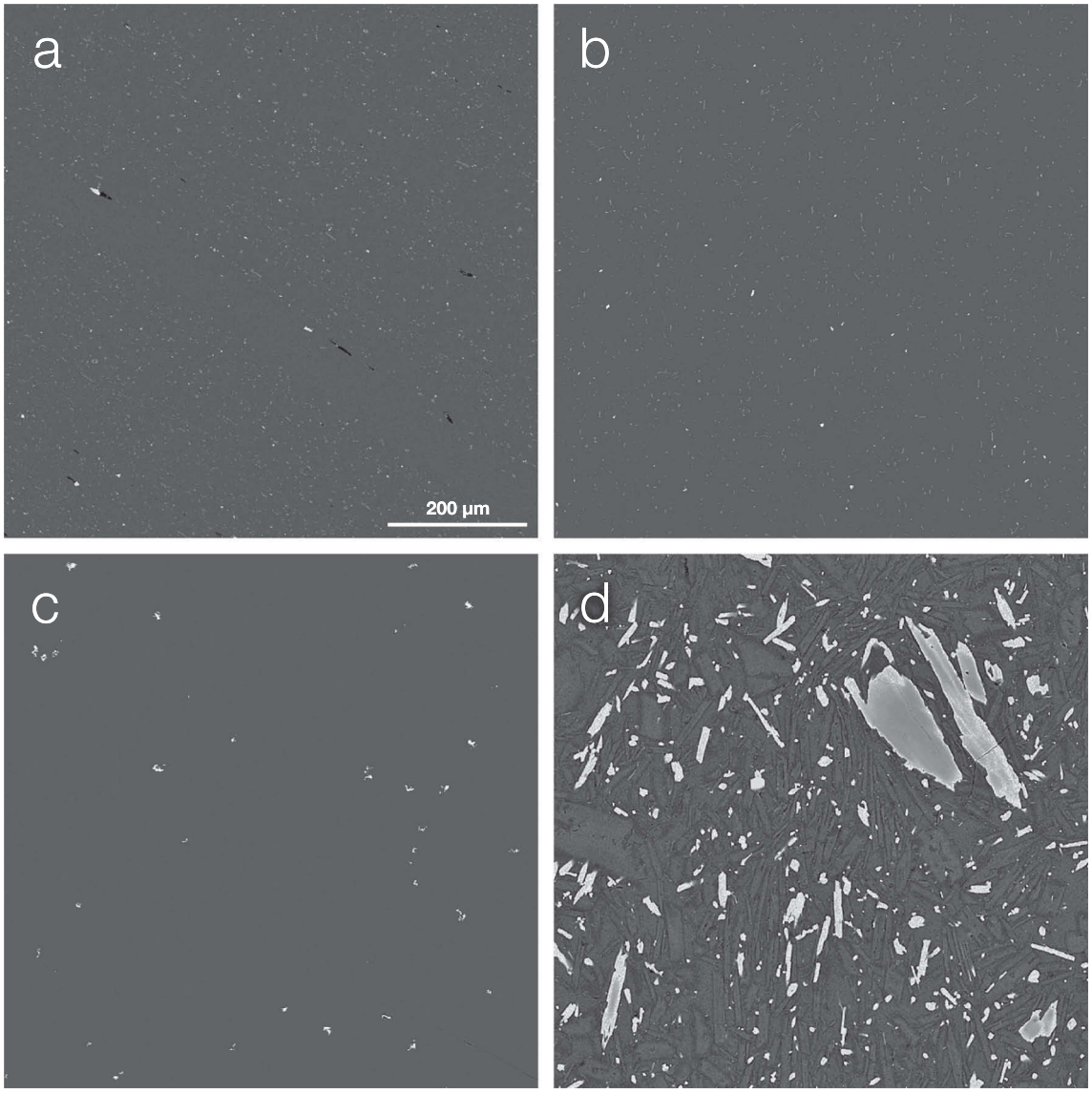

Fig. 6. Backscattered electron (BSE) microscopy of obsidian from (a) Aghvorik, (b) Meydan Dağ, and (c) Sarıkamış as well as (d) sanukite from Japan. Brighter minerals have a higher mean atomic number than darker ones. The sanukite image reveals the presence of two microscopic minerals – orthopyroxene (magnesium-iron silicate) and plagioclase (sodium-calcium aluminosilicate) – within a glassy groundmass. The field of view for all four of these images is 0.8 × 0.8 mm. Images collected by the author at the Electron Microprobe Laboratory, University of Minnesota.

standards (Heginbotham et al., 2011; Frahm, 2017).

The 35 specimens in the PYRO sets are intended to be used in two steps: (1) 20 specimens to derive the calibration equations via linear regression and (2) 15 independent specimens to evaluate the measurements that result from applying these calibration equations, as discussed in Section 6. This is a sufficient number of calibration specimens given that FP tends to use fewer standards than empirical approaches. Specifically, Heginbotham et al. (2011:186) reported:

> The data also suggest that increasing the number of standards used for quantification does not necessarily improve the accuracy of results. In fact, the vast majority of the best performing laboratories used 20 standards or fewer, and most used fewer than 10. Even among the labs using empirical methods, increasing the number of standards was not a guarantee of improved results.

It must also be stressed that the PYRO specimens are not "international standards" (sensu Shackley, 2011a:13) or SRMs. One of the specimens – Check-01 from Glass Mountain, California, USA – is close, though, because it is the raw material for the RGM-1 and -2 powdered SRMs from the USGS. Instead, the intent with developing the PYRO sets was to organize an "open-source" series of specimens, for which all available data (e.g., source names, GPS coordinates, previous analyses) are published and which could be freely borrowed, updated, and even duplicated by others.

3.2. Why not use SRMs?

As discussed in Section 2.1, several EDXRF laboratories that specialize in sourcing obsidian artifacts routinely use SRMs – in the form of finely powdered rocks – for calibration and/or accuracy checks. Various studies mention use of "international standards" (e.g., Green, 1998; Shackley, 1998, 2011a; McCoy and Carpenter, 2014; Newlander et al., 2015; Nishiaki et al., 2019); however, in each case, the SRMs are actually products of national (e.g., USGS, Geological Survey of Japan) rather than international (e.g., International Standards Organization) bodies. Hence, SRMs such as USGS RGM-1 and NIST SRM #278 meet the criteria of national standards, not international ones (Beckhoff et al., 2006:400). More importantly, powdered SRMs are not necessarily

Table 1
Geological origins of the PYRO calibration and evaluation ("check") sets.

PYRO Calibration Set

Label	Country	Source name	More info	GPS coordinates	Alternate names
Cal-01	Armenia	Aghvorik	Shirak Province	41.08° N, 43.71° E	Ashotsk, Yeni-Ël, Sizavet, Kechut
Cal-02		Gutansar	Kotayak Province	40.37° N, 44.68° E	Djraber/Dzhraber
Cal-03		Hatis trachyte	Kotayak Province	40.27° N, 44.72° E	
Cal-04		Satanakar	Syunik Province	39.82° N, 45.81° E	Mets Satanakar, Syunik 2
Cal-05	Georgia	Chikiani 1	Javakheti Region	41.48° N, 43.87° E	Paravani Lake, Kojun Dağ
Cal-06	Turkey	Meydan Dağ	Van Province	39.20° N, 43.27° E	Gürgürbaba Tepe
Cal-07		Nemrut Dağ, Cluster 6	Bitlis Province	38.60° N, 42.26° E	Nemrut Dağ F
Cal-08		Sarıkamış 1	Kars Province	40.27° N, 42.72° E	Sarıkamış North
Cal-09	Ethiopia	Balchit	Upper Awash	8.75° N, 38.64° E	Freo Amante Gurange
Cal-10		Bede Gebabe, Debre Zeyt	Oromia Region	8.67° N, 38.95° E	
Cal-11		Fantale	Oromia Region	8.97° N, 39.93° E	Mount Fentale
Cal-12	Kenya	Mt. Eburru	Naivasha-Nakuru	0.64° S, 36.25° E	Eburu GsJj50
Cal-13		Mundui	Lake Naivasha	0.78° S, 36.27° E	Sonanchi
Cal-14	Japan	Kanayama sanukite	Kagawa	34.31° N, 133.87° E	G-1
Cal-15		Suwa-Hoshigatou	Nagano	36.12° N, 138.15° E	
Cal-16		Tokachi	Hokkaido	43.10° N, 143.41° E	Tokachi-Mitsumata
Cal-17	Guatemala	El Chayal	Guatemala Dept.	14.71° N, 90.35° W	
Cal-18	Mexico	La Joya	Jalisco Province	20.84° N, 103.96° W	
Cal-19		Sierra de Pachuca	Hidago Province	20.10° N, 98.42° W	Pachuca, Sierra de las Navajas
Cal-20	Peru	Lisahuacho	Chalhuanca District	14.37° S, 73.36° W	Andahuaylas B

PYRO Check Set

Label	U.S. state	source name	More info	GPS coordinates	Alternate names
Check-01	California	Glass Mountain	Siskiyou County	41.59° N, 121.55° W	RGM, Medicine Lake Highlands
Check-02		Bodie Hills	Mono County	38.28° N, 119.11° W	Rock Springs Canyon Rhyolite
Check-03		Buck Mountain	Modoc County	41.72° N, 120.28° W	Davis Creek, numerous others
Check-04		Mt. Konocti	Lake County	38.97° N, 122.77° W	Thurston Creek Rhyolite
Check-05		Panum Crater	Mono County	37.92° N, 119.04° W	Mono Craters, Panum Dome
Check-06		Rainbow Mines	Modoc County	41.82° N, 120.30° W	Lassen Creek, California Electric Blue
Check-07		Sawmill Ridge, Casa Diablo	Mono County	37.64° N, 118.89° W	
Check-08	Nevada	Massacre Lake/Guano Valley	Washoe County	41.82° N, 119.26° W	Virgin Valley, numerous others
Check-09	Oregon	Glass ButtesAlpha	Lake County	43.57° N, 120.05° W	Glass Buttes A
Check-10		Glass ButtesBeta	Lake County	43.53° N, 120.08° W	Glass Buttes B
Check-11		Glass ButtesDelta	Lake County	43.54° N, 119.91° W	Glass Buttes D, Sand Flat
Check-12		Glass ButtesEpsilon	Lake County	43.56° N, 119.93° W	Glass Buttes E, Potato Hills
Check-13		Round Top Butte	Lake County	43.50° N, 119.96° W	Glass ButtesIota
Check-14		Wagontire	Harney County	43.36° N, 119.73° W	Egli Ridge, Egli Waterhole
Check-15	Utah	Black Rock Area	Millard County	38.74° N, 112.65° W	Coyote Hills, South Twin Peak

ideal and have their own issues that must be acknowledged (even if one ultimately opts to use them).

First, there is a long-running debate in the obsidian sourcing community – most of it outside the literature (e.g., at the bar after conference sessions), but it is mentioned by Shackley et al. (2016) – about the suitability of using powdered standards for calibration when analyzing solid obsidians. A key issue, at least theoretically, lies in differences – chemical and physical – between the standards and specimens of interest, collectively known as "matrix effects." Ideally, for quantitative analyses, these differences are best minimized in order to attain the highest accuracy, but some compromises are more acceptable than others. The X-rays will interact, to greatly varying extents, with whatever matter is placed in front of the instrument. Powdered standards, even when compressed, are likely to contain at least a little air, which includes gases (e.g., nitrogen, oxygen) and water vapor, between the particles. Pressed pellets for XRF often necessitate a binding medium (e.g., wax, cellulose) that, in effect, dilutes the material of interest, meaning that corrections are needed. Similarly, creating a fused bead for XRF involves adding the powdered material to a flux (e.g., lithium tetraborate), which yields a similar dilution effect. In each case, there is extra mass that is not the substance of interest, and the addition of these light elements introduces other effects (e.g., higher Compton scattering of X-rays and lower Rayleigh scattering, two phenomena that XRF instrument software often uses as a means to estimate the mass present; Marguí and van Grieken, 2013). Thus, one expects an analysis of powdered obsidian to yield lower trace-element values than a solid specimen would. Conversely, using powders to calibrate could result in higher values for a solid specimen. The debate is whether these effects tend to have any practical – or even measurable – consequences.

Regarding this debate, Shackley et al. (2016) hold that the use of powdered standards yields no problems for sourcing obsidian artifacts. To support this claim, Shackley et al. (2016) analyzed a pressed pellet of RMG-1 powder (99 analyses) and a flake from the original 135-kg boulder of Glass Mountain obsidian (12 analyses). This pellet contained not only air molecules trapped between the fine obsidian particles but also a "borate mix" (presumably either boric acid or a similar compound) used as a binder, all of which would have interacted with the X-rays, even if the corresponding light elements were not measured. Shackley et al. (2016) state that their results demonstrate that there is no issue: "As one can see, the variability is within 1% or less in most cases" (64). That, though, is not the case. Given the variability of microscopic magnetite (Fe_3O_4) crystals in obsidians, Fe would be anticipated to vary. Other elements, however, appear 3-6% higher in the flake, consistent with expectations (the increase is too small to be measured at very low concentrations; e.g., Nb at 9 ppm). For example, Zr was measured at 219 ± 2 ppm in the pellet ($n = 99$) and at 230 ± 4 ppm in the flake ($n = 12$), and a Student's *t*-test shows that the difference is statistically significant (p-value < 0.0001). The practical implications, on the other hand, seem minor. That is, both sides of the debate are, in a sense, correct: there *is* an effect, but its practical

Table 2
PYRO calibration specimens from Armenia.

Technique	Laboratory	Specimen/Publication	Mn (ppm)			Fe (ppm)			Zn (ppm)			Rb (ppm)			Sr (ppm)			Y (ppm)			Zr (ppm)			Nb (ppm)		
PYRO Calibration-01: Aghvorik, Armenia																										
		Recommended values	*472*	±	*24*	*12,240*	±	*690*	*48*	±	*4*	*98*	±	*5*	*198*	±	*9*	*15*	±	*6*	*236*	±	*15*	*18*	±	*4*
EDXRF	MURR Archaeometry Lab	matched specimen							54			95						12			229			14		
		Matched specimen	462			12,410						108			191			17			250			22		
		Frahm, unpublished	443	±	62				52	±	1	93	±	3				10	±	1	229	±	7	14	±	1
	NWR Obsidian Studies Lab	Matched specimen										94			204			24			241			21		
EMPA	University of Minnesota	Frahm, 2010	449	±	39	11,285	±	1830													208	±	8			
ICP-MS	IRAMAT, CNRS, Orléans	Chataigner and Gratuze, 2014				11,766	±	756				94	±	5				12	±	2				18	±	1
NAA	MURR Archaeometry Lab	matched specimen	491			12,115			47			99									250					
		matched specimen	498			12,101			44			98									249					
		Frahm, unpublished	490	±	9	12,095	±	64	49	±	2	98	±	1							222	±	11			
	Smithsonian Institution	Blackman et al., 1998				12,500	±	210	43	±	1										244	±	15			
	University of Pavia	Oddone et al., 2000				13,680	±	60				102	±	1												
PYRO Calibration-02: Gutansar, Armenia																										
		Recommended values	*641*	±	*23*	*8250*	±	*173*	*44*	±	*4*	*140*	±	*5*	*129*	±	*6*	*22*	±	*7*	*171*	±	*13*	*37*	±	*3*
EDXRF	MURR Archaeometry Lab	matched specimen							48	±	6	145	±	1	136	±	6				174	±	3			
		matched specimen	666			8477						149			122			23			171			40		
		Frahm, unpublished							50	±	3	144	±	3	137	±	6	11	±	2	182	±	5			
		Glascock and Amirkhiz, 2017							48			142						13			188			34		
	NWR Obsidian Studies Lab	matched specimen										135			124			28			162					
EMPA	University of Minnesota	matched specimen	597	±	13	8457	±	74													148	±	6			
		Frahm, 2010				8104	±	378													146	±	9			
ICP-MS	IRAMAT, CNRS, Orléans	Chataigner and Gratuze, 2014				8048	±	943	41	±	6	137	±	9				15	±	2				34	±	2
multiple	multiple laboratories	MacDonald et al., 1992				8550						140	±	2	135			32			157			43		
NAA	MURR Archaeometry Lab	matched specimen	646	±	11	8120	±	53	41	±	1	140	±	1	126	±	6									
		matched specimen	646			8175			42			139														
		Boulanger et al., 2012	641	±	10	8130	±	200	42	±	2	139	±	2							175	±	40			
		Frahm, unpublished	634	±	5	8187	±	271	42	±	2	140	±	1	130	±	14									
	Smithsonian Institution	Blackman et al., 1998				8170	±	190	39	±	3	153	±	3							191	±	17			
	University of Pavia	Oddone et al., 2000	674	±	85				50	±	4	144	±	10							181	±	15			
WDXRF	CNR, Rome, Italy	Francaviglia, 1994	616			8330	±	160				133	±	4	138	±	4	26	±	2	170	±	6			
	IGOD, RAS, Moscow	Lebedev et al., 2013	620						45			136			124			25			176			38		
	University of Freiburg	Keller and Seifried, 1990	667	±	44							135	±	2	126	±	1	24	±	1	170	±	1	35	±	1
		Keller et al., 1996	642	±	38				40	±	2	136	±	2	126	±	2	24	±	1	169	±	5	35	±	1
PYRO Calibration-03: Hatis trachyte, Armenia																										
		Recommended values	*623*			*19,940*	±	*700*	*54*			*70*			*443*	±	*24*	*19*	±	*7*	*243*	±	*12*	*27*		
EDXRF	MURR Archaeometry Lab	matched specimen				19,444						70			421			14			233			27		
	NWR Obsidian Studies Lab	matched specimen													468			24			241			27		
NAA	MURR Archaeometry Lab	matched specimen	623			20,434			54			70			441						256					
PYRO Calibration-04: Satanakar, Armenia																										
		Recommended values	*522*	±	*20*	*4580*	±	*180*	*34*	±	*2*	*192*	±	*2*	*9*	±	*2*	*8*	±	*4*	*88*	±	*10*	*36*	±	*3*
EDXRF	MURR Archaeometry Lab	matched specimen				4769						192			9			3			102			39		
		Frahm, unpublished							34			193			9						92					
	NWR Obsidian Studies Lab	matched specimen													11			12			83					
EMPA	University of Minnesota	Frahm, 2010																			78	±	24			
ICP-MS	IRAMAT, CNRS, Orléans	Chataigner and Gratuze, 2014	510			4696	±	182				193	±	1	6	±	1	7	±	1				35	±	1
NAA	MURR Archaeometry Lab	matched specimen	511			4413			35			189														
		Frahm, unpublished	535	±	23	4333	±	143	34	±	1	195	±	5												
	Oregon State Reactor	Cherry et al., 2010	550	±	39	4530	±	170	36	±	1															
	Smithsonian Institution	Blackman et al., 1998							35			192														
WDXRF	University of Freiburg	Keller et al., 1996	503	±	45	4738	±	300	29	±	4							10	±	1	83	±	5	34	±	1

Table 3
PYRO calibration specimen from Georgia.

Technique	Laboratory	Specimen/publication	Mn (ppm)			Fe (ppm)			Zn (ppm)			Rb (ppm)			Sr (ppm)			Y (ppm)			Zr (ppm)			Nb (ppm)		
PYRO Calibration-05: Chikiani 1, Georgia																										
		Recommended values	*482*	±	*40*	*5000*	±	*280*	*41*	±	*4*	*130*	±	*7*	*75*	±	*12*	*14*	±	*4*	*81*	±	*4*	*19*	±	*2*
EDXRF	MURR Archaeometry Lab	Matched specimen							37	±	1	133	±	3	83	±	3	9	±	2	86	±	1	18	±	1
		Matched specimen	575						37			144			72			15			79			23		
	NWR Obsidian Studies Lab	Matched specimen										120			72			13			75			16		
EMPA	University of Minnesota	Matched specimen	450	±	34	4440	±	770													86	±	2			
ICP-AES/MS	IEMS, Plouzané, France	Le Bourdonnec et al., 2012	465			5292	±	214	42	±	2	127	±	2	76	±	5	15			79	±	6	22	±	3
ICP-MS	IRAMAT, CNRS, Orléans, France	Chataigner and Gratuze, 2014				4922	±	511	48	±	12	127	±	6	55	±	6	9	±	1				18	±	2
	IRAMAT, CNRS, Orléans, France	Biagi et al., 2017	462	±	9	5018	±	471	48	±	5	129	±	6	58	±	4	10	±	1				20	±	1
NAA	MURR Archaeometry Lab	matched specimen	491	±	1	5174	±	108	44	±	1	134	±	1	90	±	9				83	±	4			
	MURR Archaeometry Lab	Matched specimen	484			4885			41			131			75											
	Smithsonian Institution	Blackman et al., 1998							37	±	1	139	±	6												
PIXE	C2RMF, Paris, France	Le Bourdonnec et al., 2012				4952	±	223	39	±	1	129	±	3				14	±	2	81	±	6	20	±	4
WDXRF	Institute of Geology, Moscow	Lebedev et al., 2008	465									124			90			21						20		
	University of Freiburg	Keller et al., 1996	462			5285	±	247	37			120	±	6				16	±	1				17	±	2

significance is questionable.

Second, powdered SRMs pose practical challenges for portable instruments and conducting analyses outside a laboratory environment. Pressed pellets are fragile, and while XRF sample cups are sufficiently robust for repeated use in the lab, they do not travel well. The X-ray-transparent film over the front of a sample cup is thin (sometimes only 0.004 mm thick), so even a small puncture in the film could mean the loss of $440 worth of powdered obsidian (i.e., the cost of NIST SRM #278). Traveling with cups of white powder is also usually regarded with suspicion by airport security and is likely to result in additional screening or disposal (Marsh and Park, 2018).

Third, the geological origins of SRMs are not always known as well as one might expect. For example, the obsidian for NIST SRM #278 "was obtained from Clear Lake, Newberry Crater, Oregon" (Reed, 1992). The problem is that Newberry Caldera does not have a "Clear Lake" – its two caldera lakes are named Paulina Lake and East Lake. Furthermore, Newberry Caldera has several obsidian flows, including Big Obsidian Flow, East Lake Flows (West and East), and East Lake Fissure, among others. Similarly, Smithsonian VG-568 is obsidian from "Yellowstone National Park" (Jarosewich et al., 1980). There are, however, multiple obsidian sources within the park. Obsidian Cliff is the best known source, but there are also the Cougar Creek, Park Point, and Tanker Curve obsidians, among others (Park, 2010). These are not insurmountable challenges, but such uncertainties are a product of SRM specimen collection during the 1970s, before the nature of obsidian sources and their differentiation were better understood (e.g., Hughes, 1984, 1988, 1989; Shackley, 1988).

3.3. Is there an effect from microscopic minerals?

USGS standard RGM-1 and its replacement RGM-2 originate from Glass Mountain, part of the Medicine Lake volcanic complex, in northern California. Based on radiocarbon dating of trees caught in the lava as well as paleomagnetism, this obsidian formed only ~900 years ago (Donnelly-Nolan et al., 1990), making it a focus of studies into rhyolitic volcanism (e.g., Eichelberger, 1975, 1981; Grove et al., 1997). The original and replacement standards somewhat differ in the particle sizes to which they were finely powdered. RGM-1 consists almost entirely (> 97% by mass) of particles < 75 μm in diameter with only trace amounts > 150 μm (Tatlock et al., 1976), whereas RGM-2 has particle sizes rather evenly distributed between 0.4 and 250 μm (Wilson, 2009). Otherwise, the RGM-2 material was collected from roughly the same location as the original RGM-1 block (Wilson, 2009), and these two standards are indistinguishable in terms of their chemical compositions.

The original USGS description of RGM-1 states that, like nearly all obsidians, Glass Mountain obsidian is not entirely free of mineral inclusions. Specifically, Tatlock et al. (1976) report that light and dark bands within this obsidian "seem to result from a concentration of microlites, too small to polarize light appreciably… Rare opaque crystallite, probably magnetite, may be seen in thin section" (12). Thirty specimens of Glass Mountain obsidian, collected by the Glass Mountain Archaeological Project to recognize any potential geochemical variability, were examined by EMPA in the University of Minnesota's Electron Microprobe Laboratory and by rock magnetic analyses at the University of Minnesota's Institute for Rock Magnetism. EMPA revealed microscopic mineral inclusions that vary in their size, amount, composition, and orientation (Fig. 4). Consistent with Tatlock et al. (1976), tiny needle-shaped microlites, most likely feldspars, are abundant within the obsidian, as are iron oxides. Magnetic analyses (Fig. 5) confirmed that the iron oxides are primarily magnetite, which, as a result of their pseudo-single domain (PSD) locations on a Day plot (Fig. 5a), span a size range of 0.1 – 20 μm. More information can be found in Frahm and Feinberg (2013) and in Frahm et al. (2014b). Despite variations in the mineral inclusions of Glass Mountain obsidian, EDXRF at the Geoarchaeological XRF Lab revealed "remarkable

Table 4
PYRO calibration specimens from Turkey.

Technique	Laboratory	Specimen/Publication	Mn (ppm)	Fe (ppm)	Zn (ppm)	Rb (ppm)	Sr (ppm)	Y (ppm)	Zr (ppm)	Nb (ppm)
PYRO Calibration-06: Meydan Dağ, Turkey										
		Recommended values	*519 ± 27*	*9520 ± 310*	*74 ± 8*	*200 ± 5*	*18 ± 3*	*52 ± 5*	*286 ± 15*	*32 ± 4*
EDXRF	JIAA, Kaman, Turkey	Kobayashi and Mochizuki, 2007				203 ± 9	13 ± 2	54 ± 4	284 ± 7	
	MURR Archaeometry Lab	Matched specimen	557	9470		202	20	53		31
		Matched specimen	492		65		20	49	280	30
		Frahm, unpublished			65 ± 3		17 ± 3	50 ± 3	274 ± 15	29 ± 4
	NWR Obsidian Studies Lab	Matched specimen				195	26	59	278	34
EMPA	University of Minnesota	Matched specimen	490						289	
ICP-MS	IRAMAT, CNRS, Orléans, France	Chataigner and Gratuze, 2014	477 ± 31	9564 ± 726	76 ± 13		12 ± 3	43 ± 11		32 ± 4
		Khalidi et al., 2009	476		87		16	58	305	36
		Khalidi et al., 2016	520 ± 12	9792 ± 700	85 ± 10	195 ± 8	15 ± 3			32 ± 2
	MURR Archaeometry Lab	Glascock and Ferguson, 2012	514	9072	68		16	50	269	31
	UBO, Brest, France	Poupeau et al., 2010	515 ± 16		84 ± 1	204 ± 10	17 ± 2	60 ± 4	292 ± 17	26 ± 1
NAA	MURR Archaeometry Lab	Matched specimen	559	9477	73		24		295	
		Boulanger et al., 2012	544 ± 10	9515 ± 680	76 ± 3	199 ± 2			299 ± 13	
		Glascock and Ferguson, 2012	538	9349	74	196			299	
PIXE	C2RMF, Paris, France	Poupeau et al., 2010			68 ± 1	206 ± 1	21 ± 2	50 ± 1	261 ± 1	37 ± 1
WDXRF	University of Freiburg	Keller and Seifried, 1990	542	9930			21	51		30
PYRO Calibration-07: Nemrut Dağ (Cluster 6), Turkey										
		Recommended values	*1380 ± 18*	*46,680 ± 3860*	*237 ± 10*	*233 ± 8*	*2 ± 1*	*145*	*1308 ± 82*	*76 ± 9*
EDXRF	MURR Archaeometry Lab	Matched specimen		39,119	235	223				73
		Matched specimen		44,769	226	238	1	145	1296	71
		Frahm, unpublished		45,516 ± 22	255 ± 22	233 ± 19		145 ± 17		71 ± 8
EMPA	University of Minnesota	Matched specimen		49,538 ± 226					1413 ± 23	
		Frahm, 2010		50,052 ± 614					1386 ± 27	
NAA	MURR Archaeometry Lab	Matched specimen	1379	45,495	227	225			1261	
		Matched specimen	1355	46,591	230	229			1152	
		Frahm, unpublished	1390 ± 35	47,862 ± 879	243 ± 4	237 ± 5			1304 ± 15	
PIXE	C2RMF, Paris, France	Poupeau et al., 2010		44,517 ± 445	242 ± 1	249 ± 5			1364 ± 25	
WDXRF	University of Freiburg	Keller and Seifried, 1990	1394	53363		230	3		1287	90
PYRO Calibration-08: Sarıkamış 1, Turkey										
		Recommended values	325 ± 14	5724 ± 337	31 ± 2	130 ± 8	22 ± 4	21 ± 4	109 ± 24	14 ± 1
EDXRF	Inst. of Anatolian Archaeo.	Kobayashi and Mochizuki, 2007				126 ± 5		24 ± 3	93 ± 6	
	MURR Archaeometry Lab	Matched specimen		6054	29	126	27	22	112	16
EMPA	University of Minnesota	Matched specimen	315 ± 18	5885 ± 98					117 ± 7	
	University of Minnesota	Frahm, 2010	315 ± 25	5966 ± 24					112 ± 5	
ICP-MS	MURR Archaeometry Lab	Glascock and Ferguson, 2012	327	5174	29	124	21	21	91	13
	IRAMAT, CNRS, Orléans	Chataigner and Gratuze, 2014				135 ± 16	17 ± 2	19 ± 1	106 ± 6	15 ± 1
		Chataigner et al., 2014	323 ± 14		33 ± 5	119 ± 5	18 ± 2	17 ± 1	76 ± 11	13 ± 1
		Khalidi et al., 2016	333 ± 6	5802 ± 210	33 ± 1	127 ± 2	18 ± 3	16 ± 2	75 ± 18	13 ± 1
NAA	MURR Archaeometry Lab	Glascock and Ferguson, 2012	351	5465	30	131	26		141	
	University of Pavia, Italy	Oddone et al., 1997				146 ± 6	23 ± 1		138 ± 3	14 ± 1
WDXRF	University of Freiburg	Keller and Seifried, 1990	310 ± 110			133 ± 9	23 ± 4	26 ± 3	137 ± 3	12 ± 2

uniformity" in the composition of the specimens (Dillian, 2002:249). That is, variability in microscopic texture had little, if any, effect on elemental values.

3.4. Are these sets useful for other techniques?

It should be emphasized that the past decade has also seen the continued development and application of additional non- and micro-destructive techniques for obsidian sourcing. Two of these analytical techniques use electron beams: EMPA (e.g., Frahm, 2012; Frahm et al., 2016; Blegen, 2017; built on earlier studies, e.g., Merrick and Brown, 1984; Weisler and Clague, 1998; Tykot, 1996, 1997) and scanning electron microscopy together with energy-dispersive X-ray spectrometry (SEM-EDS; e.g., Le Bourdonnec et al., 2010, 2015; Mulazzani et al., 2010; Poupeau et al., 2010; built on earlier studies, e.g., Biró and Pozsgai, 1984; Biró et al., 1986; Keller and Seifried, 1990). Other techniques use laser ablation, notably laser-induced breakdown spectroscopy (LIBS; e.g., Harmon et al., 2018, Syvilay et al., 2019) and laser-ablation inductively coupled mass spectrometry (e.g., LA-ICP-MS; Chataigner and Gratuze, 2014; Lee and Kim, 2015; Khalidi et al., 2016). Several researchers have also combined the electron- and laser-based approaches for obsidian artifact sourcing (e.g., Barca et al., 2012; Brown et al., 2013; Foresta Martin et al., 2017; Orange et al., 2017).

The PYRO sets, which include obsidians and other igneous rocks in their natural forms, were principally intended for pXRF/EDXRF calibration and evaluation, and might not be as well suited to micro-analytical techniques. As of this writing, the newer pXRF instruments from Olympus, Thermo Scientific, and Bruker all have nominal ~8 mm beams (~50 mm^2) with the option to use ~3 mm (~7 mm^2) collimated beams. The analytical areas of electron beam techniques are considerably smaller. For example, with EMPA, I analyzed obsidian using an electron beam diameter of 30 μm (0.03 mm), corresponding to an analytical area of ~700 μm^2 (~0.0007 mm^2; Frahm, 2012). Similarly, with SEM-EDS, Poupeau et al. (2010) measured 200–500 μm^2 on

Table 5
PYRO calibration specimens from Ethiopia.

Technique	Laboratory	Specimen/Publication	Mn (ppm)	Fe (ppm)	Zn (ppm)	Rb (ppm)	Sr (ppm)	Y (ppm)	Zr (ppm)	Nb (ppm)
PYRO Calibration-09: Balchit, Ethiopia										
		Recommended values	*311 ± 1*	*8625 ± 130*	*40 ± 3*	*179 ± 5*	*75 ± 3*	*30 ± 3*	*211 ± 7*	*53 ± 5*
EDXRF	Geoarchaeological XRF Lab	Negash et al., 2006			44 ± 5	185 ± 5	78 ± 4	27 ± 3	201 ± 5	57 ± 7
	MURR Archaeometry Lab	Matched specimen					75	30	217	54
	NWR Obsidian Studies Lab	Matched specimen				176	79	34	207	48
ICP-MS	LGCA, Grenoble, France	Poupeau et al., 2004			37 ± 1	180 ± 1	71 ± 1	27	219	49 ± 1
NAA	MURR Archaeometry Lab	Matched specimen	312	8716	40	175				
WDXRF	CNR ITABC, Rome, Italy	Francaviglia, 1990	310	8533			73 ± 4		209 ± 4	59 ± 2
PYRO Calibration-10: Bede Gebabe, Debre Zeyt, Ethiopia										
		Recommended values	*1356*	*41,200*	*279 ± 19*	*207*	*2*	*150*	*1282 ± 134*	*230 ± 4*
EDXRF	MURR Archaeometry Lab	matched specimen			292		2	150	1346	232
	NWR Obsidian Studies Lab	matched specimen							1372	227
NAA	MURR Archaeometry Lab	matched specimen	1356	41,202	265	207			1128	
PYRO Calibration-11: Fantale, Ethiopia										
		Recommended values	*2638*	*58,130 ± 620*	*368 ± 31*	*130 ± 6*	*12 ± 6*	*153*	*1075 ± 65*	*185 ± 14*
EDXRF	Geoarchaeological XRF Lab	Negash et al., 2007			379 ± 25	130 ± 6	23 ± 3	153 ± 5	1015 ± 39	185 ± 7
	MURR Archaeometry Lab	matched specimen			391	142	10	153	1124	187
	NWR Obsidian Studies Lab	matched specimen				126			1188	201
EMPA	University of Utah	Negash et al., 2007		58,703 ± 839						
NAA	MURR Archaeometry Lab	matched specimen	2638	58,209	333	130			1033	
WDXRF	CNR ITABC, Rome, Italy	Francaviglia, 1990				134 ± 2	7 ± 2			196 ± 3
	University of Leeds	Gibson, 1970				130 ± 3	8 ± 3		1103 ± 17	163 ± 1
		Gibson, 1972		57,470		120	12		1050	
		Weaver et al., 1972				130			1014	177

Table 6
PYRO calibration specimens from Kenya.

Technique	Laboratory	Specimen/Publication	Mn (ppm)			Fe (ppm)			Zn (ppm)			Rb (ppm)			Sr (ppm)			Y (ppm)			Zr (ppm)			Nb (ppm)		
PYRO Calibration-12: Mt. Eburru, Kenya																										
		Recommended values	*1990*	±	*40*	*59,900*	±	*1500*	*436*	±	*35*	*204*	±	*13*	7	±	2	*235*	±	*58*	*1517*	±	*64*	*335*	±	*39*
EMPA	University of Utah	Brown et al., 2013	2020	±	61	58,878	±	888																		
ICP-MS	University of Utah	Brown et al., 2013							439	±	25				9	±	1	203	±	18	1468	±	129	287	±	18
NAA	MURR Archaeometry Lab	Coleman, 2010							400	±	42	217	±	10							1493	±	33			
WDXRF	University of Leicester	Weaver et al., 1972				61,000									5									377		
	University of Reading	MacDonald and Bailey, 1975							469	±	15	213	±	5				301	±	9				374	±	10
	University of Utah	Brown et al., 2013										195	±	6	7	±	2	200	±	5				322	±	5
		Merrick et al., 1994	1959									190			5						1589			316		
PYRO Calibration-13: Mundui, Kenya																										
		Recommended values	*298*	±	*35*	*13,280*	±	*220*	*114*	±	*7*	*277*	±	*2*	*5*	±	*1*	*86*	±	*1*	*445*	±	*27*	*192*	±	*1*
EMPA	University of Utah	Brown et al., 2013																								
ICP-MS	University of Utah	Brown et al., 2013													5	±	1									
NAA	MURR Archaeometry Lab	Brooks et al., 2018	325	±	58				120	±	17	278	±	6							447	±	11			
		Coleman, 2010	309	±	15				120	±	18	279	±	8							452	±	10			
WDXRF	University of Helsinki	Seitsonen et al., 2012	310			13,430												85			408					
	University of Utah	Brown et al., 2013							109	±	6	274	±	6	5	±	3	86	±	2	474	±	11	191	±	3
		Merrick and Brown, 1984	247	±	15	13,125	±	247	107	±	1	277	±	1				88	±	1				192	±	1

obsidian specimens. The analytical areas for laser ablation techniques are also small. Harmon et al. (2018) ablated a spot ~100 μm in diameter (~0.0001 mm^2) with LIBS, and the ablation spots of Chataigner and Gratuze (2014) were ~60–100 μm in diameter with LA-ICP-MS. Therefore, the area of a typical pXRF analysis is approximately half a million times larger than that of a LIBS or LA-ICP-MS measurement. Backscattered electron (BSE) images in Figs. 6a-d reveal the microscopic heterogeneity of Aghvorik, Meydan Dağ, and Sarıkamış obsidians as well as Japanese sanukite. Heterogeneity on such microscopic scales is not a significant issue for pXRF/EDXRF; however, use of the PYRO materials to calibrate or evaluate microanalytical techniques, whether based on electron beams or laser ablation, warrants caution.

The suitability of standards to one technique but not another is common. As established in Section 2.1, EDXRF facilities often analyze USGS RGM-1, a powdered obsidian from Glass Mountain or its replacement standard, RGM-2, as a calibration standard and/or accuracy check (e.g., Skinner and Thatcher, 2003; Shackley, 2011a; Hughes, 2015). NAA labs tend to use a standard from NIST: SRM #278 (Glascock et al., 1998; Cherry et al., 2010; Elizalde-Rodarte et al., 2016; Rivero-Torres et al., 2017; Santi et al., 2017). Electron analytical techniques, such as EMPA and SEM-EDS, tend to use a standard from the Smithsonian Institution – VG-568, an obsidian from "Yellowstone National Park" in Wyoming (Tryon et al., 2011; Frahm, 2012, inter alia) – or various other materials (see Kuehne et al., 2011: Table 5). In contrast, LA-ICP-MS analysts tend to use artificial glasses (e.g., NIST SRM #610; Khalidi et al., 2009; Chataigner and Gratuze, 2014; Orange et al., 2016) or synthetic obsidian (de B. Pereira et al., 2001). Therefore, it is not unusual to see researchers change standards when moving between one analytical technique and another (e.g., LA-ICP-MS in Scharlotta et al., 2011 vs. pXRF in Scharlotta and Quach, 2015). Consequently, there is a clear precedence for tailoring the calibration standards to the strengths and weaknesses of a particular analytical technique.

4. Choosing and preparing the specimens

The following sections consider influences on how the specimens were chosen for the PYRO calibration and check sets, including maximizing compatibility with other calibration schemes (e.g., the MURR/Bruker set), and the preparation methods are also documented here.

4.1. Obsidian specimen collection

The obsidian specimens in the PYRO sets originate from my research collection, which was assembled via various means over the last fifteen years. Several specimens originated from vintage rock and mineral collections collected decades ago. For example, the Bodie Hills obsidian specimen came from the mineralogical collection of George E. Masimer (1917–1968). Similarly, the specimens from Mono Craters, Glass Mountain, and Casa Diablo all originated from older geological collections that predate protections of the sources (e.g., creation of the Mono Basin National Forest Scenic Area in 1984). Other obsidians are widely available from knapping enthusiasts and suppliers (e.g., Buck Mountain [Davis Creek] and Rainbow Mines, California; Wagontire, Oregon), but all such specimens must be verified as misidentifications were encountered (e.g., most often the readily available Buck Mountain obsidian was erroneously labeled as a more uncommon obsidian). Additional specimens were collected by myself and/or my colleagues. For example, most of the specimens from Turkey were collected in 1991 by Tuncay Ercan, Directorate of Mineral Research and Exploration, Turkey and by George "Rip" Rapp, University of Minnesota. Collection locations at Glass Buttes in Oregon are those best documented, having been published in Frahm and Feinberg (2015).

Table 7
PYRO calibration specimens from Japan.

Technique	Laboratory	Specimen/Publication	Mn (ppm)	Fe (ppm)	Zn (ppm)	Rb (ppm)	Sr (ppm)	Y (ppm)	Zr (ppm)	Nb (ppm)
PYRO Calibration-14: Kanayama sanukite, Japan										
		Recommended values	*949*	*34,650 ± 35*	*75*	*119 ± 4*	*280 ± 1*	*24 ± 6*	*225 ± 11*	*10*
EDXRF	MURR Archaeometry Lab	matched specimen		34,628		122		19	223	10
	NWR Obsidian Studies Lab	matched specimen				119	279	28	215	10
NAA	MURR Archaeometry Lab	matched specimen	949	34,678	75	115	281		236	
PYRO Calibration-15: Suwa-Hoshigatou, Japan										
		Recommended values	*591 ± 39*	*4410 ± 25*	*25 ± 1*	*141 ± 4*	*41 ± 3*	*24 ± 3*	*76 ± 1*	*7 ± 2*
EDXRF	Center for Obsidian and Lithic Studies	Suda and Tsuchiya, 2016	550 ± 24	4483 ± 40	23 ± 1	141 ± 1	42 ± 1	28 ± 1	77 ± 1	9 ± 1
	MURR Archaeometry Lab	Matched specimen	642	4601		142	40	26	75	8
	NWR Obsidian Studies Lab	Matched specimen					40	23	74	5
NAA	MURR Archaeometry Lab	Matched specimen	581	4181	26	134	47			
	Rikkyo University	Suzuki et al., 2005		4370 ± 322		135 ± 12			76 ± 45	
	Values reported in Ikeya, 2015	Tomura et al., 1994				141 ± 6				
PIXE	Australian Atomic Energy Commission	Leach et al., 2018			26		42	19	76	4
WDXRF	Applied Chemistry, Meiji University	Nakayama, 2006	560	4690	26	146	37	24	76	8
WDXRF	Center for Obsidian and Lithic Studies	Masihma, 2018	620	4130		144	38	23	77	
PYRO Calibration-16: Tokachi, Japan										
		Recommended values	*391 ± 27*	*7377 ± 163*	*35 ± 7*	*145 ± 6*	*54 ± 3*	*33 ± 5*	*85 ± 7*	*6 ± 2*
EDXRF	MURR Archaeometry Lab	matched specimen	422	7584	21	152	50	31	82	6
		Ferguson et al., 2014	427 ± 89			143 ± 8	54 ± 3	32 ± 1		7 ± 2
	National Museum of Japanese History	Hall and Kimura, 2002					58 ± 4	35 ± 3		
	NWR Obsidian Studies Lab	matched specimen				144	54	26	80	7
NAA	JAEA, Rikkyo University, Japan	Suzuki et al., 2005		7535 ± 403	42 ± 1	146 ± 13			90 ± 1	
	MURR Archaeometry Lab	matched specimen	365	7198	36	139				
		Ferguson et al., 2014	374 ± 3	7400 ± 100	40 ± 4	140 ± 1	53 ± 3			
		Kuzmin and Glascock, 2007	369 ± 6	7200 ± 100	36	139 ± 1		42 ± 4		
PIXE-PIGME	Australian Atomic Energy Commission	Leach et al., 2018				152 ± 3			95 ± 7	2 ± 2
WDXRF	Hokkaido University	Wada et al., 2014	387	7344	36	154	52	34	80	7

Table 8
PYRO calibration specimen from Guatemala.

Technique	Laboratory	Specimen/Publication	Mn (ppm)			Fe (ppm)			Zn (ppm)			Rb (ppm)			Sr (ppm)			Y (ppm)			Zr (ppm)			Nb (ppm)		
PYRO Calibration-17: El Chayal, Guatemala																										
		Recommended values	*647*	±	*22*	*6080*	±	*80*	*37*	±	*4*	*145*	±	*5*	*148*	±	*7*	*19*	±	*2*	*104*	±	*9*	*11*	±	*1*
EDXRF	Geoarchaeological XRF Lab	Shackley, 1997	594	±	36							149	±	9	150	±	6	21	±	3	109	±	1	12	±	3
		Silva de la Mora, 2018										156	±	7	153	±	6	21	±	2	108	±	5	12	±	4
	MURR Archaeometry Lab	matched specimen	683			6200						146			136			16			102			11		
	NWR Obsidian Studies Lab	matched specimen										145			142			18			106			10		
	University of California-Berkeley	Giauque et al., 1993	651	±	25	6070	±	230	44	±	2	147	±	3	151	±	3	17	±	1	106	±	2			
		Hughes, 1988	657	±	26							137	±	5	137	±	3	23	±	2	100	±	4			
		Jackson and Love, 1991							32	±	6	150	±	7	148	±	10	19	±	3	108	±	9	11	±	2
NAA	Lawrence Berkeley Laboratory	Andrews et al., 1989	649	±	13							149	±	8	153						117					
	MURR Archaeometry Lab	matched specimen	646			6024			36			140			159											
		Cobean et al., 1991	635	±	33	6010	±	60	36	±	6	141	±	1							88	±	15			
		Glascock et al., 1990	652	±	17	5980	±	70	36	±	1	138	±	2							88	±	13			
		Nazaroff et al., 2010	644	±	17							139	±	2	152	±	13				112	±	26			
	Smithsonian Institution	Harbottle et al., 1994										147	±	8												
WDXRF	Shell Development Company	Stevenson et al., 1971				6100						145									100			10		
WDXRF/NAA	Lawrence Berkeley Laboratory	Healey et al., 1984	655	±	6	6167	±	332													115	±	3			

4.2. Compatibility with other schemes

As discussed in Section 2.1, archaeological EDXRF facilities in North America tend to use the USGS standards RMG-1 or 2 for calibration and/or evaluation of obsidian analyses (e.g., Skinner and Thatcher, 2003; Carter et al., 2013; Hughes, 2015; Shackley et al., 2016). The source material of the two standards is Glass Mountain obsidian. It is the alkaline – specifically, calc-alkaline – geochemical variety of obsidian, which is typical of most obsidian sources within tectonic subduction zones such as the North American Pacific Coast, meaning that it is broadly geochemically similar to most of the obsidians in the American West. This, in turn, has made RMG-1 and 2 popular in these laboratories; however, Glass Mountain obsidian differs considerably in composition from, for example, phonolitic and trachytic obsidians of the East Africa Rift. Nevertheless, given its prevalence as a standard, Glass Mountain obsidian is included among the PYRO check specimens. Consequently, researchers, should they so desire, can still report accuracy relative to Glass Mountain obsidian.

As discussed in Section 2.2, various researchers (e.g., McCoy et al., 2014; Pintar et al., 2016; Reepmeyer et al., 2016; Fernández et al., 2017; Gaffney and Summerhayes, 2018; Grebennikov et al., 2018; Lynch et al., 2018; Matsumoto et al., 2018) have relied on the MURR/Bruker calibration for obsidian analyses (Glascock and Ferguson, 2012; Speakman, 2012). Therefore, a factor in choosing obsidian specimens to include in the PYRO sets was continuity with the MURR/Bruker set. The final choice was that one in five (20%) obsidians should be common between these two schemes. Hence, four obsidians in the PYRO calibration sets – La Joya (MURR/Bruker #16), Sierra de Pachuca (#30), Meydan Dağ (#36), and Sarıkamış (#37) – and three in the PYRO check sets – Panum Crater (Mono Craters; #7), Sawmill Ridge-Casa Diablo (#10), and Buck Mountain (Davis Creek; #27) – function to increase compatibility with the MURR/Bruker calibration. In addition, thanks to an inter-laboratory "round robin" organized and reported by Glascock (1999), Sierra de Pachuca obsidian became a de facto standard for researchers using InnovX pXRF instruments (e.g., Williams et al., 2012; Kellett et al., 2013; Moholy-Nagy et al., 2013; Millhauser et al., 2015). The inclusion of these obsidians in the PYRO sets will aid reproducibility with respect to these calibration schemes.

Other obsidians in the PYRO sets were used by researchers in previous decades to calibrate and evaluate XRF measurements. For example, Mt. Konocti obsidian was used by Stross et al. (1971) to check the repeatability of their data, and Davis et al. (1998) used Bodie Hills obsidian to test the effects of surface irregularity on EDXRF analyses of obsidian artifacts. El Chayal obsidian was used routinely as a calibration standard at Lawrence Berkeley National Lab in California (e.g., Burger and Asaro, 1977; Fowler et al., 1987; Andrews et al., 1989; Asaro et al., 1994). Consequently, these three obsidians also have long "pedigrees" as calibration standards used for sourcing.

Furthermore, I wanted the PYRO sets to be compatible with my prior calibration set, which I developed in 2012 (see Section 2.3). Consequently, the PYRO sets include six duplicates from that original set: Sarıkamış 1 and Meydan Dağ in Turkey; Chikiani 1 in Georgia; and Aghvorik, Gutansar, and Satanakar in Armenia. I have, however, updated the recommended values from 2012 to include additional analyses of matched specimens as well as datasets from the literature.

4.3. Designed to include the East African Rift

The PYRO sets were designed, from the initial planning phase, to include obsidians from the East African Rift, which are geochemically distinct from most other sources around the world due to their tectonic setting (Brown et al., 2013). In short, the divergent plate boundary of the East African Rift produces obsidians unlike those created by subduction zones. Ferguson (2012:406–407) notes what occurred when the MURR/Bruker calibration was first applied to Kenyan obsidians:

Table 9
PYRO calibration specimens from Mexico.

Technique	Laboratory	Specimen/Publication	Mn (ppm)			Fe (ppm)			Zn (ppm)			Rb (ppm)			Sr (ppm)			Y (ppm)			Zr (ppm)			Nb (ppm)		
PYRO Calibration-18: La Joya, Mexico																										
		Recommended values	*583*	±	*13*	*19,220*	±	*210*	*135*	±	*9*	*161*	±	*7*	*3*	±	*4*	*69*	±	*7*	*811*	±	*8*	*62*	±	*1*
EDXRF	MURR Archaeometry Lab	matched specimen				19,509			131			171			1			68			817			61		
		Glascock et al., 2010				19,300	±	1800	153	±	15	156	±	5	5	±	1	71	±	13				62	±	7
	NWR Obsidian Studies Lab	matched specimen													9			80						64		
ICP-MS	MURR Archaeometry Lab	Glascock and Ferguson, 2012										172			1			61								
		Glascock and Ferguson, 2012	577			19,034			134			154			1			66			805			61		
NAA	MURR Archaeometry Lab	matched specimen	602			19,234			129			159														
		Glascock and Ferguson, 2012	582						129			157														
		Glascock et al., 2010	572	±	23	19,000	±	200	131	±	11	157	±	2												
PYRO Calibration-19: Sierra de Pachuca, Mexico																										
		Recommended values	*1083*	±	*68*	*16,280*	±	*570*	*219*	±	*11*	*201*	±	*15*	*4*	±	*3*	*108*	±	*4*	*979*	±	*42*	*91*	±	*5*
EDXRF	Ashe Analytics, Montana	Glascock, 1999	1095	±	70	16,400	±	1100	224	±	14	200	±	8	2	±	1				991	±	35	91	±	4
	Geoarchaeological XRF Lab	Silva de la Mora, 2018										220	±	8	4	±	3				933	±	13	92	±	2
	MURR Archaeometry Lab	matched specimen	1032			15,660						201			2			106			979			89		
		Glascock, 2011				15,900	±	1200	207	±	19	189	±	3	10	±	4	108	±	19	957	±	62	84	±	8
	NWR Obsidian Studies Lab	matched specimen										182			13						954			95		
		Glascock, 1999	1124	±	48	17,200	±	600	224	±	8	225	±	3	5	±	1				985	±	9	99	±	2
EMPA	University of Minnesota	Frahm, 2010	1084	±	85	16,867	±	233													953	±	40			
ICP-AES/MS	CNRS, Grenoble, France	Glascock, 1999	1231	±	50	16,200	±	600				185	±	2	2	±	1				1005	±	12	91	±	1
	PUCRio de Janeiro, Brazil	Glascock, 1999				16,600						181			2			100						84		
ICP-MS	California State University	Carballo et al., 2007	1116	±	53	16,333	±	756				212	±	12							949	±	50			
	CNRS, Orléans, France	Glascock, 1999	1049	±	40	16,600	±	100	219	±	2	203	±	1	2	±	1	111	±	18	1058	±	143			
	PUCRio de Janeiro, Brazil	de B. Pereira et al., 2001							212	±	16				2						1000			85	±	2
		de B. Pereira et al., 2001	989	±	15										2						947	±	37	98	±	2
		de B. Pereira et al., 2001	1040	±	20										2						941	±	12	85	±	3
NAA	CNRS, Orléans, France	Glascock, 1999	990	±	140	17,200	±	1000	240	±	2	219	±	13				112	±	7	1020	±	5	91	±	1
	MURR Archaeometry Lab	matched specimen	1112			16,060			206			195														
		Cobean et al., 1991	1070	±	130	15,500	±	1000				187	±	15							903	±	72			
		Glascock, 2011	1148	±	25	15,800	±	200				192	±	3												
PIXE	CNRS, Grenoble, France	Glascock, 1999	1006	±	24	15,600	±	200	221	±	4	211	±	8				109	±	9	1006	±	13	97	±	13
PIXE/PIGME	ANSTO, Australia	Glascock, 1999										224	±	15	3	±	1									
WDXRF	CNR-ITABC, Rome, Italy	Glascock, 1999	1161									194			5						1055			91		

Table 10
PYRO calibration specimen from Peru.

Technique	Laboratory	Specimen/Publication	Mn (ppm)			Fe (ppm)			Zn (ppm)			Rb (ppm)			Sr (ppm)			Y (ppm)			Zr (ppm)			Nb (ppm)		
PYRO Calibration-20: Lisahuacho, Peru																										
		Recommended values	*451*	±	*13*	*8607*	±	*92*	*55*	±	*4*	*152*	±	*5*	*271*	±	*45*	*12*	±	*3*	*178*	±	*19*	*16*	±	*1*
EDXRF	MURR Archaeometry Lab	matched specimen	442									150			242			13			161			17		
		Glascock et al., 2007	472	±	17	8547	±	135				150	±	2	310	±	8	14	±	3	198	±	6	15	±	4
ICP-MS	Chicago Field Museum	Kellett et al., 2013				8711	±	556	56	±	3	158	±	6	206	±	12	9	±	1	155	±	14			
NAA	Lawrence Berkeley Lab	Burger et al., 2006	454	±	4	8622	±	429				158	±	4	300	±	65									
	MURR Archaeometry Lab	matched specimen	450			8484			51			146			299						184					
		Burger et al., 2006	438	±	17	8673	±	195	59	±	2	150	±	3							194	±	9			

The initial calibration included samples from 40 well-known obsidian sources in the Americas. For these obsidians, iron rarely exceeds 6–7 percent, zirconium is rarely above 1000 ppm, and niobium is rarely over 200 ppm. It was clear from the spectral overlay that many of the Kenyan samples had abnormally high concentrations of these three elements, yet the concentrations calculated by the calibration produced lower concentrations as the peak areas increased… The problem was corrected by including a couple Kenya obsidian samples with high iron, zirconium, and niobium concentrations.

The solution was adding two Kenyan obsidians – Eburu GsJj53 and Kedong Road – to the calibration. In contrast, five (25%) of the 20 PYRO calibration specimens originate from Kenyan and Ethiopian obsidian sources. I previously used one of the five obsidians – Mt. Eburru (GsJj50, not GsJj53) – as a calibration check when sourcing Kenyan obsidian artifacts (Frahm et al., 2017a).

4.4. Compositionally beyond obsidians

In anticipation of encountering geochemically atypical volcanic glass, two non-obsidians are included among the calibration specimens. One is a trachyte (~65% SiO_2, lower silica than rhyolite but more than dacite) from Hatis volcano in Armenia. This extrusive igneous rock is aphanitic – that is, its texture is so fine-grained that the constituent minerals appear indistinguishable to the naked eye. I found this trachyte during a survey of obsidian outcrops at this volcano in a location that had previously been mapped as rhyolitic lavas (Karapetian et al., 2001). This material flakes well, and a fresh surface has a somewhat glossy appearance. It likely would have been exploited as a toolstone in the past if not for abundant obsidian available only dozens of meters away. The other is sanukite from Kanayama in Japan (Higashimura and Warashina, 1975; Warashina et al., 1978). This extrusive igneous rock, which was used to fashion stone tools for millennia, is an andesite with microscopic minerals (primarily orthopyroxene and plagioclase) in a glassy groundmass. The two non-obsidians contain, for example, Sr at higher concentrations than typically occur in obsidian (440 and 280 ppm, respectively); however, such levels can be encountered in East Africa Rift obsidians (e.g., 214 ppm in Mackinder 1 and 2 from the Lake Baringo area in Kenya; Brown et al., 2013).

4.5. Replicating an archaeological assemblage

Another consideration that influenced the "check specimens" of the PYRO sets was creating a largely authentic archaeological test case. There is little point to assessing whether Mesoamerican obsidians can be chemically distinguished from, for instance, East African or Central Mediterranean obsidians using a given instrument or analytical technique. That is not a scenario one should expect to encounter. Hence, the check specimens were selected, in part, to mimic a potential assemblage at an archaeological site near the junction of Oregon, California, and Nevada in the northwestern United States. Reaux et al. (2018) report their obsidian sourcing results from sites within the Catnip Creek Delta region, very near this junction. More than 30 obsidian sources across these three states were recognized, including Buck Mountain, Massacre Lake/Guano Valley, Rainbow Mines, and Wagontire as well as three Glass Buttes sources. Therefore, the check specimens were intended to double as a way to evaluate how an instrument would perform in a "real world" scenario.

4.6. Cutting and mounting specimens

The specimens were cut to their target size (10–20 mm diameter) using a Hi-Tech Diamond slab saw with a 25-cm diamond-embedded saw blade. This size was considered adequate given that many recent pXRF models have a standard 8-mm beam diameter (and optional

Table 11
PYRO check specimens from California (United States).

Technique	Laboratory	Specimen/Publication	Mn (ppm)			Fe (ppm)			Zn (ppm)			Rb (ppm)			Sr (ppm)			Y (ppm)			Zr (ppm)			Nb (ppm)		
PYRO Check-01: Glass Mountain, California																										
		Recommended values	*278*	±	*16*	*12,930*	±	*290*	*34*	±	*2*	*150*	±	*3*	*108*	±	*2*	*25*	±	*1*	*222*	±	*4*	*9*	±	*1*
EDXRF	Geoarchaeological XRF Lab	Shackley, 2017, inter alia	292	±	15	13,307	±	389	36	±	3	149	±	3	108	±	4	25	±	1	221	±	4	9	±	1
	Geochemical Research Lab	Hughes, 2007, 2015, inter alia	284	±	18	13,201	±	162				149	±	4	108	±	4	25	±	2	219	±	3	9	±	1
	MURR Archaeometry Lab	matched specimen				12,245						156			107			23			230			9		
	NWR Obsidian Studies Lab	matched specimen										151			113			28			227			10		
	NWR Obsidian Studies Lab	Skinner et al., 1997, inter alia	302	±	28	12,947	±	988	35	±	5	150	±	3	106	±	4	26	±	1	219	±	3	10	±	2
	University of California-Berkeley	Hughes, 1982, 1986										146	±	35	104	±	16	25	±	4	218	±	35	8	±	1
ICP-MS/AES	CNRS, Grenoble, France	Bellot-Gurlet et al., 2008	263			12,800						154			107			26						10		
multiple	CNRS, France	Govindaraju, 1994	279			12,998			32			149			108			25			219			9		
	combined datasets	Gladney and Roelandts, 1988	282	±	30	13,000	±	400	32	±	6	149	±	8	108	±	10				219	±	20			
	Max-Planck-Institut fuer Chemie	Jochum et al., 2016	245	±	13	13,086	±	210	33	±	1	150	±	2	105	±	2	23	±	1	228	±	4	9	±	1
	United States Geological Survey	Smith, 1995	280	±	30	13,009	±	210	32			150	±	8	110	±	10	25			220	±	20	9	±	1
	United States Geological Survey	Wilson, 2009	273	±	8	13,000	±	300	33	±	2	147	±	5	108	±	5	24	±	2	222	±	17	9		
NAA	MURR Archaeometry Lab	matched specimen	280			12,649			38			147														
PYRO Check-02: Bodie Hills, California																										
		Recommended values	*433*	±	*48*	*4655*	±	*548*	*30*	±	*5*	*184*	±	*12*	*96*	±	*7*	*12*	±	*2*	*98*	±	*6*	*15*	±	*2*
EDXRF	BioSystems Obsidian Studies Lab	Davis et al., 1998	487	±	7				32	±	5	180	±	2	89	±	2	14	±	1	107	±	2			
	Geoarchaeological XRF Lab	Shackley and Skinner, 2015	438									195						14			104			15		
		Shackley, 2005	411									171			100			7			95			17		
	Geochemical Research Lab	Burton, 2010										192	±	4				12	±	3	99	±	4	15	±	3
		Haarklau et al., 2005	353									185	±	2	97	±	2	12	±	1	98	±	1	13	±	3
		Rice, 2015										194	±	30				13	±	2	95	±	5	17	±	1
		Starek, 2013				5409	±	176				197	±	13				13	±	1	94	±	7	17	±	1
		Wills, 2013				5338	±	372				188	±	7	101	±	4	12	±	1	94	±	4	16	±	2
	NWR Obsidian Studies Lab	Montague, 2010	402	±	64	4329	±	353	35	±	10	193	±	10	104	±	4	13	±	1	106	±	8	16	±	1
		Skinner and Thatcher, 2006	424	±	35	4268	±	96	29	±	6	184	±	6	101	±	3	13	±	1	104	±	4	16	±	3
ICP-MS	California State University	Draucker, 2007	373			4004			31			158			80									16		
		George, 2013	487	±	176							167	±	44										19	±	2
		Scharlotta et al., 2011	416	±	6	4410	±	139	32	±	4	193	±	2							86	±	2	15	±	1
ICP-MS/AES	SGS Minerals Analytical Lab	John et al., 2012							28	±	15	167	±	28							98	±	36	13	±	2
WDXRF	Brigham Young University	Nelson, 1984	480			4830						182			95									14		
	University of CaliforniaBerkeley	Jack and Carmichael, 1968	490						20			195			95			13			98			13		
PYRO Check-03: Buck Mountain, California																										
		Recommended values	*414*	±	*28*	*5380*	±	*160*	*28*	±	*2*	*109*	±	*6*	*66*	±	*7*	*18*	±	*2*	*94*	±	*5*	*11*	±	*2*
EDXRF	Geoarchaeological XRF Lab	Dillian et al., 2009	393						29			103			71			16			99			8		
		Shackley and Hughes, 2014	396	±	13							113	±	3	69	±	3	17	±	2	94	±	1	13	±	1
		Shackley, 2012a										110	±	1	72	±	1	18	±	1	92	±	1	10	±	3
	Geochemical Research Lab	LaLande, 1990										119	±	5	53	±	3	22	±	3				9	±	4
		Macko et al., 2005	429	±	13							105	±	3	62	±	3	16	±	2	89	±	3	8	±	3
		Rice, 2015										115	±	4	72	±	3	19	±	2	97	±	4	11	±	2
	MURR Archaeometry Lab	matched specimen	449			5617						110			60			14			88			13		
	NWR Obsidian Studies Lab	matched specimen										101			62			18			92			8		
		Skinner and Thatcher, 2016										103	±	5	66	±	4	18	±	1	92	±	4	11	±	1
		Smith and Kielhofer, 2011							31	±	11	110	±	4	71	±	9	20	±	3	99	±	10	10	±	2
		Thatcher, 2000										117	±	5	74	±	7	20	±	3				12	±	2
	University of California-Berkeley	Hughes, 1986										116	±	6	69	±	5	20	±	3	95	±	5	12	±	3
		Ritter, 1989										106	±	4	53	±	3	14	±	4	103	±	4			
ICP-MS	MURR Archaeometry Lab	Glascock and Ferguson, 2012	382			5316			27			100			58			16			88			11		
	California State University	George, 2013	404	±	118																88	±	35	14	±	2
multiple	multiple analytical labs	MacDonald et al., 1992	465						24	±	1	117	±	9	70			17	±	6	100			15	±	1
NAA	MURR Archaeometry Lab	matched specimen	397			5305			27			106			59											
		Glascock and Ferguson, 2012	410			5283			28			108			75											

(*continued on next page*)

Table 11 (*continued*)

Technique	Laboratory	Specimen/Publication	Mn (ppm)			Fe (ppm)			Zn (ppm)			Rb (ppm)			Sr (ppm)			Y (ppm)			Zr (ppm)			Nb (ppm)		
PYRO Check-04: Mt. Konocti, California																										
		Recommended values	*216*	±	*13*	*9444*	±	*112*	*32*	±	*8*	*212*	±	*10*	*74*	±	*6*	*37*	±	*2*	*200*	±	*11*	*12*	±	*2*
EDXRF	Biosystems Analysis	Psota, 1994										220	±	2	68	±	6	39	±	2	198	±	8	11	±	2
	Geoarchaeological XRF Lab	Shackley, 2012c							35						74			38			194			12		
	Geochemical Research Lab	Gillette, 2011										207	±	20	75	±	4	36	±	4	197	±	11	13	±	2
		Psota, 1994							48	±	4	221	±	23	67	±	3	38	±	1	194	±	9	10		
	MURR Archaeometry Lab	matched specimen	227			9329			23			216			64			34			201			11		
	NWR Obsidian Studies Lab	matched specimen										218			71			35			180			10		
	University of California-Berkeley	Jackson, 1989										212			75			39			204			15		
		Silliman, 2005	223												76			38			209					
Multiple	Multiple analytical laboratories	MacDonald et al., 1992	230			9450			25			208			72									13		
		Stimac and Hickmott, 1994							37	±	6	222	±	25	85	±	18	39	±	4	210	±	19	16	±	2
NAA	Berkeley Research Reactor	Bowman et al., 1973	195	±	13				35	±	3	221	±	22												
	MURR Archaeometry Lab	matched specimen	209			9552			32			206			84						222					
WDXRF	Los Alamos National Laboratory	Goff et al., 2001	225						24			194			73			36			192			12		
	Shell Development Company	Stevenson et al., 1971	205									195														
PYRO Check-05: Panum Crater, California																										
		Recommended values	*356*	±	*39*	*7737*	±	*841*	*43*	±	*2*	*183*	±	*9*	*8*	±	*4*	*26*	±	*3*	*110*	±	*6*	*23*	±	*5*
EDXRF	MURR Archaeometry Lab	matched specimen	389			7746						189			6			26			112			24		
	NWR Obsidian Studies Lab	matched specimen										166			12			27			109			21		
		Brady, 2007	354	±	71	7291	±	986	45	±	8	194	±	9	14	±	1	30	±	2	119	±	3	21	±	1
		Montague, 2010	299	±	22	6545	±	513	43	±	8				14	±	1	29	±	1	119	±	5	21	±	1
	University of California-Berkeley	Hughes, 1989	422	±	6							179	±	1	10	±	1	28	±	1	114	±	2	21	±	1
ICP-MS	MURR Archaeometry Lab	Glascock and Ferguson, 2012	343			7325			41			175			6			24			104			20		
		Glascock and Ferguson, 2012	308			8641			47			173			4									23		
MS & SIMS	GFZ & UCLA	Schmitt and Simon, 2004	310			5880									5			21								
multiple	multiple analytical laboratories	MacDonald et al., 1992	387			7630			41			186			8			26			105			23		
NAA	MURR Archaeometry Lab	matched specimen	342			7768			43			180														
		Glascock and Ferguson, 2012	357			7773			43			180														
WDXRF	Brigham Young University	Nelson, 1984	395	±	12	8680	±	308				181	±	3	12	±	2	30	±	3						
	Michigan State University	Vogel et al., 1989	310			8550	±	233				181			6						118					
	University of California-Berkeley	Hughes, 1989							40	±	4	193	±	3	5	±	1	25	±	3	108	±	4	22	±	4
		Jack & Charmichael 1968										195			5			25			105			30		
WDXRF & AAS	U.S. Geological Survey	MacDonald et al., 1992	387			8217			41			186	±	11	8						105			24	±	2
WDXRF & NAA	Imperial College & Kings College	Thompson et al., 1984	387			8540			42			195			7			23			107			21		
PYRO Check-06: Rainbow Mines, California																										
		Recommended values	*348*	±	*24*	*7354*	±	*153*	*25*	±	*4*	*127*	±	*6*	*70*	±	*6*	*20*	±	*1*	*138*	±	*6*	*11*	±	*1*
EDXRF	Geoarchaeological XRF Lab	Shackley, 2015a										122			65			20								
	Geochemical Research Lab	Amick, 2013										130	±	7	78	±	6	19	±	2	147	±	13	9	±	2
	MURR Archaeometry Lab	matched specimen	365			7462			22			130			63			19			131			12		
	NWR Obsidian Studies Lab	matched specimen										126			73			22			138			12		
		Skinner and Thatcher, 2016										121	±	7	73	±	1	20	±	1	134	±	6	11	±	1
	University of California-Berkeley	Hughes, 1986										137	±	6	73	±	9.4	22	±	3	141	±	7	11	±	3
NAA	MURR Archaeometry Lab	matched specimen	331			7246			27			124			63											

(*continued on next page*)

Table 11 (*continued*)

Technique	Laboratory	Specimen/Publication	Mn (ppm)			Fe (ppm)			Zn (ppm)			Rb (ppm)			Sr (ppm)			Y (ppm)			Zr (ppm)			Nb (ppm)		
PYRO Check-07: Sawmill Ridge, Casa Diablo, California																										
		Recommended values	*286*	±	*27*	*9495*	±	*504*	*33*	±	*3*	*150*	±	*3*	*121*	±	*11*	*18*	±	*2*	*194*	±	*9*	*13*	±	*1*
EDXRF	Geoarchaeological XRF Lab	Shackley, 2011b													106			19			191			12		
	Geochemical Research Lab	Brady, 2007	251	±	27	9092	±	770	35	±	10	153	±	5	117	±	9	19	±	3	192	±	10	12	±	2
		Hughes, 1994	324	±	5	9757	±	121	36	±	5	151	±	2	114	±	2	18	±	2	189	±	2	14	±	1
		Starek, 2013				10,211	±	140				150	±	4	122	±	4	18	±	2	184	±	4	14	±	2
		Farrell and Burton, 2010										149	±	1	125	±	2	16	±	2	193	±	7	17	±	1
	MURR Archaeometry Lab	matched specimen	304			9978			30						114			15			198			14		
	NWR Obsidian Studies Lab	matched specimen										151			127			20			194			13		
		Montague, 2010	309	±	84				39	±	10	154	±	4	119	±	1	18	±	1	191	±	4	13	±	1
ICP-MS	MURR Archaeometry Lab	Glascock and Ferguson, 2012	260			8802			30						108						189			12		
NAA	MURR Archaeometry Lab	matched specimen	278			9346			31			148			139											
		Glascock and Ferguson, 2012	279			9278			33			145			140						218					

Table 12
PYRO check specimen from Nevada (United States).

Technique	Laboratory	Specimen/Publication	Mn (ppm)			Fe (ppm)			Zn (ppm)			Rb (ppm)			Sr (ppm)			Y (ppm)			Zr (ppm)			Nb (ppm)		
PYRO Check-08: Massacre Lake/Guano Valley, Nevada																										
		Recommended values	*922*	±	*44*	*14,290*	±	*1450*	*135*	±	*6*	*215*	±	*9*	*4*	±	*4*	*89*	±	*4*	*582*	±	*13*	*31*	±	*2*
EDXRF	Geochemical Research Lab	Rice, 2015										216	±	4							601	±	6	32	±	3
	MURR Archaeometry Lab	matched specimen	881			14,230						217			1			85			611			30		
	NWR Obsidian Studies Lab	matched specimen										205			12						572			35		
		Camp, 2009	881	±	85	14,734	±	1065	131	±	11	222	±	6	8	±	4	89	±	3	575	±	7	30	±	2
		Jew et al., 2015										204	±	16	4	±	1	89	±	2	574	±	8	34	±	2
		LaValley, 2013				11,825	±	1316	133	±	14	231	±	14	8	±	3	88	±	6	579	±	24	32	±	3
		Lyons et al., 2001							141	±	11	228	±	9	4	±	1	91	±	3	590	±	16	33	±	2
		Rick et al., 2001										206	±	4				85	±	3				27	±	2
		Skinner and Thatcher, 2016										213	±	7	2	±	1	90	±	2	587	±	14	32	±	1
		Skinner, 2013										203	±	13	3	±	1	86	±	4	571	±	11	32	±	1
		Smith and Kielhofer, 2011	923	±	218	13,668	±	2168	128	±	19	214	±	34	8	±	2	85	±	4	567	±	22	30	±	2
		Thatcher, 2000							145	±	5	221	±	1	2	±	3	90	±	3	577	±	1	33	±	6
	University of California-Berkeley	Hughes, 1986										230	±	11	1	±	1	98	±	6				27	±	5
NAA	MURR Archaeometry Lab	matched specimen	918			14,061			138			205									581					
WDXRF	Brigham Young University	Nelson, 1984	1000			16,650						218	±	7	2	±	1									
	WSU GeoAnalytical Labs	Coble and Mahood, 2016	930			14,850			131			210			0			91			579			30		

Table 13
PYRO check specimens from Oregon (United States).

Technique	Laboratory	Specimen/Publication	Mn (ppm)			Fe (ppm)			Zn (ppm)			Rb (ppm)			Sr (ppm)			Y (ppm)			Zr (ppm)			Nb (ppm)		
PYRO Check-09: Glass ButtesAlpha, Oregon																										
		Recommended values	*332*	±	*40*	*5738*	±	*131*	*36*	±	*5*	*85*	±	*3*	*25*	±	*4*	*50*	±	*3*	*93*	±	*6*	*11*	±	*2*
EDXRF	Geoarchaeological XRF Lab	Dillian et al., 2009	396									87			28			49			92			14		
		Shackley, 2014b	348									88			33			55			103			11		
	MURR Archaeometry Lab	matched specimen	384			5903			27			87			22			45			87			11		
	NWR Obsidian Studies Lab	matched specimen													25			41			84			8		
		Helzer, 2001	281	±	32				39	±	18	87	±	2	28	±	1	54	±	1	96	±	3	12	±	1
		Parfitt and McCutcheon, 2017										84	±	2	23	±	1	51	±	2	95	±	2	11	±	1
		Skinner and Thatcher, 2003							40	±	6	88	±	6	26	±	2	53	±	3	98	±	4	12	±	2
		Sparaga, 2017										88	±	4	24	±	1	48	±	1	91	±	10	9	±	1
		Thatcher, 2000							38	±	10				28	±	1	53	±	1	99	±	3	11	±	5
	University of California-Berkeley	Hughes, 1986													26	±	3	57	±	5	93	±	6	11	±	2
ICP-MS	Oregon State University	Ford, 2012										83			22											
ICP-MS/XRF	Oregon State University	Ford, 2012	318			5674			30			82			24			50			85			10		
NAA	MURR Archaeometry Lab	matched specimen	312			5691			36			81														
		Ambroz et al., 2001	314	±	11	5580	±	80	39	±	7	81	±	1	18	±	6									
WDXRF	University of Oregon	Skinner, 1983	303	±	22	5840	±	47							19	±	2	44	±	2	91	±	2	9	±	2
PYRO Check-10: Glass ButtesBeta, Oregon																										
		Recommended values	*309*	±	*18*	*6510*	±	*130*	*38*	±	*6*	*72*	±	*2*	*49*	±	*5*	*45*	±	*5*	*117*	±	*11*	*12*	±	*1*
EDXRF	MURR Archaeometry Lab	matched specimen				6657			26			73			44			42			106			11		
	NWR Obsidian Studies Lab	matched specimen													45			38			100			12		
		Helzer, 2001	290	±	13				36	±	1	73	±	1	58	±	1	48	±	1	126	±	2	13	±	4
		Skinner and Thatcher, 2003							43	±	8	74	±	3	53	±	4	49	±	2	121	±	5	11	±	1
		Thatcher, 2000	298	±	28				41	±	3	73	±	2	53	±	4	49	±	2	122	±	4	11	±	1
NAA	MURR Archaeometry Lab	matched specimen	329			6391			38			70			46						126					
		Ambroz et al., 2001	318	±	7	6490	±	110	42	±	5	68	±	1	45	±	10									
PYRO Check-11: Glass ButtesDelta, Oregon																										
		Recommended values	*425*	±	*52*	*4750*	±	*70*	*43*	±	*11*	*116*	±	*7*	*8*	±	*3*	*66*	±	*4*	*84*	±	*6*	*14*	±	*1*
EDXRF	MURR Archaeometry Lab	matched specimen	495						28			122			4			63			79			13		
	NWR Obsidian Studies Lab	matched specimen										107			10						82			14		
		Skinner and Thatcher, 2003	368	±	44				46	±	6	124	±	7	9	±	1	69	±	3	91	±	3	14	±	2
NAA	MURR Archaeometry Lab	matched specimen	420			4797			44			116														
		Ambroz et al., 2001	416	±	5	4700	±	1000	55	±	6	111	±	2												
PYRO Check-12: Glass ButtesEpsilon, Oregon																										
		Recommended values	*463*	±	*48*	*4805*	±	*30*	*45*	±	*10*	*126*	±	*8*	*4*	±	*3*	*69*	±	*7*	*83*	±	*8*	*14*	±	*1*
EDXRF	MURR Archaeometry Lab	Matched specimen	541						33			136			1			70			79			13		
	NWR Obsidian Studies Lab	Matched specimen										117			7			60			88			14		
		Skinner and Thatcher, 2003	410	±	30				50	±	6	138	±	6	5	±	1	76	±	3	90	±	3	16	±	3
ICP-MS/XRF	Oregon State University	Ford, 2012	450			4820			39			123			2			71			74			13		
NAA	MURR Archaeometry Lab	matched specimen	468			4825			46			121														
		Ambroz et al., 2001	447	±	4	4770	±	1000	58	±	5	121	±	2												
PYRO Check-13: Round Top Butte, Oregon																										
		Recommended values	*527*	±	*57*	*4596*	±	*166*	*27*	±	*12*	*131*	±	*6*	*28*	±	*6*	*31*	±	*3*	*69*	±	*2*	*12*	±	*2*
EDXRF	Geochemical Research Lab	Jenkins and Connolly, 1990										140	±	5	19	±	3	34	±	2						
	MURR Archaeometry Lab	matched specimen	539			4761			18			139			27			31			69			12		
	NWR Obsidian Studies Lab	matched specimen										128			35			28			70			10		
	Oregon State University	Meigs et al., 2009	465			4430						131			31						67			13		
ICP-MS	Oregon State University	Ford, 2012										127			31											
NAA	MURR Archaeometry Lab	matched specimen	578			4597			35			131			26											
	Portland State University	Roche, 1987										123	±	23												
PYRO Check-14: Wagontire, Oregon																										
		Recommended values	*478*			*13,110*			*63*	±	*15*	*102*	±	*7*	*40*	±	*4*	*55*	±	*4*	*340*	±	*13*	*22*	±	*1*

(*continued on next page*)

Table 13 (*continued*)

Technique	Laboratory	Specimen/Publication	Mn (ppm)	Fe (ppm)	Zn (ppm)	Rb (ppm)	Sr (ppm)	Y (ppm)	Zr (ppm)	Nb (ppm)
EDXRF	Geochemical Research Lab	Jenkins and Connolly, 1990			80 ± 9		41 ± 3	51 ± 2	351 ± 6	23 ± 4
	MURR Archaeometry Lab	matched specimen			47	106	38	51	344	21
	NWR Obsidian Studies Lab	matched specimen				91	46	59	353	
		Thatcher, 2000			73 ± 9	105 ± 3	41	58 ± 2	328 ± 2	21 ± 1
ICP-MS	Rice University	Savov et al., 2009			49	109	35			
NAA	MURR Archaeometry Lab	matched specimen	478	13,114	68	97			325	

Table 14
PYRO check specimen from Utah (United States).

Technique	Laboratory	Specimen/Publication	Mn (ppm)	Fe (ppm)	Zn (ppm)	Rb (ppm)	Sr (ppm)	Y (ppm)	Zr (ppm)	Nb (ppm)
PYRO Check-15: Black Rock Area, Utah										
		Recommended values	*445 ± 56*	*6396 ± 224*	*42 ± 8*	*273 ± 7*	*11 ± 4*	*58 ± 7*	*100 ± 6*	*32 ± 3*
EDXRF	Geoarchaeological XRF Lab	Dillian et al., 2007	468 ± 1		42 ± 8	264 ± 5	10 ± 3	60 ± 1	102 ± 1	29 ± 8
		Shackley, 2014a	412			285	8	63	105	30
		Shackley, 2015b	389			272	16	59	100	35
	Geochemical Research Lab	Hughes, 2015					9 ± 3	60 ± 2	93 ± 5	31 ± 3
		Moore, 2009			56 ± 8	269 ± 11	13 ± 3	52 ± 3	100 ± 3	30 ± 3
		Yentsch et al., 2009					8 ± 3	61 ± 3	98 ± 4	31 ± 3
	MURR Archaeometry Lab	matched specimen	488	6693	34	277	7	58	100	32
	NWR Obsidian Studies Lab	matched specimen				277	14	49	87	31
		Estes, 2009	334 ± 27		40 ± 7		6 ± 9	70 ± 3	109 ± 7	37 ± 1
multiple	multiple analytical laboratories	MacDonald et al., 1992	465	6444 ± 85	37 ± 4	269 ± 6	8 ± 1	46 ± 4	101 ± 1	36 ± 2
NAA	MURR Archaeometry Lab	matched specimen	454	6211	43					
WDXRF	Brigham Young University	Nelson and Holmes, 1979	491 ± 13	6235 ± 94		270 ± 12	15 ± 2		104 ± 17	
		Nelson, 1984	503 ± 15				14 ± 2		102 ± 10	

Table 15
Summary of recommended values for all PYRO specimens.

Label	Mn (ppm)			Fe (ppm)			Zn (ppm)			Rb (ppm)			Sr (ppm)			Y (ppm)			Zr (ppm)			Nb (ppm)		
PYRO Calibration Set																								
Cal-01	472	±	24	12,240	±	690	48	±	4	98	±	5	198	±	9	15	±	6	236	±	15	18	±	4
Cal-02	641	±	23	8250	±	173	44	±	4	140	±	5	129	±	6	22	±	7	171	±	13	37	±	3
Cal-03	623			19,940	±	700	54			70			443	±	24	19	±	7	243	±	12	27		
Cal-04	522	±	20	4580	±	180	34	±	2	192	±	2	9	±	2	8	±	4	88	±	10	36	±	3
Cal-05	482	±	40	5000	±	280	41	±	4	130	±	7	75	±	12	14	±	4	81	±	4	19	±	2
Cal-06	519	±	27	9520	±	310	74	±	8	200	±	5	18	±	3	52	±	5	286	±	15	32	±	4
Cal-07	1380	±	18	46,680	±	3860	237	±	10	233	±	8	2	±	1	145			1308	±	82	76	±	9
Cal-08	325	±	14	5724	±	337	31	±	2	130	±	8	22	±	4	21	±	4	109	±	24	14	±	1
Cal-09	311	±	1	8625	±	130	40	±	3	179	±	5	75	±	3	30	±	3	211	±	7	53	±	5
Cal-10	1356			41,200			279	±	19	207			2			150			1282	±	134	230	±	4
Cal-11	2638			58,130	±	620	368	±	31	130	±	6	12	±	6	153			1075	±	65	185	±	14
Cal-12	1990	±	40	59,900	±	1500	436	±	35	204	±	13	7	±	2	235	±	58	1517	±	64	335	±	39
Cal-13	298	±	35	13,280	±	220	114	±	7	277	±	2	5	±	1	86	±	1	445	±	27	192	±	1
Cal-14	949			34,650	±	35	75			119	±	4	280	±	1	24	±	6	225	±	11	10		
Cal-15	591	±	39	4410	±	25	25	±	1	141	±	4	41	±	3	24	±	3	76	±	1	7	±	2
Cal-16	391	±	27	7377	±	163	35	±	7	145	±	6	54	±	3	33	±	5	85	±	7	6	±	2
Cal-17	647	±	22	6080	±	80	37	±	4	145	±	5	148	±	7	19	±	2	104	±	9	11	±	1
Cal-18	*583*	±	13	19,220	±	210	135	±	9	161	±	7	3	±	4	69	±	7	811	±	8	62	±	1
Cal-19	*1083*	±	68	16,280	±	570	219	±	11	201	±	15	4	±	3	108	±	4	979	±	42	91	±	5
Cal-20	*451*	±	13	8607	±	92	55	±	4	152	±	5	271	±	45	12	±	3	178	±	19	16	±	1
PYRO Check Set																								
Check-01	278	±	16	12,930	±	290	34	±	2	150	±	3	108	±	2	25	±	1	222	±	4	9	±	1
Check-02	433	±	48	4655	±	548	30	±	5	184	±	12	96	±	7	12	±	2	98	±	6	15	±	2
Check-03	414	±	28	5380	±	160	28	±	2	109	±	6	66	±	7	18	±	2	94	±	5	11	±	2
Check-04	216	±	13	9444	±	112	32	±	8	212	±	10	74	±	6	37	±	2	200	±	11	12	±	2
Check-05	356	±	39	7737	±	841	43	±	2	183	±	9	8	±	4	26	±	3	110	±	6	23	±	5
Check-06	348	±	24	7354	±	153	25	±	4	127	±	6	70	±	6	20	±	1	138	±	6	11	±	1
Check-07	286	±	27	9495	±	504	33	±	3	150	±	3	121	±	11	18	±	2	194	±	9	13	±	1
Check-08	922	±	44	14,290	±	1450	135	±	6	215	±	9	4	±	4	89	±	4	582	±	13	31	±	2
Check-09	332	±	40	5738	±	131	36	±	5	85	±	3	25	±	4	50	±	3	93	±	6	11	±	2
Check-10	309	±	18	6510	±	130	38	±	6	72	±	2	49	±	5	45	±	5	117	±	11	12	±	1
Check-11	425	±	52	4750	±	70	43	±	11	116	±	7	8	±	3	66	±	4	84	±	6	14	±	1
Check-12	463	±	48	4805	±	30	45	±	10	126	±	8	4	±	3	69	±	7	83	±	8	14	±	1
Check-13	527	±	57	4596	±	166	27	±	12	131	±	6	28	±	6	31	±	3	69	±	2	12	±	2
Check-14	478			13,110			63	±	15	102	±	7	40	±	4	55	±	4	340	±	13	22	±	1
Check-15	445	±	56	6396	±	224	42	±	8	273	±	7	11	±	4	58	±	7	100	±	6	32	±	3

collimation down to 3 mm) and a built-in aiming camera. Similar beam sizes are possible for benchtop XRF instruments (e.g., 1, 3.5, 9, and 15 mm for a Thermo Scientific ARL Quant'X). Additionally, to assuage concerns about sufficient thickness for accurate analyses (see Frahm, 2016:448–450 and references within), these specimens were cut as thickly as possible (~5–15 mm) given the available material. A greater thickness is required to analyze Ba accurately in obsidian (~18 mm using the Kα X-ray), and this is a reason that, in subsequent sections, Ba is not reported for these specimens.

The obsidian specimens were encapsulated in epoxy resin to protect them from chipping in transit (and users from small, fresh chips off the specimens). Specifically, EpoxySet from Allied High Tech Products was chosen for this purpose. It has low viscosity (300 cP), so it easily surrounds and adheres to specimens. It also has high clarity, hardness (89 Shore D), and strength (7600 psi tensile strength). The resin consists of Bisphenol-A [$(CH_3)_2C(C_6H_4OH)_2$] and epichlorhydrin [C_3H_5ClO], and the curing agent is triethylenetetramine [$(CH_2NHCH_2CH_2NH_2)_2$]. The specimens were placed in two-part mounting cups (25 mm diameter), and the liquid epoxy was poured over the specimens, filling the cups. Hardened epoxy prepared without a specimen was analyzed by pXRF, and as anticipated, these organic compounds contained no elements that would interfere with obsidian sourcing. The prepared specimens were cut using a diamond-embedded wafering blade on a Buehler IsoMet saw and/or ground using silicon carbide paper on a Buehler MiniMet 1000 polisher.

5. Data and recommended values

Whenever possible, the elemental data from multiple analytical techniques and laboratories were employed to establish the recommended values for the PYRO sets. Reference standards based on chemical analysis in a single laboratory or by only one technique have occasionally been shown to have inaccuracies in their data. Consider, for instance, the previously mentioned VG-568 obsidian standard (Jarosewich, 2002). In the official values reported by Jarosewich et al. (1980), Ti is listed as 720 ppm (0.12% TiO_2). More recent studies, however, found consistently lower values for Ti: 480 ± 180 ppm in Streck and Wacaster (2006), 480 ± 60 ppm in Rowe et al. (2008), and 450 ± 55 ppm in Frahm (2010, 2012). As argued by Hancock and Carter (2010:245), "although analytical chemistry is not a democratic process, the agreement of specific elemental concentration data" from different laboratories and techniques "adds credibility to the relative accuracy of their numbers." Thus, there is great value in using standards that are not predicated on one value from a single technique or lab, which might exhibit some sort of systematic error or bias. Instead, it is better to seek measurements from independent labs, remove outliers, and find a consensus among them.

5.1. Comparative elemental data

Many of the PYRO specimens were analyzed at the MURR Archaeometry Laboratory, thanks to Michael D. Glascock and Jeffrey R. Ferguson, as well as the Northwest Research Obsidian Studies Laboratory (NWROSL), thanks to Alex J. Nyers and Craig E. Skinner. None of them, however, should be held responsible for my interpretations of their elemental measurements. NAA at MURR followed their standard procedures for obsidian characterization (Glascock, 2011:174), including both short- and long-irradiation measurements.

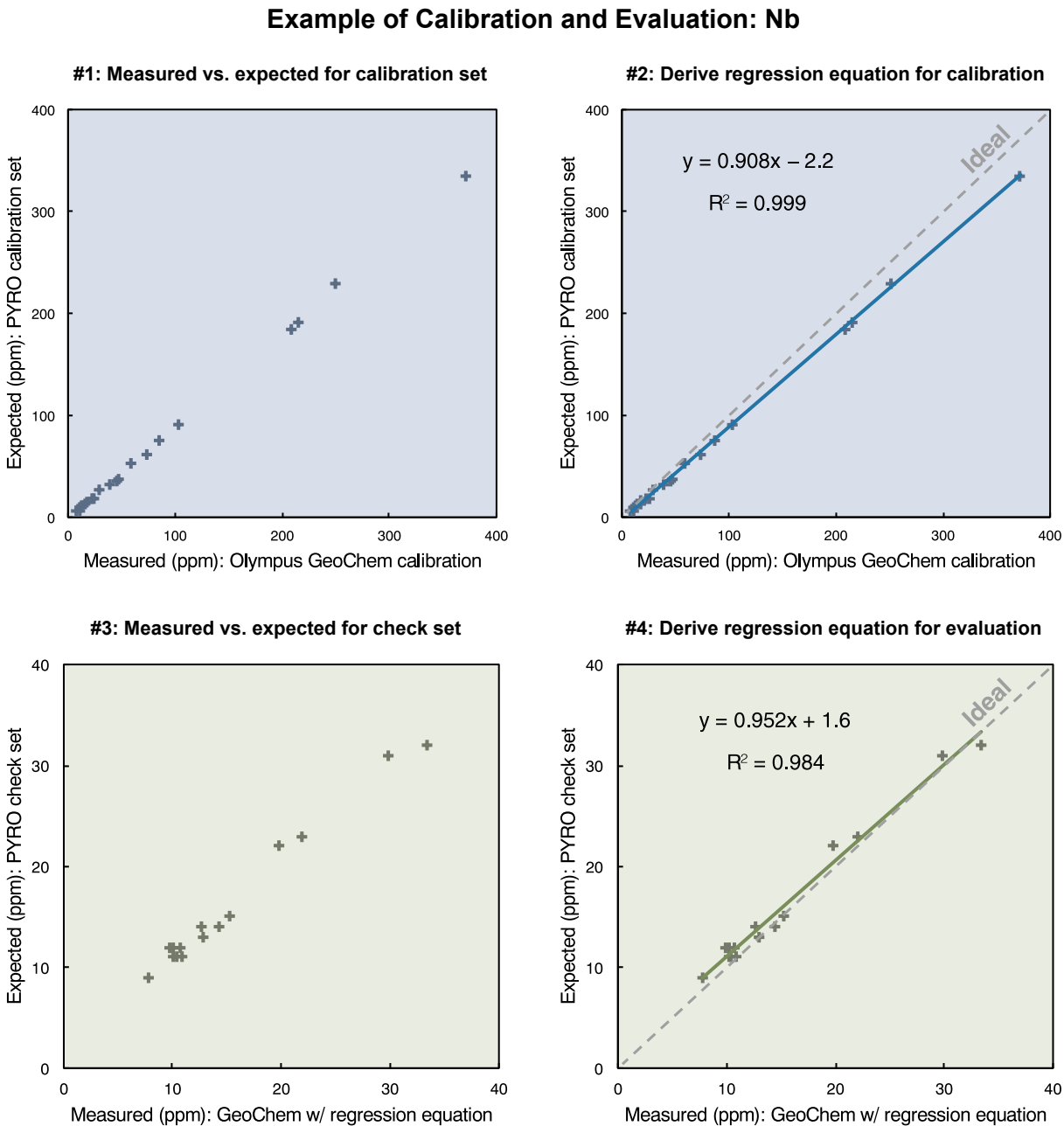

Fig. 7. Four steps in use of the PYRO calibration and check sets with Nb. First, one measures the 20 calibration set specimens and compares them to the expected values reported here. Second, one uses linear regression analysis in order to derive a calibration equation that can be input either into the pXRF software (e.g., "cal factors" in Olympus terminology, "user factors" in Thermo terminology) or applied to the data in spreadsheet software (e.g., Excel). Third, one measures the check set with the new applied calibration equations. Fourth, one again uses linear regression, but this time one is quantifying how well the measured values reproduce the expected ones.

Their EDXRF data reflect measurements using either an older ElvaX (Elvatech, Ltd., Ukraine) instrument (Glascock, 2011:174175) or a newer Thermo Scientific ARL Quant'X instrument (Maziar and Glascock, 2017:34). EDXRF measurements at NWROSL were conducted using a Thermo Electron QuantX-EC instrument. I also analyzed several specimens using EMPA at the University of Minnesota using published protocols (Frahm, 2012).

5.2. Published datasets

In addition to the MURR and NWROSL data, the literature – both published and "grey" – was searched for other measurements of the obsidians. For the North American obsidians, relevant data were often found in laboratory reports for clients of GRL and the Geoarchaeological XRF Lab. For the Kenyan obsidians, datasets from Brown et al. (2013) proved invaluable, as they have before (Frahm et al., 2017a). As noted in Section 4.2, several of these obsidians have a history of use as calibration and/or check specimens in obsidian artifact sourcing, so there are existing data for them. Data from pXRF instruments were avoided to prevent any bias from the protocols discussed in Section 2.2. For datasets found in the literature or laboratory reports, average values and standard deviations were calculated if multiple measurements per source were given. Three specimens – Hatis trachyte (which I identified while testing outcrops) from Armenia, Kanayama sanukite from Japan, and Bede Gebabe obsidian from Ethiopia – have no published measurements that could be located.

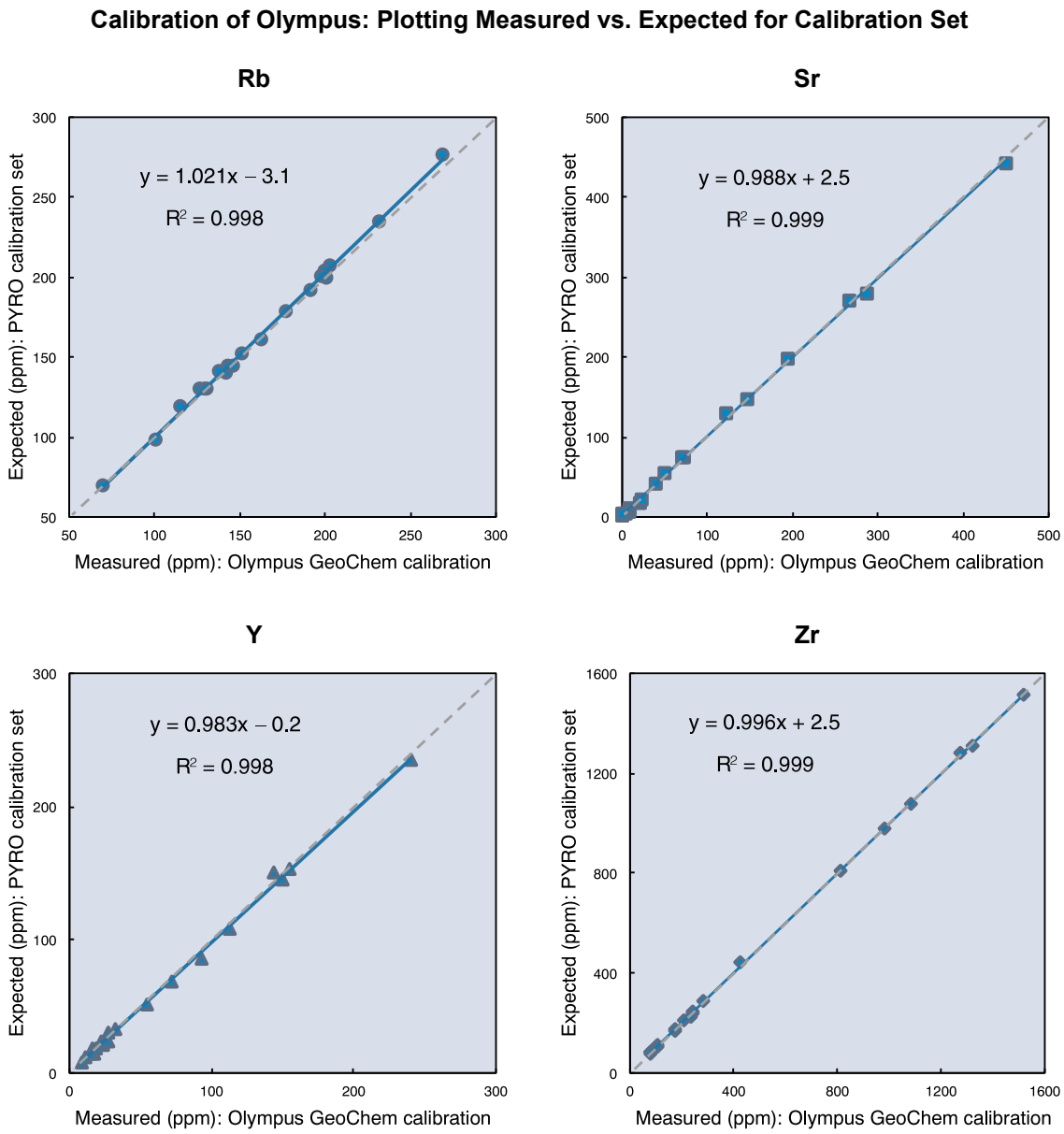

Fig. 8. Use of the PYRO calibration specimens with Rb, Sr, Y, and Zr to derive linear regression equations to apply to the factory-set Olympus Vanta GeoChem calibration.

5.3. Element selection and omission

Eight elements are reported here: Mn, Fe, Zn, Rb, Sr, Y, Zr, and Nb. This list of elements was, in large part, limited by the availability and agreement of comparative datasets. Ti was one element that I had to omit for now. It was not until 2010 that MURR developed a procedure to measure Ti in obsidian (Coleman, 2010). Several of the five Ti isotopes do not readily absorb neutrons to become radioactive, whereas others result in radioisotopes also produced by other elements. Consequently, NAA has relatively poor sensitivity for Ti (i.e., three to four orders of magnitude worse than Mn), and as a result, it is often left unmeasured or unreported (Glascock, 2017). In addition, with EDXRF, there is a concern about an overlap of Ti Kα X-rays (4.51 keV) and Ba Lα X-rays (4.47 keV). Ti X-rays also have much lower energies than those for Rb (13.40 keV) to Nb (16.62 keV) and, therefore, are more sensitive to irregular surfaces (Forster et al., 2011). For these reasons, the analyses at NWOSL and MURR did not include Ti, and the published values for Ti were highly variable. Hopefully the list of recommended values can eventually be expanded to include Ti, among others.

5.4. Recommended values

Table 1 lists the 20 specimens in the PYRO calibration set and the 15 specimens in the check set along with their GPS coordinates and alternative names. Any outlier values were identified using standard techniques (e.g., ≥1.5 times the interquartile range) and removed. Tables 2 to 10 give the recommended values and the corresponding measurements – both published datasets and matched specimens – for the PYRO calibration set, divided by country. Tables 11 to 14 list them for the check set, divided by state. Table 15 summarizes the recommended values for all

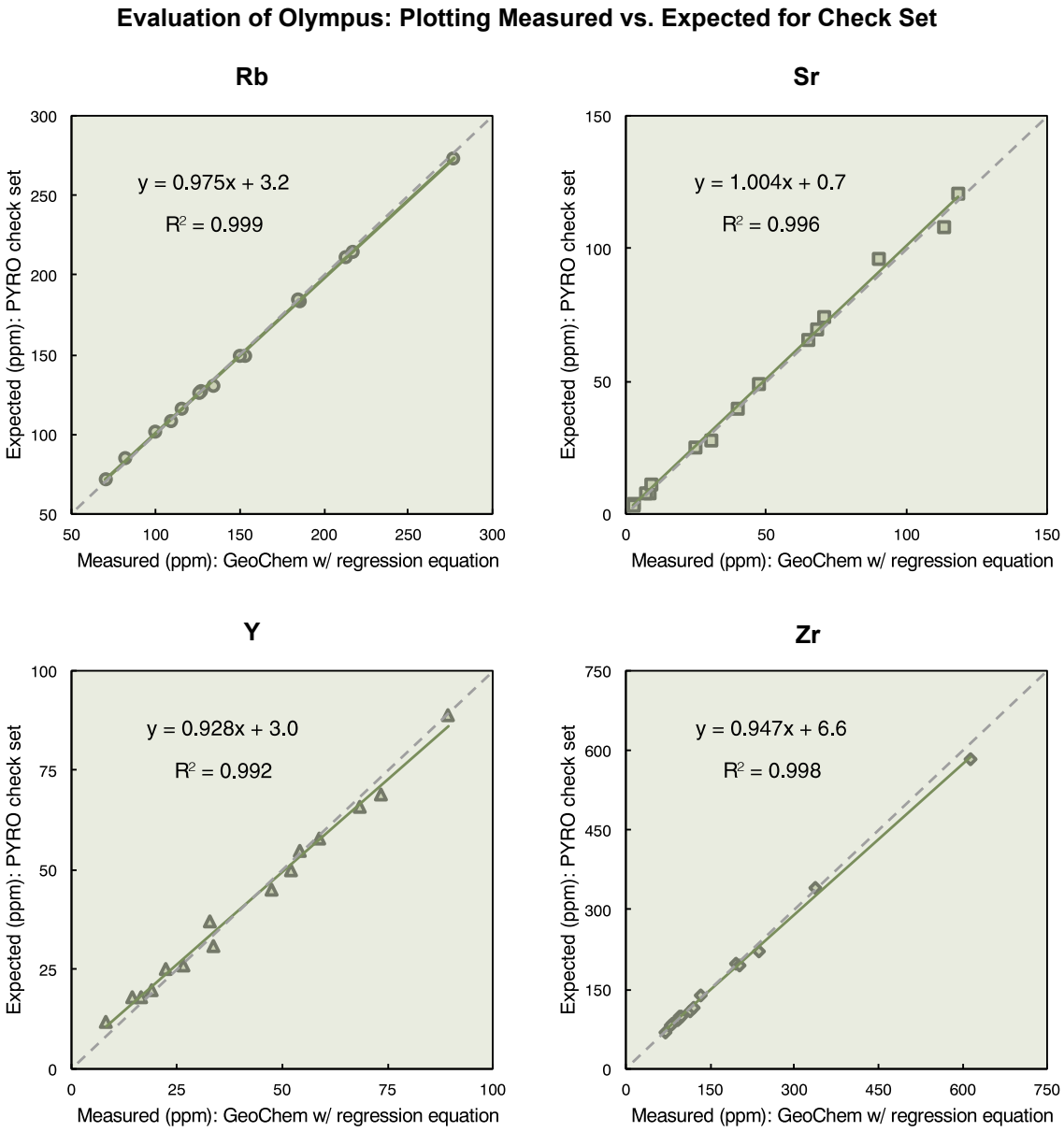

Fig. 9. Use of the PYRO check specimens with Rb, Sr, Y, and Zr to evaluate the PYRO-calibrated data for Olympus Vanta instrument.

PYRO calibration and check specimens in a single table. No claim is made that these recommended values are equivalent in accuracy to the certified values of SRMs. There is, though, much greater transparency in how these data and the corresponding facilities are reported in comparison to many SRMs (e.g., "a round robin study involving a select set of international laboratories," Wilson, 2009).

6. PYRO use and reproducibility

Measurements of the PYRO calibration and check specimens using two pXRF instruments in different facilities can demonstrate the sets' use. First, the PYRO specimens were analyzed using an Olympus Vanta M-series pXRF instrument, which is equipped with a Rh anode, 4 W X-ray tube, and 40 mm^2 Si drift detector (SDD) with a very high spectral resolution ($\lesssim$ 140 eV). In the "GeoChem" mode, the voltage automatically varies in combination with X-ray filters to fluoresce the heavy (40 kV) and light (10 kV) portions of the periodic table. This mode uses the FP correction scheme (see Section 3.1) and has been calibrated by the manufacturer using a collection of ~40 geological SRMs (what is called the "FP with standards" approach by Heginbotham et al., 2011).

Fig. 7 illustrates the calibration and assessment of Nb measurements. First, the calibration specimens, which span a wide range of concentrations (6–335 ppm) are analyzed, and the measured Nb values are plotted against the expected values reported here. Second, regression analysis yields a linear equation that describes how the measured values are best arithmetically converted into the expected ones. The slope and *y*-axis intercept of the regression equation are then used to adjust the factory calibration. In the Olympus Vanta software, these numbers are input as "cal factors" for Nb, whereas they are input as "user factors" in the Thermo Niton software. Next, the check specimens, which cover a narrower range of values (9–32 ppm), are measured using the fine-tuned calibration. Lastly, a second regression analysis describes how well measured values for these check specimens reproduce the expected ones. This process brings the Nb measurements into closer agreement with the recommended values. Figs. 8 and 9 illustrate this calibration and evaluation process for other elements (i.e.,

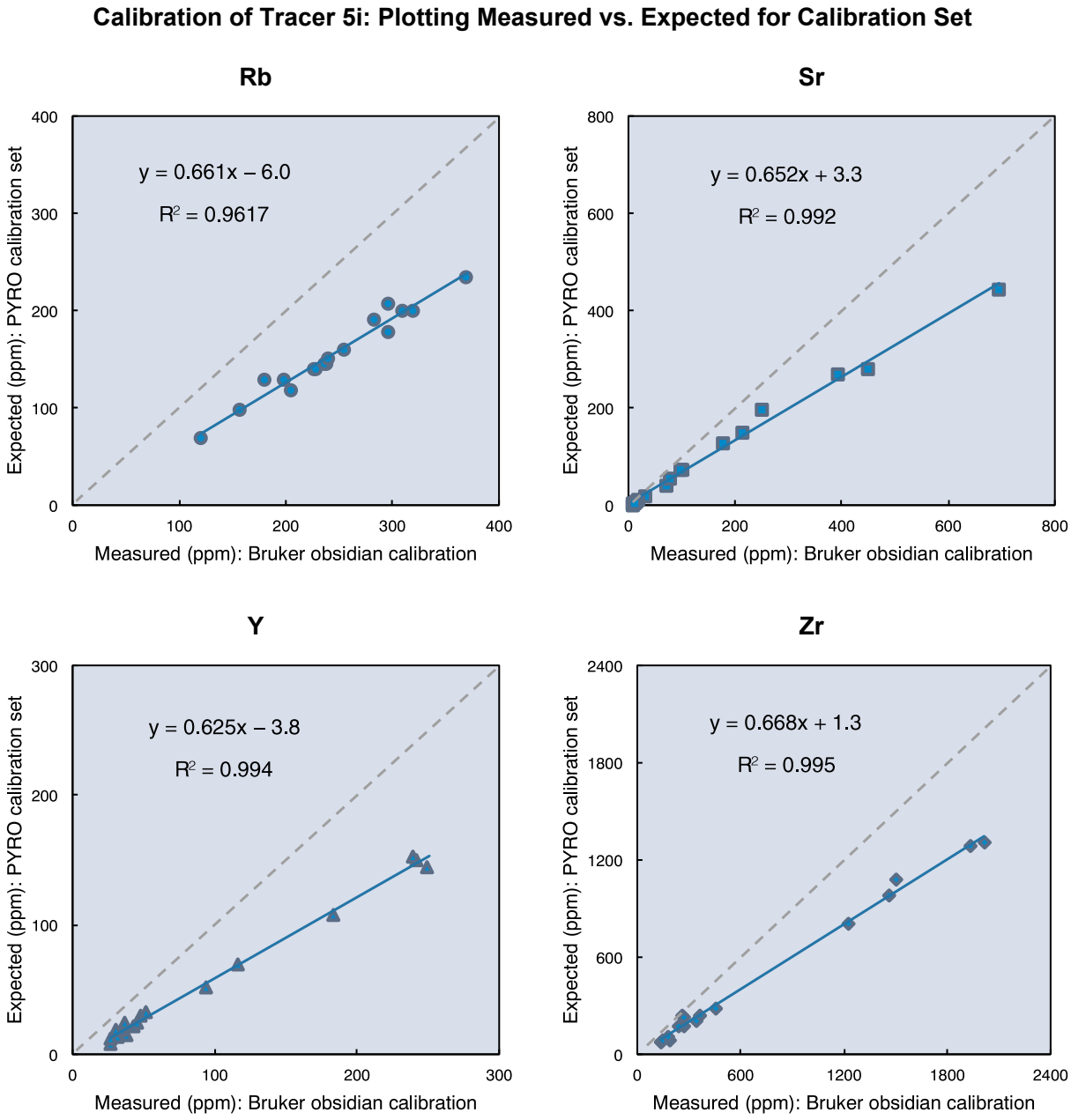

Fig. 10. Use of the PYRO calibration specimens with Rb, Sr, Y, and Zr to derive linear regression equations to apply to the factory-set Bruker Tracer 5i "obsidian" calibration.

Rb, Sr, Y, and Zr), which required less adjustment than Nb.

In September 2018, Jeffrey Ferguson at MURR analyzed 31 of the 35 PYRO specimens (17 of 20 calibration specimens, 14 of 15 check specimens) with a new Bruker Tracer 5i pXRF instrument. This model has a Rh anode, 4 W tube, and 20 mm^2 SDD with a high resolution ($\lesssim$140 eV), and it used the MURR-developed and Bruker-installed obsidian calibration that Ferguson helped to devise and test in 2012 (Glascock and Ferguson, 2012). The Tracer 5i consistently reported higher elemental values relative to the Thermo benchtop EDXRF instrument at MURR. Fig. 10 illustrates these trends for four elements (i.e., Rb, Sr, Y, and Zr). Applying the same regression analysis protocol, as shown in Fig. 11, reveals how these measurements can also align with the PYRO data.

Most importantly, Fig. 12 illustrates how the PYRO-calibrated Olympus Vanta and Tracer 5i datasets reproduce each other. For comparison, Fig. 13 shows the reproducibility between the MURR and NWROSL EDXRF datasets. Reproducibility between the PYRO-calibrated instruments compares favorably. Additionally, plotting the two pXRF datasets together (Fig. 14) further demonstrates their compatibility, despite considerable differences in their correction scheme (i.e., FP vs. empirical) and factory calibration (i.e., ~40 geological SRMs vs. 40 MURR-characterized obsidians).

7. Peabody loan policies and accession

The PYRO sets are intended to be freely available to researchers via a loan (i.e., a temporary physical transfer without an ownership transfer) arranged with the Yale University Archaeological Laboratories, where most sets will reside. The precise loan policies will likely be refined over time; however, the guidelines reflect those of Yale's Peabody Museum of Natural History. Specifically, the loan of a

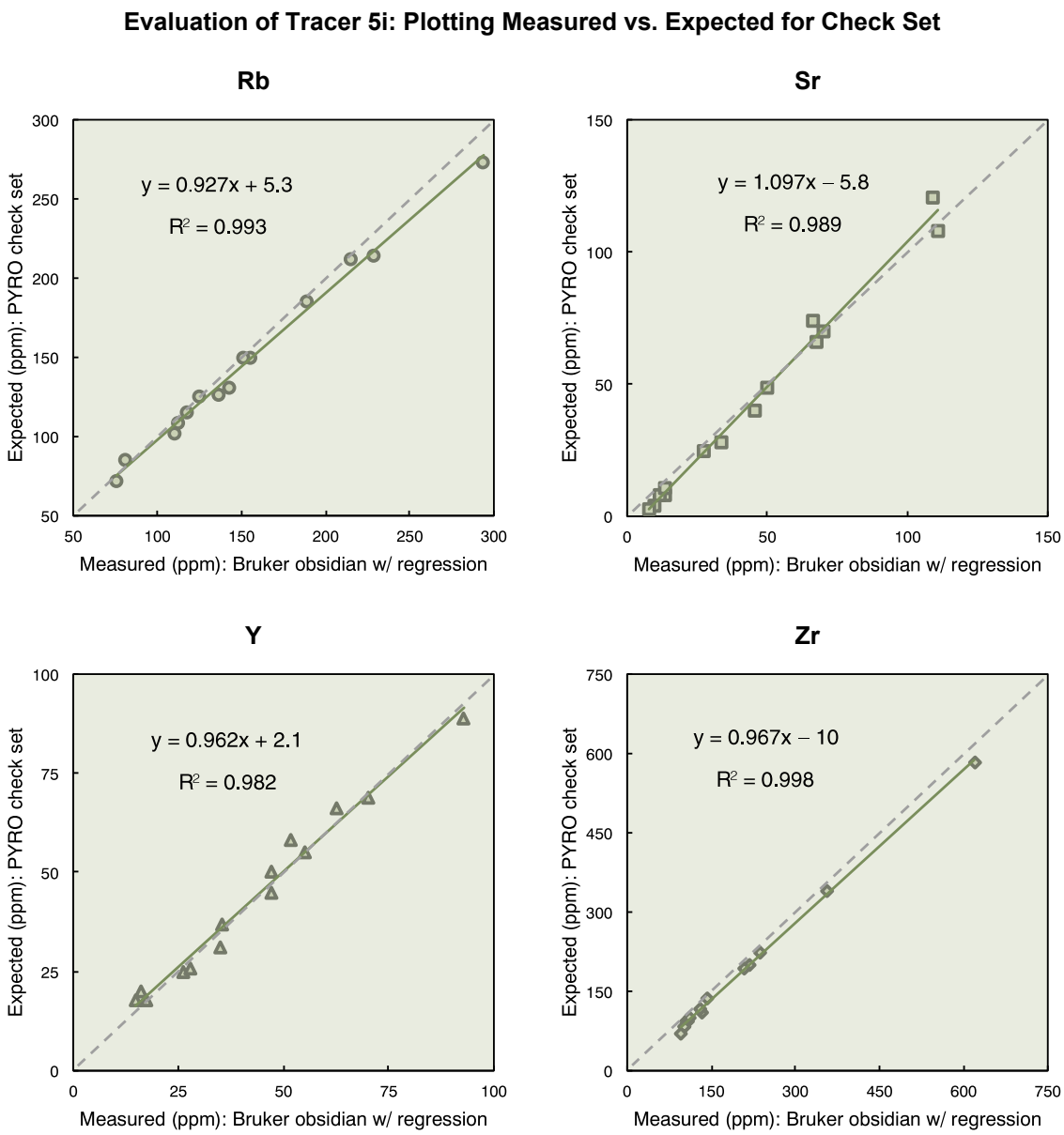

Fig. 11. Use of the PYRO check specimens with Rb, Sr, Y, and Zr to evaluate the PYRO-calibrated data for Bruker Tracer 5i instrument.

PYRO set will be subject to the following stipulations:

- Loans are made for non-commercial and scholarly purposes (i.e., without financial gain; e.g., a borrower cannot charge someone a fee to calibrate an instrument with a loaned PYRO set). A loaned set will only be sent to an accredited educational or research institution.
- Loan requests should be made in writing on institutional letterhead. A request should state the purpose of the loan, a brief project description, where and under whose responsibility a set would be housed while on loan, and the requested length of the loan period.
- A loan is made to institutions, not individuals. Students, postdoctoral scholars, and visiting researchers cannot enter into formal agreements on behalf of their institutions. Therefore, a permanent faculty member or department head should submit a request on their behalf and assume responsibility, as an institutional representative, for the care and custody of a set. A set cannot be transferred to a third party without prior written authorization.
- Specimens in the set should not be sampled, remounted, or altered in any way. Many, but not all, of the PYRO specimens have corresponding unmounted material that may be requested, if a sufficient amount is available, for destructive compositional analyses.

As an alternative to a formal loan, qualified researchers may analyze a PYRO set using their instrument during a scheduled visit to the Yale University Archaeological Laboratories.

To aid the longevity of the PYRO sets, one set will be accessioned by the Peabody Museum of Natural History. Founded in 1866, the museum has been a center of geological, anthropological, and biological research at Yale for > 150 years, and its collections will be available to scholars for the next 150 years. Archaeological and geological interest in obsidian at the Peabody dates to its nineteenth-century origins (Dana, 1869; Iddings, 1885, 1888; Iddings and Penfield, 1890;

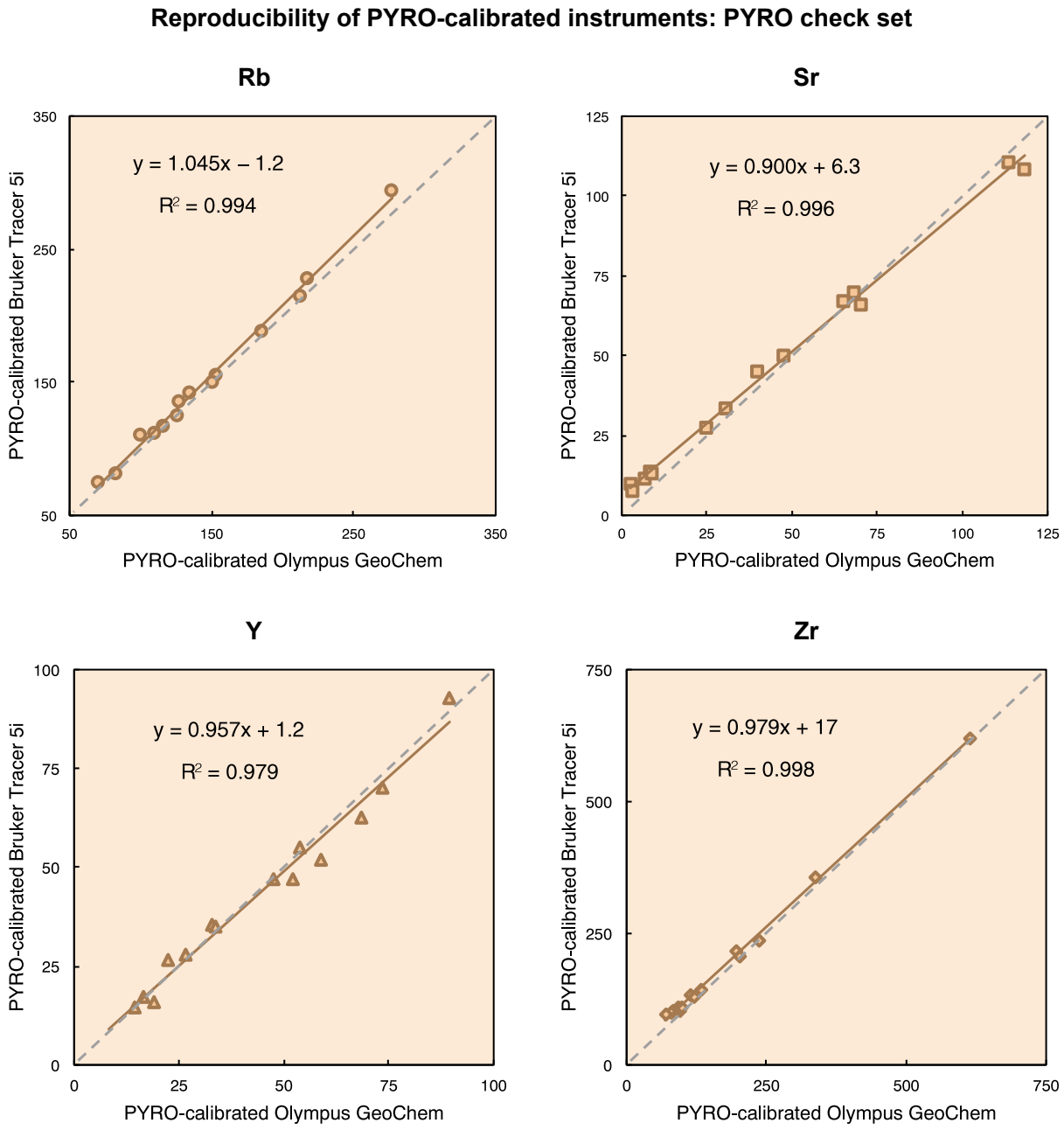

Fig. 12. Reproducibility of two PYRO-calibrated pXRF instruments for Rb, Sr, Y, and Zr based on 14 PYRO specimens from the check sets, which are intended for evaluating calibrated elemental data.

MacCurdy, 1900), and Yale researchers later played central roles in the developing XRF techniques for obsidian sourcing. Following his work on obsidian artifacts, technology, and sources in Guatemala (Coe, 1960; Coe and Flannery, 1964), Michael Coe initiated a Mesoamerican obsidian characterization program in collaboration with Robert Cobean (a Harvard graduate student at the time) and Yale geochemists Karl Turekian, Edward Perry, and Dinkar Kharkar. The Guatemalan and Mexican obsidian collected between 1969 and 1972 became known in the literature as the "Yale Collection" (Vogt et al., 1982), and the specimens were analyzed using XRF in the Department of Geology and Geophysics (Cobean et al., 1971; Zeitlin, 1979, 1982; Zeitlin and Heimbuch, 1978). Coincidentally, Cobean and colleagues later surveyed and sampled obsidian sources across central Mexico, a project that eventually led to the creation of the Archaeometry Lab at MURR (Glascock et al., 2007). Hence, researchers also have the option to access a PYRO set as a visiting scholar at the Peabody Museum.

8. Concluding remarks

This project, which has been no small endeavor, is meant to facilitate, not mandate, a shift to more settled calibration and evaluation protocols among archaeologists – especially those with less experience – using EDXRF and pXRF to source obsidian artifacts. Falling back on Killick's metaphor of the "awkward adolescence of archaeological science," adolescence is, of course, a time of difficult, sometimes painful, developmental challenges, which, it seems, is what Killick (2015) had

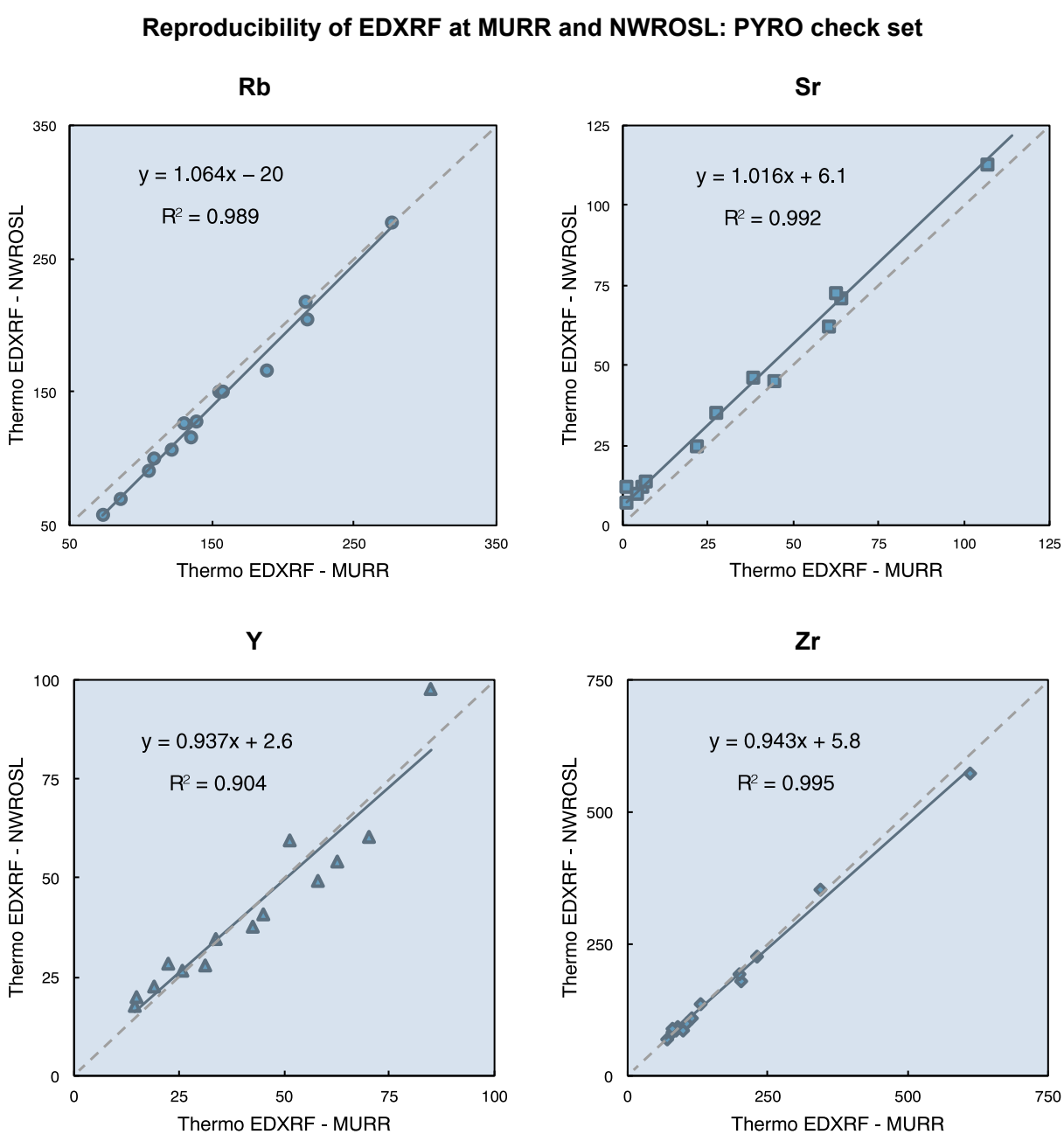

Fig. 13. Reproducibility of benchtop EDXRF (Thermo instruments) measurements at MURR and NWROSL for Rb, Sr, Y, and Zr based on 14 PYRO specimens from the check sets, which are intended for evaluating calibrated elemental data. The MURR instrument is calibrated using a version of the MURR/Bruker calibration (as described in Section 2.2), while the NWROSL instrument is calibrated using a collection of geological SRMs (as described in Section 2.1).

in mind. It is also, however, a time of experimentation and greater independence. As mentioned at the start of this paper, EDXRF experts' critiques of pXRF use have been, on the whole, more programmatic than pragmatic. Notably, Killick (2015) also cautioned about disparities in access to the techniques and tools of archaeological science. Portable instruments, such as pXRF, are certainly more accessible to archaeologists around the world than, for instance, varieties of mass spectrometry. Whether we are considering the adolescence or accessibility of pXRF in obsidian artifact sourcing, experts have issued (sometimes strongly worded) advice in the literature, at conferences, and in peer reviews. Whether or not they are correct is beside the point. The point is that we know, based on studies into learning and lithic technologies, that such an approach can be largely ineffective (e.g., Tostevin, 2012; Lombao et al., 2017; Ranhorn et al., forthcoming). It might seem obvious that a novice flintknapper could not replicate a Levallois point or a Mesoamerican prismatic blade after simply encountering one on the landscape. Nor can novices effectively replicate such tools by following a list of instructions handed to them. Left on their own, novices would be unlikely to select the proper implements to make such tools. Instead, active guidance is much more effective for a novice to learn the proper techniques and attain the desired outcome. This, we can predict, holds true not only for making stone tools but also for conducting elemental analyses of them. Consequently, the proximate goal of the PYRO sets is to serve as a tool for almost anyone to meet – and to exceed – experts' practices regarding accuracy, reproducibility, and scientific transparency, whereas the ultimate aim is to facilitate collaborations and "big data" projects. Making the PYRO sets freely available and "open-source" (i.e., all the source information is shared here) will hopefully aid in the realization of these goals.

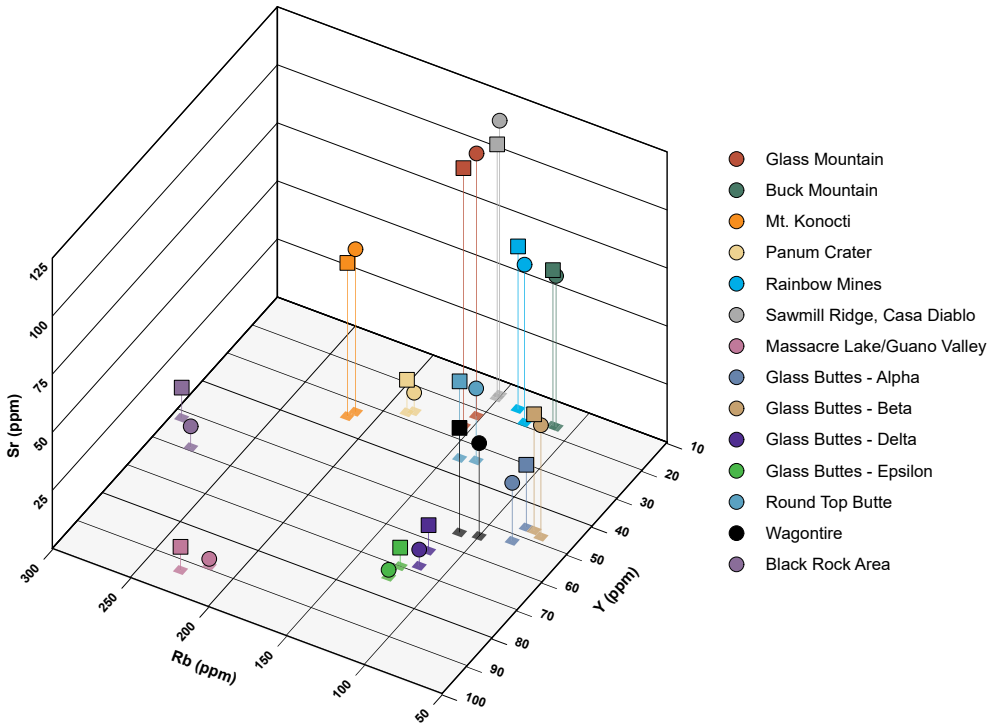

Fig. 14. Three-dimensional scatterplot of Rb, S, and Y for two PYRO-calibrated pXRF instruments' (Fig. 12) measurements of 14 check set specimens from the North American West, demonstrating the resulting similarities between their calibrated analyses for these obsidians.

Declaration of competing interest

The author declares that there is no conflict of interest.

Acknowledgements

Jeff Ferguson and Mike Glascock (MURR Archaeometry Lab) as well as Craig Skinner and Alex Nyers (Northwest Research Obsidian Studies Lab) graciously provided analytical data for many specimens in the PYRO sets (and other specimens that did not make the final cut). Funding for NAA conducted at MURR was provided by Yale's Council on Archaeological Studies and Anthropology Department, which also funded all of the supplies, consumables, and equipment. The sets (and acronym) were, in part, inspired by the Copper CHARM Set, spearheaded by Arlen Heginbotham at the J. Paul Getty Museum. An undergraduate intern, Steven Newman, conducted the rock magnetic measurements at the University of Minnesota's Institute for Rock Magnetism, where we had invaluable assistance from Josh Feinberg, Mike Jackson, and Peter Sølheid. Electron microscopy was conducted in the University of Minnesota's Electron Microprobe Laboratory. The Glass Mountain obsidian specimens studied by electron microscopy and magnetic analysis were lent by Carolyn Dillian. Specimen preparation was supported by Liev Frahm. An earlier version of this calibration set was a component of my project *Portable XRF Applications in Archaeology* with Roger Doonan at the University of Sheffield under the NARNIA Project, a Marie Curie research network funded by the FP7 and the European Union (Grant #265010). Other support came, at one time or another, from the Anthropology and Earth Sciences Departments at the University of Minnesota; the University of Minnesota's Undergraduate Research Opportunity Program (UROP); the University of Minnesota's Grant-in-Aid of Research, Artistry, and Scholarship Program; the Pleistocene Archaeology, Geochronology, and Environment of the Southern Caucasus (PAGES) Project funded by the Leverhulme Trust (Grant RPG-2016-102); and the Hrazdan Gorge Palaeolithic Project (HGPP) funded by the University of Connecticut and Leakey Foundation. The Olympus Vanta instrument in this study was purchased thanks to the support from Yale's Offices of the Vice Provost for Research, Dean of Science, and Dean of Social Science. Other contributors to the project and related ones – at one point or another – include, in alphabetical order: Tsegaye Abebe Adhana, Daniel Adler, Elizabeth Anthony, Pavel Avetisyan, Frank Brown, Gaye Demir, Hasan Diker, Tuncay Ercan, LeRoy Frahm, Vincenzo Francaviglia, Boris Gasparyan, Katherine Hayes, Charissa Johnson, Sergei Karapetian, Suren Kesejyan, François-Xavier Le Bourdonnec, Khachatur Meliksetian, Harry Merrick, George Rapp, Jean-Paul Raynal, Ming Hua Ren, Nino Sadradze, and Keith Wilkinson. Steve Shackley said in the Fryxell Award session held in his honor at the 2019 Society for American Archaeology annual meeting: “You can blame me for Ellery Frahm” – credit where credit is due. Many students had to put up with this project, from noise of the rock saw and unpleasant smells of curing epoxy to dealing with bags of obsidian spread out all over the Archaeomaterials Suite lab tables for nearly two years. Three anonymous reviewers are thanked for their positive response to this work. All errors and interpretations are my own.

References

Abedi, A., Varoutsikos, B., Chataigner, C., 2018. Provenance of obsidian artifacts from the Chalcolithic site of Dava Göz in NW Iran using portable XRF. J. Archaeol. Sci. Rep. 20, 756–767.

Ambroz, J.J., Glascock, M.D., Skinner, C.E., 2001. Chemical differentiation of obsidian within the glass buttes complex, Oregon. J. Archaeol. Sci. 28, 741–746.

Amick, D.S., 2013. Way out west: Cody complex occupations from the northwestern Great Basin. In: Knell, E.J., Muniz, M.P. (Eds.), Paleoindian Lifeways of the Cody Complex. University of Utah Press, pp. 215–245.

Andrews, A.P., Asaro, F., Michel, H.V., Stross, F.H., Rivero, P.C., 1989. The obsidian trade at Isla Cerritos, Yucatán. Mexico. Journal of Field Archaeology 16, 355–363.

Asaro, F., Salazar, E., Michel, H., Burger, R., Stross, F., 1994. Ecuadorian obsidian sources used for artifact production and methods for provenience assignments. Lat. Am. Antiq. 5 (3), 257–277.

Barca, D., Lucarini, G., Fedele, F.G., 2012. The provenance of obsidian artefacts from the Wādī Ath-Thayyilah 3 Neolithic site (Eastern Yemen Plateau) by LA–ICP–MS. Archaeometry 54, 603–622.

Barrett, T., Shannon, R., Wade, J., Lang, J., 2012. XRF analysis of historical paper in open books. In: Shugar, A.N., Mass, J.L. (Eds.), Handheld XRF for Art and Archaeology. University Press, Leuven 191124.

Beckhoff, B., Kanngießer, B., Langhoff, N., Wedell, R., Wolff, H., 2006. Handbook of Practical X-Ray Fluorescence Analysis. Springer-Verlag.
Bellot-Gurlet, L., Dorighel, O., Poupeau, G., 2008. Obsidian provenance studies in Colombia and Ecuador: Obsidian sources revisited. J. Archaeol. Sci. 35, 272–289.
Biagi, P., Nisbet, R., Gratuze, B., 2017. Obsidian mines and their characterization: New aspects of the exploitation of the obsidian sources of Mt. Chikiani (Koyun Dağ) in the Lesser Caucasus of Georgia. The Quarry 12, 2–24.
Biró, T.K., Pozsgai, I., 1984. Obszidian Lelöhely-Azonositas Elektronsugaras Mikroanalizis Segitsegevel (obsidian characterization by electron microprobe analysis). In: Iparregeszet 2 (Industrial Archaeology II), pp. 25–38.
Biró, T.K., Pozsgai, I., Vlader, A., 1986. Electron beam microanalyses of obsidian samples from geological and archaeological sites. Acta Archaeologica Academiae Scientiarum Hungaricae 38, 257–278.
Bishop, R.L., 1992. Comments on section II: Variation. In: Neff, H. (Ed.), Chemical Characterization of Ceramic Pastes in Archaeology. Prehistory Press, Madison, WI, pp. 167–170.
Bishop, R.L., Olin, J.S., Blackman, M.J., 1983. SARCAR: a new archaeometric resource. In: ICOM Committee for Conservation, 7th Triennial Meeting Preprints, pp. 84.8.1–84.8.2.
Blackman, M.J., Bishop, R.L., 2007. The Smithsonian-NIST partnership: the application of instrumental neutron activation analysis to archaeology. Archaeometry 49, 321–341.
Blackman, M.J., Badalian, R., Kikodze, Z., Kohl, P.L., 1998. Chemical characterization of Caucasian obsidian geological sources. In: Cauvin, M.-C., Gourgaud, A., Gratuze, B., Arnaud, N., Poupeau, G., Poidevin, J.L., Chataigner, C. (Eds.), L'obsidienne au Proche et Moyen-Orient: Du Volcan à l'Outil. BAR International Seriespp. 205–231.
Blegen, N., 2017. The earliest long-distance obsidian transport: Evidence from the ~200 ka middle stone age Sibilo school road site, Baringo, Kenya. J. Hum. Evol. 103, 1–19.
Boulanger, M.T., Davis, R.S., Glascock, M.D., 2012. Preliminary characterization and regional comparison of the Dasht-i-Nawur obsidian source near Ghazni, Afghanistan. J. Archaeol. Sci. 39 (7), 2320–2328.
Bowman, H.R., Asaro, F., Perlman, I., 1973. On the uniformity of composition in obsidians and evidence for magmatic mixing. The Journal of Geology 81 (3), 312–327.
Brady, R.T., 2007. Prehistoric Wetland Use in the Mono Lake Basin, Eastern California. Master's thesis. Department of Anthropology, California State University.
Brooks, A.S., Yellen, J.E., Potts, R., Behrensmeyer, A.K., Deino, A.L., et al., 2018. Long-distance stone transport and pigment use in the earliest middle stone age. Science 360 (6384), 90–94.
Brown, F.H., Nash, B.P., Fernandez, D.P., Merrick, H.V., Thomas, R.J., 2013. Geochemical composition of source obsidians from Kenya. J. Archaeol. Sci. 40, 3233–3251.
Burger, R.L., Asaro, F., 1977. Trace Element Analysis of Obsidian Artifacts from the Andes: New Perspectives on Pre-Hispanic Economic Interaction in Peru and Bolivia. UC-Berkeley Archaeological Research Facility (Lawrence Berkeley Laboratory report number LBL6343).
Burger, R.L., Fajardo Rios, F.A., Glascock, M.D., 2006. Potreropampa and Lisahuacho obsidian sources: geological origins of Andahuaylas A and B type obsidians in the province of Aymaraes, Department of Apurimac, Peru. Ñawpa Pacha 28 (1), 109–127.
Burton, J.F., 2010. Data recovery and monitoring at the Snowcreek site (CA-MNO-3) Mammoth Lakes, California. In: Trans-Sierran Archaeological Research Contributions to Trans-Sierran Archaeology, No. 67.
Camp, A.J., 2009. Pre-Archaic Occupations in the West Arm of the Black Rock Desert. Master's thesis. Department of Anthropology, University of Nevada-Reno.
Campbell, S., Healey, E., 2016. Multiple sources: the pXRF analysis of obsidian from Kenan Tepe, S.E. Turkey. J. Archaeol. Sci. Rep. 10, 377–389.
Cann, J.R., Renfrew, C., 1964. The characterization of obsidian and its application to the Mediterranean Region. Proceedings of the Prehistoric Society 30, 111–133.
Carballo, D.M., Carballo, J., Neff, H., 2007. Formative and classic period obsidian procurement in Central Mexico: a compositional study using laser ablation–inductively coupled plasma–Mass spectrometry. Lat. Am. Antiq. 18 (1), 27–43.
Carter, T., Grant, S., Kartal, M., Coşkun, A., Özkaya, V., 2013. Networks and Neolithisation: sourcing obsidian from Körtik Tepe (SE Anatolia). J. Archaeol. Sci. 40, 556–569.
Carter, T., Strasser, T.F., Panagopoulou, E., Campeau, K., Mihailović, D.D., 2018. Obsidian circulation in the early Holocene Aegean: A case study from Mesolithic Damnoni (SW Crete). J. Archaeol. Sci. Rep. 17, 173–183.
Chataigner, C., Gratuze, B., 2014. New data on the exploitation of obsidian in the southern Caucasus (Armenia, Georgia) and Eastern Turkey, part 1: source characterization. Archaeometry 56, 25–47.
Chataigner, C., Işıklı, M., Gratuze, B., Çil, V., 2014. Obsidian sources in the regions of Erzurum and Kars (north-east Turkey). Archaeometry 56, 351–374.
Cherry, J.F., Faro, E.Z., Minc, L., 2010. Field survey and geochemical characterization of the southern Armenian obsidian sources. J. Field Archaeol. 35 (2), 147–163.
Cobean, R.H., Coe, M.D., Perry, E.A., Turekian, K.K., Kharkar, D.P., 1971. Obsidian Trade at San Lorenzo Tenochtitlan, Mexico. Science 174, 666–671.
Cobean, R.H., Vogt, J.R., Glascock, M.D., Stocker, T.L., 1991. High-precision trace-element characterization of major Mesoamerican obsidian sources and further analyses of artifacts from San Lorenzo Tenochtitlan, Mexico. Lat. Am. Antiq. 2 (1), 69–91.
Coble, M.A., Mahood, G.A., 2016. Geology of the High Rock caldera complex, northwest Nevada, and implications for intense rhyolitic volcanism associated with flood basalt magmatism and the initiation of the Snake River Plain–Yellowstone trend. Geosphere 12 (1), 58–113.
Coe, M.D., 1960. A fluted point from Highland Guatemala. Am. Antiq. 25 (3), 412–413.
Coe, M.D., Flannery, K.V., 1964. The pre-Columbian obsidian industry of El Chayal, Guatemala. Am. Antiq. 30 (1), 43–49.
Coleman, M.E., 2010. Radioanalytical Multi-elemental Analysis: New Methodology and Archaeometric Applications. Ph.D. dissertation. University of Missouri-Columbia.
Dana, J.D., 1869. A System of Mineralogy: Descriptive Mineralogy, Comprising the Most Recent Discoveries. J. Wiley & Son.
Davis, M.K., Jackson, T.L., Shackley, M.S., Teague, T., Hampel, J.H., 1998. Chapter 7: Factors affecting the energy-dispersive X-ray fluorescence (EDXRF) analysis of archaeological obsidian. In: Shackley, M.S. (Ed.), Archaeological Obsidian Studies: Method and Theory. vol. 3. Advances in Archaeological and Museum Science, pp. 159–180.
de B. Pereira, C., Miekeley, N., Poupeau, G., Küchler, I., 2001. Determination of minor and trace elements in obsidian rock samples and archaeological artifacts by laser ablation inductively coupled plasma mass spectrometry using synthetic obsidian standards. Spectrochim. Acta B At. Spectrosc. 56 (10), 1927–1940.
Dillian, C., 2002. More Than Toolstone: Differential Utilization of Glass Mountain Obsidian. PhD dissertation. University of California-Berkeley.
Dillian, C.D., Bello, C.A., Shackley, M.S., 2007. Crossing the Delaware: documenting super-long distance obsidian exchange in the mid-Atlantic. Archaeol. East. N. Am. 35, 93–104.
Dillian, C.D., Bello, C.A., Shackley, M.S., 2009. Chapter 2: long-distance exchange of obsidian in the mid-Atlantic United States. In: Dillian, C.D., White, C.L. (Eds.), Trade and Exchange: Archaeological Studies from History and Prehistory. Springer, pp. 17–35.
Donnelly-Nolan, J.M., Champion, D.E., Miller, C.D., Grove, T.L., Trimble, D.A., 1990. Post-11,000-year volcanism at medicine Lake volcano, Cascade Range, northern California. J. Geophys. Res. 704 (95B:19) 693619.
Draucker, A.C., 2007. Geochemical characterization of obsidian subsources from the Coso Range. In: California Using Laser Ablation Inductively Coupled Plasma Mass Spectrometry as a Tool for Archaeological Investigations. Department of Geology, California State University, Bakersfield Master's thesis.
Dunlop, D.J., 2002. Theory and application of the day plot (Mrs/Ms versus Hcr/Hc), 1. Theoretical curves and tests using titanomagnetite data. J. Geophys. Res. 107 (B3) (EPM 4-14-22).
Ebert, C.E., Dennison, M., Hirth, K.G., McClure, S.B., Kennett, D.J., 2015. Formative period obsidian exchange along the Pacific coast of Mesoamerica. Archaeometry 57, 54–73.
Eichelberger, J.C., 1975. Origin of andesite and dacite: evidence of mixing at Glass Mountain and other Circum-Pacific volcanoes. Geol. Soc. Am. Bull. 86, 1381–1391.
Eichelberger, J.C., 1981. Mechanism of magma mixing at Glass Mountain, medicine Lake Highland volcano, California. In: Johnston, D.A., Donnelly-Nolan, J. (Eds.), US Geological Survey Circular. vol. 838. pp. 183–189.
Elizalde-Rodarte, S.V., Tenorio, D., Jiménez-Reyes, M., 2016. Three Mayan archaeological sites of the eastern coast of the Yucatan Peninsula: Source identification of obsidian artifacts by NAA. J. Archaeol. Sci. Rep. 8, 22–27.
Estes, M.B., 2009. Paleoindian Occupations in the Great Basin: A Comparative Study of Lithic Technological Organization, Mobility, and Landscape Use from Jakes Valley, Nevada. Master's thesis. Department of Anthropology, University of Nevada, Reno.
Farrell, M.M., Burton, J.F., 2010. Plum family Mammoth Lakes partnership Mammoth Lakes, California (TPM 10-01) archaeological survey and evaluation. In: Trans-Sierran Archaeological Research Contributions to Trans-Sierran Archaeology No. 68.
Ferguson, J.R., 2012. Chapter 12: X-ray fluorescence of obsidian: approaches to calibration and the analysis of small samples. In: Shugar, A.N., Mass, J.L. (Eds.), Handheld XRF for Art and Archaeology. Leuven University Press, Leuven, pp. 401–422.
Ferguson, J.R., Glascock, M.D., Izuho, M., Mukai, M., Wada, K., Sato, H., 2014. Multi-method characterisation of obsidian source compositional groups on Hokkaido Island (Japan). In: Ono, A., Suda, Y., Glascock, M.D. (Eds.), Methodological Issues of Obsidian Provenance Studies and the Standardization of Geologic Obsidian. BAR International Series, Oxford, pp. 13–32.
Fernández, M.V., Barberena, R., Rughini, A.A., Giesso, M., Cortegoso, V., Durán, V., Villanueva, G.R., Borrazzo, K., Lucero, G., Garvey, R., MacDonald, B.L., Glascock, M.D., 2017. Obsidian geochemistry, geoarchaeology, and lithic technology in northwestern Patagonia (Argentina). J. Archaeol. Sci. Rep. 13, 372–381.
Ford, M.T., 2012. Rhyolitic Magmatism of the High Lava Plains and Adjacent Northwest Basin and Range, Oregon: Implications for the Evolution of Continental Crust. Doctoral dissertation. Oregon State University.
Foresta Martin, F., Di Piazza, A., D'Oriano, C., Carapezza, M.L., Paonita, A., Rotolo, S.G., Sagnotti, L., 2017. New insights into the provenance of the obsidian fragments of the island of Ustica (Palermo, Sicily). Archaeometry 59, 435–454.
Forster, N., Grave, P., Vickery, N., Kealhofer, L., 2011. Non-destructive analysis using PXRF: methodology and application to archaeological ceramics. X-Ray Spectrom. 40, 389–398.
Fowler, W.R., Kelley, J.H., Asaro, F., Michel, H.V., Stross, F.H., 1987. The chipped stone industry of Cihuatan and Santa Maria, El Salvador, and sources of obsidian from Cihuatan. Am. Antiq. 52 (1), 151–160.
Frahm, E., 2007. An evaluation of portable X-ray fluorescence for artifact sourcing in the field: Can a handheld device differentiate Anatolian obsidian sources? Geological Society of America annual meeting, Denver, Colorado, 28-31 October. Geol. Soc. Am. Abstr. Programs 39 (6), 29.
Frahm, E., 2010. The Bronze-Age Obsidian Industry at Tell Mozan (Ancient Urkesh), Syria. Ph.D. dissertation. Department of Anthropology, University of MinnesotaTwin Cities.
Frahm, E., 2012. Non-destructive sourcing of Bronze-Age Near Eastern obsidian artefacts: redeveloping and reassessing electron microprobe analysis for obsidian sourcing. Archaeometry 54 (4), 623–642.
Frahm, E., 2013. Validity of “off-the-shelf” handheld portable XRF for sourcing Near Eastern obsidian chip debris. J. Archaeol. Sci. 40 (2), 1080–1092.
Frahm, E., 2014. Characterizing obsidian sources with portable XRF: Accuracy, reproducibility, and field relationships in a case study from Armenia. J. Archaeol. Sci. 49, 105–125.

Frahm, E., 2016. Can I get chips with that? Obsidian sourcing down to the microdebitage with portable XRF. J. Archaeol. Sci. Rep. 9, 448–467.
Frahm, E., 2017. First hands-on tests of an Olympus Vanta portable XRF analyzer to source Armenian obsidian artifacts. International Association for Obsidian Studies Bulletin 58, 8–23.
Frahm, E., 2019. Beyond the Technical Revolution: Epistemological Shifts in Archaeological XRF (or: "The World of XRF Will Never be the Same Again"). Society for American Archaeology Annual Meeting, Albuquerque, New Mexico (10-14 April).
Frahm, E., Doonan, R.C.P., 2013. The technological versus methodological revolution of portable XRF in archaeology (review). J. Archaeol. Sci. 40 (2), 1425–1434.
Frahm, E., Feinberg, J.M., 2013. From flow to quarry: magnetic properties of obsidian and changing the scales of archaeological sourcing. J. Archaeol. Sci. 40, 3706–3721.
Frahm, E., Feinberg, J.M., 2015. Reassessing obsidian field relationships at Glass Buttes, Oregon. J. Archaeol. Sci. Rep. 2, 654–665.
Frahm, E., Tryon, C.A., 2018a. Origins of Epipalaeolithic obsidian artifacts from Garrod's excavations at Zarzi cave in the Zagros foothills of Iraq. Journal of Archaeological Sci. Reports 21, 472–485.
Frahm, E., Tryon, C.A., 2018b. Later Stone Age toolstone acquisition in the Central Rift Valley of Kenya: Portable XRF of Eburran obsidian artifacts from Leakey's excavations at Gamble's Cave II. J. Archaeol. Sci. Rep. 18, 475–486.
Frahm, E., Doonan, R.C.P., Kilikoglou, V., 2014a. Handheld portable X-ray fluorescence of Aegean obsidians. Archaeometry 56, 228–260.
Frahm, E., Feinberg, J.M., Schmidt-Magee, B.A., Wilkinson, K.N., Gasparyan, B., Yeritsyan, B., Karapetian, S., Meliksetian, Kh., Muth, M.J., Adler, D.S., 2014b. Sourcing geochemically identical obsidian: Multiscalar magnetic variations in the Gutansar volcanic complex and implications for Palaeolithic research in Armenia. J. Archaeol. Sci. 47, 164–178.
Frahm, E., Campbell, S., Healey, H., 2016. Caucasus connections? New data and interpretations for Armenian obsidian in Northern Mesopotamia. J. Archaeol. Sci. Rep. 9, 543–564.
Frahm, E., Goldstein, S.T., Tryon, C.A., 2017a. Late Holocene forager-fisher and pastoralist interactions along the Lake Victoria shores, Kenya: Perspectives from portable XRF of obsidian artifacts. J. Archaeol. Sci. Rep. 11, 717–742.
Frahm, E., Sherriff, J., Wilkinson, K.N., Beverly, E.J., Adler, D.S., Gasparyan, B., 2017b. Ptghni: A new obsidian source in the Hrazdan River Basin, Armenia. J. Archaeol. Sci. Rep. 14, 55–64.
Francaviglia, V., 1990. Characterization of Mediterranean obsidian sources by classical petrochemical methods. Preistoria Alpina 20, 311–332.
Francaviglia, V., 1994. L'origine des Outils en Obsidienne de Tell Magzalia, Tell Sotto, Yarim Tepe et Kül Tepe, Iraq. Paléorient 20 (2), 18–31.
Gaffney, D., Summerhayes, G.R. 2018. Coastal mobility and lithic supply lines in northeast New Guinea. Archaeol. Anthropol. Sci.. doi.org/https://doi.org/10.1007/s12520-018-0713-8.
George, R.J., II. 2013. Obsidian Use by Coastal Hunter-Gatherers in Southern California: Provenance Analysis of Obsidian Artifacts from CA-ORA-64 Comparing XRF and LA-TOF-ICP-MS. Master's thesis, Department of Anthropology, California State University-Fullerton.
Giauque, R.D., Asaro, F., Stross, F.H., Hester, T.R., 1993. High-precision non- destructive x-ray fluorescence method applicable to establishing the provenance of obsidian artifacts. X-Ray Spectrom. 22, 44–53.
Gibson, I.L., 1970. A Pantelleritic welded ash-flow tuff from the Ethiopian Rift Valley. Contr. Mineral. and Petrol. 28, 89–111.
Gibson, I.L., 1972. The chemistry and petrogenesis of a suite of pantellerites from the Ethiopian rift. J. Petrol. 13, 31–34.
Gillette, D.L., 2011. Cultural Markings on the Landscape: The PCN Pecked Curvilinear Nucleated Tradition in the Northern Coastal Ranges of California. Doctoral thesis. Department of Anthropology, University of California-Berkeley.
Gladney, E.S., Roelandts, I., 1988. 1987 compilation of elemental concentration data for USGS BHVO-1, MAG-1, QLO-1, RGM-1, SCo-1, SDC-1, SGR-1 and STM-1. Geostand. Newslett. 12, 253–362.
Glascock, M.D., 1999. An inter-laboratory comparison of element compositions for two obsidian sources. Int. Assoc. Obsidian Stud. Bull. 23, 13–25.
Glascock, M.D., 2011. Comparison and contrast between XRF and NAA: used for characterization of obsidian sources in Central Mexico. In: Shackley, M.S. (Ed.), X-ray Fluorescence Spectrometry (XRF) in Geoarchaeology. Springer, pp. 161–192.
Glascock, M.D., 2017. Overview of neutron activation analysis. MURR website. Online at Archaeometry Laboratoryhttp://archaeometry.missouri.edu/naa_overview.html.
Glascock, M.D., Amirkhiz, A.C., 2017. X-ray fluorescence analysis of obsidian artifacts from Cheshmeh Ali, Iran. Ir Cons Sci J 1 (1), 1–5.
Glascock, M.D., Ferguson, J.R., 2012. Report on the Analysis of Obsidian Source Samples by Multiple Analytical Methods. Prepared for Bruce Kaiser, Bruker AXS, Kennewick, WA. Archaeometry Laboratory, University of Missouri Research Reactor Report.
Glascock, M.D., Elam, J.M., Aoyama, K., 1990. Provenience analysis of obsidian artifacts from the La Entrada region, Honduras. In: Pernicka, E., Wagner, G.A. (Eds.), Archaeometry '90. Birkhäuser Verlag, Basel, pp. 395–404.
Glascock, M.D., Braswell, G., Cobean, R.H., 1998. A systematic approach to obsidian source characterization. In: Shackley, M.S. (Ed.), Archaeological Obsidian Studies: Method and Theory. Society for Archaeological Sciences, pp. 15–65.
Glascock, M.D., Speakman, R.J., Neff, H., 2007. Archaeometry at the University of Missouri Research Reactor and the provenance of obsidian artefacts in North America. Archaeometry 49, 343–357.
Glascock, M.E., Weigan, P.C., Esparza López, R., Ohnersorgen, M.A., Garduño Ambriz, M., Mountjoy, J.B., Darling, J.A., 2010. Geochemical characterisation of obsidian in western Mexico: the sources in Jalisco, Nayarit, and Zacatecas. In: Kuzmin, Y.V., Glascock, M.D. (Eds.), Crossing the Straits: Prehistoric Obsidian Source Exploitation in the North Pacific Rim. BAR International Series, vol. 2152. Archaeopress, Oxford, pp. 201–217.
Goff, F., Bergfeld, D., Janik, C.J., Counce, D., Stimac, J.A., 2001. Geochemical Data on Waters, Gases, Rocks, and Sediments from the GeysersClear Lake Region, California (19912000). Los Alamos National Laboratory.
Golitko, M., 2019. The potential of obsidian "big data". UISPP: Journal of the International Union for Prehistoric and Protohistoric Sciences 2 (1), 83–98.
Govindaraju, K., 1994. 1994 compilation of working values and sample description for 383 geostandards. Geostand. Newslett. 18 (Special Issue), 1–58.
Grave, P., Attenbrow, V., Sutherland, L., Pogson, R., Forster, N., 2012. Non-destructive pXRF of mafic stone tools. J. Archaeol. Sci. 39, 1674–1686.
Grebennikov, A.V., Kuzmin, Y.V., Glascock, M.D., Popov, V.K., Budnitskiy, S.Y., Dikova, M.A., Nozdrachev, E.A., 2018. The Lake Krasnoe obsidian source in Chukotka (Northeastern Siberia): geological and geochemical frameworks for provenance studies in Beringia. Archaeol. Anthropol. Sci. 10, 599–614.
Green, R.C., 1998. A 1990s perspective on method and theory in archaeological volcanic glass studies. In: Shackley, M.S. (Ed.), Archaeological Obsidian Studies. Springer, pp. 223–235.
Grove, T.L., Donnelly-Nolan, J.M., Housh, T.B., 1997. Magmatic processes that generated the rhyolite of Glass Mountain, Medicine Lake volcano. Contrib. Mineral. Petrol. 127 (3), 205–233.
Haarklau, L., Johnson, L., Wagner, D.L., 2005. Fingerprints in the Great Basin: The Nellis Air Force Base Regional Obsidian Sourcing Study. U.S. Army Corps of Engineers, Fort Worth District.
Hall, M., 2016. X-ray fluorescence-energy dispersive (ED-XRF) and wavelength dispersive (WD-XRF) spectrometry. In: Hunt, Alice (Ed.), The Oxford Handbook of Archaeological Ceramic Analysis. Oxford University Press.
Hall, M., Kimura, H., 2002. Quantitative EDXRF studies of obsidian sources in northern Hokkaido. J. Archaeol. Sci. 29, 259–266.
Hancock, R.G.V., Carter, T., 2010. How reliable are our published archaeometric analyses? Effects of analytical techniques through time on the elemental analysis of obsidians. J. Archaeol. Sci. 37 (2), 243–250.
Harbottle, G., Bishop, R.L., 1992. Commentary on technique. In: Neff, H. (Ed.), Chemical Characterization of Ceramic Pastes in Archaeology. Prehistory Press, Madison, WI, pp. 27–29.
Harbottle, G., Neff, H., Bishop, R.L. 1994. Appendix C: the sources of Copan Valley obsidian. In: Ceramics and Artifacts from Excavations in the Copan Residential Zone, by G.R. Willey, R.M. Leventhal, A.A. Demarest, and W.L. Fash Jr., pp. 445457. Papers of the Peabody Museum of Archaeology and Ethnology vol. 80, Harvard University.
Harmon, R.S., Throckmorton, C.S., Hard, R.R., Gottfried, J.L., Wörner, G., Harpp, K., Collins, L., 2018. Discriminating volcanic centers with handheld laser-induced breakdown spectroscopy (LIBS). J. Archaeol. Sci. 98, 112–127.
Healey, P.F., McKillop, H.I., Walsh, B., 1984. Analysis of obsidian from Moho Cay, Belize: new evidence on Classic Maya trade routes. Science 225 (4660), 414–417.
Heginbotham, A., Bezur, A., Bouchard, M., Davis, J.M., Eremin, K., Frantz, J.H., Glinsman, L., Hayek, L.-A., Hook, D., Kantarelou, V., Karydas, A.G., Lee, L., Mass, J., Matsen, C., McCarthy, B., McGath, M., Shugar, A., Sirois, J., Smith, D., Speakman, R.J., 2011. An evaluation of inter-laboratory reproducibility for quantitative XRF of historic copper alloys. In: Mardikian, P., Chemello, C., Watters, C., Hull, P. (Eds.), Metal 2010: Proceedings of the Interim Meeting of the ICOMCC Metal Working Group, October 1115, 2010, Charleston, South Carolina. Clemson University Press.
Heginbotham, A., Bassett, J., Bourgarit, D., Eveleigh, C., Glinsman, L., Hook, D., Smith, D., Speakman, R.J., Shugar, A., Van Langh, R., 2015. The copper CHARM set: a new set of certified reference materials for the standardization of quantitative X-ray fluorescence analysis of heritage copper alloys. Archaeometry 57, 856–868.
Heizer, R.F., Williams, H., Graham, J., 1965. Notes on Mesoamerican obsidians and their significance in archaeological studies. In: Contributions of the University of California Archaeological Research Facility. vol. 1. pp. 94–103.
Helzer, M.M., 2001. Paleoethnobotany and Household Archaeology at the Bergen Site: A Middle Holocene Occupation in the Fort Rock Basin, Oregon. Doctoral thesis. Department of Anthropology, University of Oregon.
Hibbert, D.B., 2007. Quality Assurance in the Analytical Chemistry Laboratory. Oxford University Press.
Higashimura, T., Warashina, T., 1975. Sourcing of sanukite stone implements by X-ray fluorescence analysis. J. Archaeol. Sci. 2, 169–l78.
Hughes, R.E., 1982. Age and exploitation of obsidian from the Medicine Lake Highland, California. J. Archaeol. Sci. 9, 173–185.
Hughes, R.E., 1984. Obsidian studies in the Great Basin: problems and prospects. In: Contributions of the University of California Archaeological Research Facility No. 45, Berkeley, California.
Hughes, R.E., 1986. Diachronic variability in obsidian procurement patterns in northeastern California and southcentral Oregon. In: University of California Publications in Anthropology 17, Berkeley, California.
Hughes, R.E., 1988. The Coso volcanic field reexamined: implications for obsidian sourcing and hydration dating research. Geoarchaeology 3 (4), 253–265.
Hughes, R.E., 1989. A new look at Mono Basin obsidians. In: Hughes, Richard E. (Ed.), Current Directions in California Obsidian Studies. Contributions of the University of California Archaeological Research Facility No. 48, pp. 1–12.
Hughes, R.E., 1994. Intrasource chemical variability of artefact-quality obsidians from the Casa Diablo Area, California. J. Archaeol. Sci. 21, 263–271.
Hughes, R.E., 2007. The geologic sources for obsidian artifacts from Minnesota archaeological sites. The Minnesota Archaeologist 66, 53–68.
Hughes, R.E., 2015. Prehistoric obsidian conveyance in the Eastern Great Basin: evidence from Hogup and danger caves, Utah. J. Archaeol. Sci. Rep. 4, 293–309.
Iddings, J.P., 1885. On the occurrence of fayalite in the lithophyses of obsidian and rhyolite in the Yellowstone National Park. Am. J. Sci. 30, 58–60.
Iddings, J.P., 1888. Obsidian Cliff, Yellowstone National Park. Seventh Annual Report of

the United States Geological Survey to the Secretary of the Interior. Government Printing Office, Washington, D.C., pp. 255–295.
Iddings, J.P., Penfield, S.L., 1890. Fayalite in the obsidian of Lipari. Am. J. Sci. 40, 75–78.
Ikeya, N., 2015. Maritime transport of obsidian in Japan during the Upper Paleolithic. In: Kaifu, Y., Izuho, M., Goebel, T., Sato, H., Ono, A. (Eds.), Emergence and Diversity of Modern Human Behavior in Paleolithic Asia. Texas A&M University Press, pp. 362–375.
Jack, R.N., Carmichael, I.S.E., 1968. The chemical "fingerprinting" of acid volcanic rocks. In: California Division of Mines Special Report. vol. 100. pp. 17–32.
Jackson, T.L., 1989. Late prehistoric obsidian production and exchange in the North Coast Ranges, California. In: Hughes, R.E. (Ed.), Current Directions in California Obsidian Studies. Contributions of the University of California Archaeological Research Facility No. 48pp. 79–94.
Jackson, T., Love, M., 1991. Blade running: Middle Preclassic obsidian exchange and the introduction of prismatic blades at La Blanca, Guatemala. Anc. Mesoam. 2 (1), 47–59.
Jarosewich, E., 2002. Smithsonian microbeam standards. J. Res. Natl. Inst. Stand. Technol. 107, 681–685.
Jarosewich, E., Nelen, J.A., Norberg, J.A., 1980. Reference samples for electron microprobe analysis. Geostand. Newslett. 4, 43–47.
Jenkins, D.L., Connolly, T.J., 1990. Archaeology of Indian grade spring: A special function site on Stinkingwater, mountain, Harney County, Oregon. In: University of Oregon Anthropological Papers No. 42.
Jew, N.P., Ainis, A.F., Endzweig, P.E., Erlandson, J.M., Skinner, C., Sullivan, K.J., 2015. Chipped stone crescents from America's Far West: descriptive and geochemical analyses from the Northern Great Basin. North American Archaeologist 36 (2), 119–140.
Jochum, K.P., Weis, U., Schwager, B., Stoll, B., Wilson, S.A., Haug, G.H., Andreae, M.O., Enzweiler, J., 2016. Reference values following ISO guidelines for frequently requested rock reference materials. Geostand. Geoanal. Res. 40 (3), 333–350.
John, D.A., du Bray, E.A., Blakely, R.J., Fleck, R.J., Vikre, P.G., Box, S.E., Moring, B.C., 2012. Miocene magmatism in the Bodie Hills volcanic field, California and Nevada: a long-lived eruptive center in the southern segment of the ancestral Cascades arc. Geosphere 8 (1), 44–97.
Karapetian, S.G., Jrbashian, R.T., Mnatsakanian, A.Kh., 2001. Late collision rhyolitic volcanism in the north-eastern part of the Armenian Highland. J. Volcanol. Geotherm. Res. 112, 189–220.
Keller, J., Seifried, C., 1990. The present status of obsidian source identification in Anatolia and the Near East. PACT 25: Volcanology and archaeology. In: Proceedings of the European Workshops of Ravello. vol. 25. pp. 57–87.
Keller, J., Djerbashian, E., Pernicka, E., Karapetian, S., Nasedkin, V., 1996. Armenian and Caucasian obsidian occurrences as sources for the Neolithic trade: volcanological setting and chemical characteristics. In: Archaeometry 94: The Proceedings of the 29th International Symposium on Archaeometry; Ankara, 914 May 1994, pp. 69–86.
Kellett, L.C., Golitko, M., Bauer, B.S., 2013. A provenance study of archaeological obsidian from the Andahuaylas region of southern Peru. J. Archaeol. Sci. 40, 1890–1902.
Khalidi, L., Gratuze, B., Boucetta, S., 2009. Provenance of obsidian excavated from Late Chalcolithic levels at the sites of Tell Hamoukar and Tell Brak, Syria. Archaeometry 51, 879–893.
Khalidi, L., Gratuze, B., Stein, G., McMahon, A., Al-Quntar, S., Carter, R., Cuttler, R., Drechsler, P., Healey, E., Inizan, M.-L., Mouralis, D., Pernicka, E., Robin, A.-K., 2016. The growth of early social networks: New geochemical results of obsidian from the Ubaid to Chalcolithic Period in Syria, Iraq and the Gulf. J. Archaeol. Sci. Rep. 9, 743–757.
Killick, D., 2015. The awkward adolescence of archaeological science. J. Archaeol. Sci. 56, 242–247.
Kobayashi, K., Mochizuki, A., 2007. Source Identification of Obsidian Projectile Points from Kaman-Kalehöyük. Kaman-Kalehöyük, pp. 16.
Kuehne, S.C., Froese, D.G., Shane, P.A.R., 2011. The INTAV intercomparison of electron-beam microanalysis of glass by tephrochronology laboratories: results and recommendations. Quat. Int. 246, 19–47.
Kuhn, T.S., 1962. The Structure of Scientific Revolutions. University of Chicago Press.
Kuzmin, Y.V., Glascock, M.D., 2007. Two islands in the ocean: prehistoric obsidian exchange between Sakhalin and Hokkaido, Northeast Asia. J. Island & Coastal Archaeology 2, 99–120.
LaLande, J., 1990. Summary Report on the 1989 Obsidian-Sourcing Project. (Rogue River National Forest, C.R. Job RR-909).
LaValley, S.J., 2013. Late Holocene Toolstone Procurement and Land-Use Strategies in the Black Rock Desert and High Rock Country of Northwest Nevada. Master's thesis. Department of Anthropology, University of Nevada, Reno.
Le Bourdonnec, F.-X., Bontempi, J.-M., Marini, N., Mazet, S., Neuville, P.F., Poupeau, G., Sicurani, J., 2010. SEM-EDS characterization of western Mediterranean obsidians and the Neolithic site of A Fuata (Corsica). J. Archaeol. Sci. 37, 92–106.
Le Bourdonnec, F.-X., Nomade, S., Poupeau, G., Guillou, H., Tushabramishvili, N., Moncel, M.-H., Pleurdeau, D., Agapishvili, T., Voinshet, P., Mgeladze, A., Lordkipanoidze, D., 2012. Multiple origins of Bondi Cave and Ortvale Klde (NW Georgia) obsidians and human mobility in Transcaucasia during the Middle and Upper Palaeolithic. J. Archaeol. Sci. 39, 1317–1330.
Le Bourdonnec, F.-X., D'Anna, A., Poupeau, G., Lugliè, C., Bellot-Gurlet, L., Tramoni, P., Marchesi, H., 2015. Obsidians artefacts from Renaghju (Corsica Island) and the Early Neolithic circulation of obsidian in the Western Mediterranean. Archaeol. Anthropol. Sci. 7, 441–462.
Leach, B.F., Oda, S., Bird, R., 2018. Characterisation of 15 sources of Japanese obsidian: PIXEPIGME analysis, and identification of archaeological specimens. Tuhinga, Records of the Museum of New Zealand. Te Papa Tongarewa 29, 77–89.
Lebedev, V.A., Bubnov, S.N., Dudauri, O.Z., Vashakidze, G.T., 2008. Geochronology of Pliocene volcanism in the Dzhavakheti Highland (the Lesser Caucasus). Part 2: Eastern part of the Dzhavakheti Highland. Regional geological correlation. Stratigr. Geol. Correl. 16, 553–574.
Lebedev, V.A., Chernyshev, I.V., Shatagin, K.N., Bubnov, S.N., Yakushev, A.I., 2013. The Quaternary Volcanic Rocks of the Geghama Highland, Lesser Caucasus, Armenia: Geochronology, Isotopic SrNd Characteristics, and Origin. J. Volcanol. Seismol. 7 (3), 204–229.
Lee, G., Kim, J., 2015. Obsidians from the Sinbuk archaeological site in Korea — evidences for strait crossing and long-distance exchange of raw material in Paleolithic Age. J. Archaeol. Sci. Rep. 2, 458–466.
Liebmann, M.J., 2017. From landscapes of meaning to landscapes of signification in the American Southwest. Am. Antiq. 82 (4), 642–661.
Lombao, D., Guardiola, M., Mosquera, M., 2017. Teaching to make stone tools: new experimental evidence supporting a technological hypothesis for the origins of language. Sci. Rep. 7 (Article #14394).
Lynch, S.C., Kato, H., Weber, A.W., 2018. Obsidian resource use from the Jomon to Okhotsk period on Rebun Island: an analysis of archaeological obsidian. J. Archaeol. Sci. Rep. 17, 1007–1017.
Lyons, W.H., Thomas, S.P., Skinner, C.E., 2001. Changing Obsidian Sources at the Lost Dune and McCoy Creek Sites, Blitzen Valley, Southeast Oregon. J. Calif. Gt. Basin Anthropol. 23 (2), 273–296.
MacCurdy, G.G., 1900. The obsidian razor of the Aztecs. Am. Anthropol. 2 (3), 417–421 New Series.
MacDonald, R., Bailey, D.K., 1975. Part 1. The chemistry of the peralkaline oversaturated obsidians. Chapter N. chemistry of igneous rocks. In: Data of Geochemistry, 6th ed. Geological Survey Professional Paper 440-N-I.
MacDonald, R., Smith, R.L., Thomas, J.E., 1992. Chemistry of the Subalkalic silicic obsidians. In: United States Geological Survey Professional Paper. vol. 1523.
Macko, M.E., Couch, J.S., Koerper, H.C., 2005. Implications of ritual biface caches from the Irvine site. J. Calif. Gt. Basin Anthropol. 25 (1), 93–108.
Marguí, E., van Grieken, R., 2013. X-Ray Fluorescence Spectrometry and Related Techniques: An Introduction. Momentum Press.
Marsh, R., Park, M., 2018. Got powder in your carry-on? You may want to check it. 20 June 1998. Online at CNNhttps://www.cnn.com/2018/06/20/politics/tsa-powder-carry-on-bags/index.html.
Masihma, H., 2018. Nondestructive analyses of bulk rock compositions of obsidian using a handheld XRF Delta Premium DP-6000. Natural Resource Environment and Humans 8, 109–118.
Matsumoto, Y., Nesbitt, J., Glascock, M.D., Cavero Palomino, Y.I., Burger, R.L., 2018. Interregional obsidian exchange during the late initial period and early horizon: new perspectives from Campanayuq Rumi, Peru. Lat. Am. Antiq. 29 (1), 44–63.
Maziar, S., Glascock, M.D., 2017. Communication networks and economical interactions: Sourcing obsidian in the Araxes River basin. J. Archaeol. Sci. Rep. 14, 31–37.
McCoy, M.D., Carpenter, J., 2014. Strategies for obtaining obsidian in pre-European contact era New Zealand. PLoS One 9 (1), e84302.
McCoy, M.D., Ladefoged, T.N., Codlin, M., Sutton, D.G., 2014. Does Carneiro's circumscription theory help us understand Maori history? An analysis of the obsidian assemblage from Pouerua Pa, New Zealand (Aotearoa). J. Archaeol. Sci. 42, 467–475.
Meigs, A., Scarberry, K., Grunder, A., Carlson, R., Ford, M.T., Fouch, M., Grove, T., Hart, W.K., Iademarco, M., Jordan, B., Milliard, J., 2009. Geological and Geophysical Perspectives on the Magmatic and Tectonic Development, High Lava Plains and Northwest Basin and Range. The Geological Society of America Field Guide, vol. 15.
Mendelsohn, R.R., 2018. Obsidian sourcing and dynamic trade patterns at Izapa, Chiapas, Mexico: 100 BCE400 CE. J. Archaeol. Sci. Rep. 20, 634–646.
Merrick, H.V., Brown, F.H., 1984. Obsidian sources and patterns of source utilization in Kenya and northern Tanzania: some initial findings. The African Archaeological Review 2, 129–152.
Merrick, H.V., Brown, F.H., Nash, W.P., 1994. Use and movement of obsidian in the early and middle stone ages of Kenya and northern Tanzania. In: Childs, S.T. (Ed.), Society, Culture, and Technology in Africa. Masca Research Papers in Science and Archaeology, pp. 29–44.
Millhauser, J.K., Fargher, L.F., Heredia Espinoza, V.Y., Blanton, R.E., 2015. The geopolitics of obsidian supply in Postclassic Tlaxcallan: a portable X-ray fluorescence study. J. Archaeol. Sci. 58, 133–146.
Moholy-Nagy, H., Meierhoff, J., Golitko, M., Kestle, C., 2013. An analysis of pXRF obsidian source attributions from Tikal, Guatemala. Lat. Am. Antiq. 24 (1), 72–97.
Montague, S.T., 2010. High-Elevation Prehistoric Land Use in the Central Sierra Nevada, Yosemite National Park, California. Master's thesis. Department of Anthropology, California State University-Sacramento.
Moore, J., 2009. Great Basin Tool-Stone Sources: The NDOT Obsidian and Tool-Stone Sourcing Project: 2002 Progress Report. Nevada Department of Transportation.
Mulazzani, S., Le Bourdonnec, F.-X., Belhouchet, L., Poupeau, G., Zoughlami, J., Dubernet, S., Tufano, E., Lefrais, Y., Khedhaier, R., 2010. Obsidian from the Epipalaeolithic and Neolithic eastern Maghreb. A view from the Hergla context (Tunisia). J. Archaeol. Sci. 37, 2529–2537.
Nakayama, K., 2006. Glass Bead/X-ray Fluorescence Analysis of 42 Components in Silicate Rocks. Doctoral dissertation. Meiji University Graduate School of Science and Engineering.
Nazaroff, A., Prufer, K., Drake, B., 2010. Assessing the applicability of portable X-ray fluorescence spectrometry for obsidian provenance research in the Maya lowlands. J. Archaeol. Sci. 37, 885e895.
Negash, A., Shackley, M.S., Alene, M., 2006. Source provenance of obsidian artifacts from the Early Stone Age (ESA) site of Melka Konture, Ethiopia. J. Archaeol. Sci. 33 (12), 1647–1650.
Negash, A., Alene, M., Brown, F.H., Nash, B.P., Shackley, M.S., 2007. Geochemical sources for the terminal Pleistocene/early Holocene obsidian artifacts of the site of Beseka, Central Ethiopia. J. Archaeol. Sci. 34, 1205–1210.

Nelson, F., 1984. X-ray fluorescence analysis of some Western north American obsidians. In: Hughes, Richard E. (Ed.), Obsidian Studies in the Great Basin. Contributions of the University of California Archaeological Research Facility No. 45 University of California, Berkeley, pp. 27–62.
Nelson, F.W., Holmes, R.D., 1979. Trace Element Analysis of Obsidian Sources and Artifacts from Western Utah. Antiquities Section Selected Papers, vol. 6 (15). Utah State Historical Society, pp. 65–80.
Neri, L.A.M., Pawlik, A.F., Reepmeyer, C., Mijares, A.S.B., Paz, V.J., 2015. Mobility of early islanders in the Philippines during the Terminal Pleistocene/Early Holocene boundary: pXRF-analysis of obsidian artefacts. J. Archaeol. Sci. 61, 149–157.
Newlander, K., Goodale, N., Jones, G.T., Bailey, D.G., 2015. Empirical study of the effect of count time on the precision and accuracy of pXRF data. J. Archaeol. Sci. Rep. 3, 534–548.
Nishiaki, Y., Maeda, O., Kannari, T., Nagai, M., Healey, E., Guliyev, F., Campbell, S., 2019. Obsidian provenance analyses at Göytepe, Azerbaijan: Implications for understanding Neolithic socioeconomies in the southern Caucasus. Archaeometry. https://doi.org/10.1111/arcm.12457.
Oddone, M., Yeğingil, Z., Bigazzi, G., Ercan, T., Özdogan, M., 1997. Chemical Characterisations of Anatolian obsidians by instrumental and epithermal neutron activation analysis. J. Radioanal. Nucl. Chem. 224 (1), 27–38.
Oddone, M., Bigazzi, G., Keheyan, Y., Meloni, S., 2000. Characterisation of Armenian obsidians: implications for raw material supply for prehistoric artifacts. Journal of Radioanaytical and Nuclear Chemistry 243 (3), 673–682.
Orange, M., Le Bourdonnec, F.-B., Scheffers, A., Joannes-Boyau, R., 2016. Sourcing obsidian: A new optimized LA-ICP-MS protocol. STAR: Science & Technology of Archaeological Research 2 (2), 192–202.
Orange, M., Le Bourdonnec, F.-X., Bellot-Gurlet, L., Lugliè, C., Dubernet, S., Bressy-Leandri, C., Scheffers, A., Joannes-Boyau, R., 2017. On sourcing obsidian assemblages from the Mediterranean area: Analytical strategies for their exhaustive geochemical characterisation. J. Archaeol. Sci. Rep. 12, 834–844.
Panich, L.M., 2016. Beyond the colonial curtain: Investigating indigenous use of obsidian in Spanish California through the pXRF analysis of artifacts from Mission Santa Clara. J. Archaeol. Sci. Rep. 5, 521–530.
Parfitt, A.B., McCutcheon, P.T., 2017. Chemical sourcing of obsidian artifacts from the Grissom site (45-KT-301) to study source variability. Journal of Northwest Anthropology 51, 37–72.
Park, R.J., 2010. A Culture of Convenience? Obsidian Source Selection in Yellowstone National Park. Master's thesis. Department of Anthropology and Archaeology, University of Saskatchewan, Saskatoon, Canada.
Pintar, E., Martínez, J.G., Aschero, C.A., Glascock, M.D., 2016. Obsidian use and mobility during the early and middle Holocene in the salt Puna, NW Argentina. Quat. Int. 422, 93–108.
Poupeau, G., Kieffer, G., Raynal, J.-P., Milton, A., Delerue, S., 2004. Trace element geochemistry in Balchit obsidian (Upper Awash, Ethiopia). In: Chavaillon, J., Piperno, M. (Eds.), Studies on the Early Paleolithic Site of Melka Kunture, Ethiopia. Istituto Italiano di Preistoria e Protostoria, Florence, pp. 103–110.
Poupeau, G., Le Bourdonnec, F.-X., Carter, T., Delerue, S., Shackley, M.S., Barrat, J.A., Dubernet, S., Moretto, P., Calligaro, T., Milić, M., Kobayashi, K., 2010. The use of SEM-EDS, PIXE and EDXRF for obsidian provenance studies in the Near East: a case study from Neolithic Çatalhöyük (central Anatolia). J. Archaeol. Sci. 37 (11), 2705–2720.
Psota, S., 1994. Native American Use of Non-Quarry Obsidian in Northern Sonoma County: A Preliminary Assessment. Master's thesis. Cultural Resources Management, Sonoma State University.
Reaux, D.J., Smith, G.M., Adams, K.D., Jamaldin, S., George, N.D., Mohr, K., Rosencrance, R.L., 2018. A first look at the terminal Pleistocene/Early Holocene record of Guano Valley, Oregon, USA. PaleoAmerica. https://doi.org/10.1080/20555563.2018.1460183.
Reed, W.P., 1992. Certificate: Standard Reference Material 278, Obsidian Rock. National Institute of Standards and Technology, Department of Commerce.
Reepmeyer, C., O'Connor, S., Maloney, T., Kealy, S., 2016. Late Pleistocene/Early Holocene maritime interaction in Southeastern Indonesia-Timor Leste. J. Archaeol. Sci. 76, 21–30.
Renfrew, C., Dixon, J., Cann, J., 1966. Obsidian and early cultural contact in the Near East. Proceedings of the Prehistoric Society 2, 30–72.
Renfrew, C., Cann, J., Dixon, J., 1965. Obsidian in the Aegean. Annual of the British School at Athens 60, 225–247.
Renfrew, C., Dixon, J., Cann, J., 1968. Further analysis of Near Eastern obsidians. Proceedings of the Prehistoric Society 34, 319–331.
ResearchGate, 2019. Q&A discussion page. https://bit.ly/2WhrkeZ, Accessed date: May 2019.
Rice, P.M., 1996. Recent ceramic analysis: 2. Composition, production, and theory. J. Archaeol. Res. 4 (3), 165–202.
Rice, S.K., 2015. Analysis of Paleoindian Site Structure and Toolstone Procurement at the Overlook Site (26CH3413), Churchill County, Nevada. Master's thesis. Department of Anthropology, University of Nevada-Reno.
Rick, T.C., Skinner, C.E., Erlandson, J.M., Vellanoweth, R.L., 2001. Obsidian source characterization and human exchange systems on California's Channel Islands. Pacific Coast Archaeological Society Quarterly 37 (3), 27–44.
Riebe, D.J., Feinman, G.M., Nash, S.E., 2018. P-XRF compositional analysis of obsidian from O Block Cave, New Mexico. J. Archaeol. Sci. Rep. 18, 26–42.
Ritter, E.W., 1989. Sheep Rock Shelter (CA-Sis-266) Archaeological Test Excavations in Shasta Valley. Bureau of Land Management.
Rivero-Torres, S.E., Jiménez-Reyes, M., Tenorio, D., 2017. Obsidian artifacts from the southeastern structure of the Lagartero Acropolis, Chiapas, Mexico. J. Archaeol. Sci. Rep. 15 (2017), 219–225.
Roche, R.L., 1987. Stratigraphic and Geochemical Evolution of the Glass Buttes Complex, Oregon. Master's thesis. Department of Geology, Portland State University.
Rowe, M., Thornber, C., Gooding, D., Pallister, S., 2008. Catalog of Mount St. Helens 20042005 tephra samples with major- and trace-element geochemistry. In: United States Geological Survey, Open-File Report 20081131.
Santi, P., Renzulli, A., Oddone, M., Martinez, E.L., Gonzalez Rivera, C.A., 2017. Long-distance provenance for obsidian artifacts of Mesoamerica Preclassic and Early Classic periods found in the Los Naranjos Archaeological Park (Honduras). Archaeol. Anthropol. Sci. 9, 555–566.
Savov, I.P., Leeman, W.P., Lee, C.A., Shirey, S.B., 2009. Boron isotopic variations in NW USA rhyolites: Yellowstone, Snake River Plain, Eastern Oregon. J. Volcanol. Geotherm. Res. 188, 162–172.
Scharlotta, I., Quach, T.T., 2015. Provenance analysis of porphyritic volcanic materials in San Diego using portable X-ray fluorescence. J. Archaeol. Sci. Rep. 3, 285–294.
Scharlotta, I., Gilstrap, W., Neff, H., 2011. No stone unburned: a compositional analysis of obsidian microdebitage by laser ablation TOF-ICP-MS. Archaeometry 53 (5), 873–889.
Schmitt, A.K., Simon, J.I., 2004. Boron isotopic variations in hydrous rhyolitic melts: a case study from Long Valley, California. Contrib. Mineral. Petrol. 146, 590–605.
Seitsonen, O., Sonninen, E., Heikkilä, P.A., 2012. Pastoral Neolithic studies in northern Tanzania: an interim report on XRF and stable isotope analyses in the Engaruka area. Nyame Akuma 77, 11–23.
Shackley, M.S., 1988. Sources of archaeological obsidian in the southwest: an archaeological, petrological, and geochemical study. Am. Antiq. 53, 752–772.
Shackley, M.S., 1997. An energy dispersive X-ray fluorescence analysis of the obsidian artifacts from Chan Chich, Belize. In: Houk, B.A. (Ed.), The 1997 Season of the Chan Chich Archaeological Project. Papers of the Chan Chich Archaeological Project, Number 3 Center for Maya Studies, San Antonio, Texas, pp. 67–72.
Shackley, M.S., 1998. Current issues and future directions in archaeological volcanic glass studies: an introduction. In: Shackley, M.S. (Ed.), Archaeological Obsidian Studies: Method and Theory. Plenum Press, New York, pp. 1–14.
Shackley, M.S., 2005. Source Provenance of Obsidian Artifacts from the Ellis Landing Site (CA-CCO-295), Contra Costa County, California. UC Berkeley Archaeological X-ray Fluorescence Reports.
Shackley, M.S., 2010. Is there reliability and validity in portable X-ray fluorescence spectrometry (PXRF)? In: The SAA Archaeological Record, pp. 17–20 November issue.
Shackley, M.S., 2011a. An introduction to X-ray fluorescence (XRF) analysis in archaeology. In: Shackley, M.S. (Ed.), X-ray Fluorescence Spectrometry (XRF) in Geoarchaeology. Springer, pp. 7–44.
Shackley, M.S., 2011b. Source provenance of obsidian Artifacts from CA-SMA-113, west-Central California. In: UC Berkeley Archaeological X-ray Fluorescence Reports.
Shackley, M.S., 2012a. Source Provenance of Obsidian Artifacts from CA-SCR-276, Santa Cruz, California. UC Berkeley Archaeological X-ray Fluorescence Reports.
Shackley, M.S., 2012b. Portable X-ray fluorescence spectrometry (pXRF): the good, the bad, and the ugly (online essay). Archaeol. Southwest Mag. 26 (Spring issue).
Shackley, M.S., 2012c. An Energy-dispersive X-ray Fluorescence Analysis of Obsidian Projectile Points and Fragments from CA-COL-33, Southern Colusa County, Northern California. UC Berkeley Archaeological X-ray Fluorescence Reports.
Shackley, M.S., 2014a. Source Provenance of Obsidian Artifacts from Various Sites in the Goodman Point Project, Montezuma County, Southwest Colorado. UC Berkeley Archaeological X-ray Fluorescence Reports.
Shackley, M.S., 2014b. X-ray fluorescence (XRF) analysis of major oxide and trace element concentrations for an obsidian projectile point from a site at furnace creek, Cumberland Furnace, Tennessee. In: UC Berkeley Archaeological X-Ray Fluorescence Reports.
Shackley, M.S., 2015a. Source Provenance of Unknown Obsidian Samples. UC Berkeley Archaeological X-ray Fluorescence Reports.
Shackley, M.S., 2015b. Source provenance of obsidian Artifacts from Zion National Park, Utah and pipe spring National Monument, Arizona. In: UC Berkeley Archaeological X-ray Fluorescence Reports.
Shackley, M.S., 2017. ThermoFisher scientific Quant'X analysis and instrumentation. Geoarchaeological XRF Laboratory website, updated 12 December 2017. http://www.swxrflab.net/anlysis.htm.
Shackley, M.S., Hughes, R.E., 2014. Source Provenance of Obsidian Artifacts from the Spring Creek Site (CA-SHA-69), Shasta County, California. UC Berkeley Archaeological X-ray Fluorescence Reports.
Shackley, M.S., Skinner, C., 2015. Source Provenance of Obsidian Paleoindian and Early Archaic Artifacts from the Great Basin. UC Berkeley Archaeological X-ray Fluorescence Reports.
Shackley, M.S., Goff, F., Dolan, S.G., 2016. Geologic origin of the source of Bearhead rhyolite (Paliza canyon) obsidian, Jemez Mountains, northern New Mexico. N. M. Geol. 38 (3), 52–65.
Silliman, S.W., 2005. Obsidian studies and the archaeology of 19th-century California. J. Field Archaeol. 30 (1), 75–94.
Silva de la Mora, F.G., 2018. Obsidian procurement and distribution in the northwestern Maya lowlands during the Maya classic, a regional perspective. J. Archaeol. Sci. Rep. 18, 577–586.
Skinner, C.E., 1983. Obsidian Studies in Oregon: An Introduction to Obsidian and an Investigation of Selected Methods of Obsidian Characterization Utilizing Obsidian Collected at Prehistoric Quarry Sites in Oregon. Master's Terminal Project, Interdisciplinary Studies, University of Oregon.
Skinner, C.E., 2013. X-Ray Fluorescence Analysis of Artifact Obsidian from the Cal Schmidt Clovis Site (35-HA-850), Harney County, Oregon. Northwest Research Obsidian Studies Laboratory Report 201304.
Skinner, C.E., Thatcher, J.J., 2003. X-ray Fluorescence Analysis and Obsidian Hydration

Rim Measurement of Artifact Obsidian from 34 Archaeological Sites Associated with the Proposed FTV Western Fiber Build Project, Deschutes, Lake, Harney, and Malheur Counties, Oregon. Northwest Research Obsidian Studies Laboratory Report 199856.
Skinner, C.E., Thatcher, J.J., 2006. X-ray fluorescence analysis and obsidian hydration measurement of artifact obsidian from several sites in the Mojave National Preserve, San Bernardino County, California. In: Northwest Research Obsidian Studies Laboratory Report 2006116.
Skinner, C.E., Thatcher, J.J., 2016. Obsidian studies: geochemical sourcing (X-ray fluorescence and hydration rim measurement). In: Ruby Pipeline Project Archaeological Site Testing and Evaluation and Data Recovery Oregon Segment: Lake and Klamath Counties. Archaeological Investigations Northwest, Portland, Oregon (Report 3346).
Skinner, C.E., Thatcher, J.J., Davis, M.K., 1997. X-Ray Fluorescence Analysis and Obsidian Hydration Rim Measurement of Artifact Obsidian from 35-DS-193 and 35-DS-201, Surveyor Fire Rehabilitation Project, Deschutes National Forest, Oregon. Northwest Research Obsidian Studies Laboratory Report. (98-96).
Smith, D.B., 1995. Rhyolite, Glass Mountain RGM-1. Certificate of Analysis. United States Geological Survey.
Smith, G.M., Kielhofer, J., 2011. Through the High Rock and beyond: placing the Last Supper Cave and Parman Paleoindian lithic assemblages into a regional context. J. Archaeol. Sci. 38 (12), 3568–3576.
Sparaga, J., 2017. Thee Stones they Chose: Lithic Analysis and Design Selections at Číxwicən Village (45CA523). Master's thesis. Western Washington University.
Speakman, R.J., 2012. Evaluation of Bruker's tracer family factory obsidian calibration for handheld portable XRF studies of obsidian. Report prepared for Bruker AXS, Kennewick, WA. In: Center for Applied Isotope Studies Report. University of Georgia.
Speakman, R.J., Shackley, M.S., 2013. Commentary: silo science and portable XRF in archaeology: a response to Frahm. J. Archaeol. Sci. 40, 1435–1443.
Speakman, R.J., Little, N.C., Creel, D., Miller, M.R., Iñañe, J.G., 2011. Sourcing ceramics with portable XRF spectrometers? A comparison with INAA using Mimbres pottery from the American Southwest. J. Archaeol. Sci. 38, 3483–3496.
Starek, G.M., 2013. The Temporal Dating and Analysis of the Archaeological Assemblage Recovered from a Portion of Prehistoric Site, *"Satos Rini Rumaytak"* (At the Hill Above the River Site) CA-SCR-12. Master's thesis. Department of Anthropology, San Jose State University.
Stevenson, D.P., Stross, F.H., Heizer, R.F., 1971. An evaluation of X-ray fluorescence analysis as a method for correlating obsidian artifacts with source location. Archaeometry 13, 17–25.
Stimac, J., Hickmott, D., 1994. Trace-element partition coefficients for ilmenite, orthopyroxene and pyrrhotite in rhyolite determined by micro-PIXE analysis. Chem. Geol. 117 (14), 313–330.
Streck, M., Wacaster, S., 2006. Plagioclase and pyroxene hosted melt inclusions in basaltic andesites of the current eruption of arenal volcano, Costa Rica. J. Volcanol. Geotherm. Res. 157 (13), 236–253.
Stross, F.H., Stevenson, D.P., Weaver, J.R., Wyld, G., 1971. Analysis of American obsidians by X-ray fluorescence and neutron activation analysis. In: Brill, R.H. (Ed.), Science and Archaeology. MIT Press, pp. 210–221.
Suda, Y., Tsuchiya, M., 2016. The Provenance of Obsidian Artifacts from the Hiroppara Site Group (Kirigamine, Central Japan). Petrological Analysis of Relics Excavated from the Site of IV Hirohara I and II. Meiji University Kurosoishi Research Center Materials and Reports.
Suzuki, M., Watanabe, K., Tomura, K., 2005. Constructing Data-Base for Sourcing Archaeological Obsidians by INAA Using Middle- and Long-lived Nuclides. Progress Report of the Inter-University Collaborative Use of JAEA Facilities.
Syvilay, D., Bousquet, B., Chapoulie, R., Orange, R., Le Bourdonnec, F.-X., 2019. Advanced statistical analysis of LIBS spectra for the sourcing of obsidian samples. J. Anal. At. Spectrom. https://doi.org/10.1039/C8JA00340H. Advance article.
Tatlock, D.B., Flanagan, F.L., Bastron, H., Berman, S., Sutton, A.L., Jr. 1976. Rhyolite, RGM-1, from Glass Mountain, California. In: F.L. Flanagan, ed., Descriptions and Analyses of Eight New USGS Rock Standards. U.S. Geological Survey Professional Paper vol. 850: 1114.
Thatcher, J.J., 2000. The Distribution of Geologic and Artifact Obsidian from the Silver Lake/Sycan Marsh Geochemical Source Group, South-Central Oregon. Master's thesis. Interdisciplinary Studies, Oregon State University.
Thompson, R.N., Morrison, M.A., Hendry, G.L., Parry, S.J., Simpson, P.R., Hutchison, R., O'Hara, M.J., 1984. An assessment of the relative roles of crust and mantle in magma genesis: an elemental approach [and discussion]. Philosophical Transactions of the Royal Society of London. Series A, Mathematical and Physical Sciences 310 (1514), 549–590.
Tomura, K., Koshimizu, T., Nobuyama, I., Mochizuki, A., 1994. Identification of obsidian implements from Doteue site, Numazu City, using NAA. In: Abstract Volume of the 38th Houshakagaku Touronkai, pp. 91–92.
Tostevin, G., 2012. Seeing Lithics: A Middle-Range Theory for Testing for Cultural Transmission in the Pleistocene. American School of Prehistoric Research Monograph Series Harvard University, Oxbow Books.
Tryon, C.A., Kuhn, S.L., Slimak, L., Logan, A.M.V., Balkan-Atlı, N., 2011. Scale in tephrostratigraphic correlation: An example from Turkish Pleistocene archaeological sites. Quat. Int. 246 (12), 124–133.
Tykot, R.H., 1996. Obsidian procurement and distribution in the central and Western Mediterranean. J. Mediterr. Archaeol. 9 (1), 39–82.
Tykot, R.H., 1997. Characterization of the Monte arci (Sardinia) obsidian sources. J. Archaeol. Sci. 24 (5), 467–479.
Vogel, T.A., Eichelberger, J.C., Younker, L.W., Schuraytz, B.C., Horkowitz, J.P., Stockman, H.W., Westrich, H.R., 1989. Petrology and emplacement dynamics of intrusive and extrusive rhyolites of obsidian dome, Inyo craters volcanic chain, eastern California. J. Geophys. Res. 94 (B12), 17937–17956.
Vogt, J.R., Graham, C.C., Glascock, M.D., Cobean, R.H., 1982. A study of Mesoamerican obsidian sources using activation analysis. J. Radioanal. Chem. 69, 271–289.
Wada, K., Mukai, M., Sano, K., Izuho, M., Sato, H., 2014. Chemical composition of obsidians in Hokkaido Island, northern Japan: The importance of geological and petrological data for source studies. In: Ono, A., Glascock, M.D., Kuzmin, Y.V., Suda, Y. (Eds.), Methodological Issues for Characterization and Provenance Studies of Obsidian in Northeast Asia. Archaeopress, pp. 67–84.
Wang, D., Van der Voo, R., 2004. The hysteresis properties of multidomain magnetite and titanomagnetite/titanomaghemite in mid-ocean ridge basalts. Earth Planet. Sci. Lett. 220, 175–184.
Warashina, T., Kamaki, Y., Higashimura, T., 1978. Sourcing of sanukite implements by X-ray fluorescence analysis II. J. Archaeol. Sci. 5 (3), 283–291.
Weaver, J.R., Stross, F.H., 1965. Analysis by X-ray fluoresce of some American obsidians. In: Contributions of the University of California Archaeological Research Facility. vol. 1. pp. 89–93.
Weaver, S.D., Steal, J.S.C., Gibson, I.L., 1972. Trace-element data relevant to the origin of trachytic and Pantelleritic lavas in the east African rift system. Contr. Mineral. and Petrol. 36, 181–194.
Weisler, M.I., Clague, D.A., 1998. Characterisation of archaeological volcanic glass from Oceania: the utility of three techniques. In: Shackley, M.S. (Ed.), Archaeological Obsidian Studies: Method and Theory. Society for Archaeological Sciences, pp. 103–128.
Williams, P.R., Dussubieux, L., Nash, D.J., 2012. Provenance of Peruvian Wari obsidian: comparing INAA, LA-ICP-MS, and portable XRF. In: Liritzis, I., Stevenson, C.M. (Eds.), Obsidian and Ancient Manufactured Glasses. University of New Mexico Press, pp. 75–85.
Wills, W., 2013. A Home in the Yosemite Wilderness: An Archaeological Investigation of Prehistory at Laurel Lake, Site CA-TUO-4818, Tuolumne County, California. Master's thesis. Cultural Resources Management, Sonoma State University.
Wilson, S., 2009. Rhyolite, Glass Mountain RGM-2. Certificate of Analysis. United States Geological Survey.
Yentsch, A.T., Rood, R.J., Jones, K.T., Fenner, L.A., 2009. Archaeological investigations at the prison site (42SL186). Antiquities Section Selected Papers 8 (17).
Zeitlin, R.N., 1979. Prehistoric Long-distance Exchange on the Southern Isthmus of Tehuantepec, Mexico. Doctoral dissertation. Yale University.
Zeitlin, R.N., 1982. Toward a more comprehensive model of interregional commodity distribution: political variables and prehistoric obsidian procurement in Mesoamerica. Am. Antiq. 47 (2), 260–275.
Zeitlin, R.N., Heimbuch, R.C., 1978. Trace element analysis and the archaeological study of obsidian procurement in Precolumbian Mesoamerica. In: Davis, D.D. (Ed.), Lithics and Subsistence: The Analysis of Stone Tool Use in Prehistoric Economies. vol. 20. Vanderbilt University Publications in Anthropology, pp. 117–159.